SHIP PRODUCTION COMMITTEE
FACILITIES AND ENVIRONMENTAL EFFECTS
SURFACE PREPARATION AND COATINGS
DESIGN/PRODUCTION INTEGRATION
HUMAN RESOURCE INNOVATION
MARINE INDUSTRY STANDARDS
WELDING
INDUSTRIAL ENGINEERING
EDUCATION AND TRAINING

November 15, 2000
NSRP 0569
N1-95-2

THE NATIONAL SHIPBUILDING RESEARCH PROGRAM

A Shipyard Program for NPDES Compliance
Appendix F - Bay/Estuary Model (B.E.S.T.) Documentation

U.S. DEPARTMENT OF THE NAVY
CARDEROCK DIVISION,
NAVAL SURFACE WARFARE CENTER

in cooperation with
National Steel and Shipbuilding Company
San Diego, California

Report Documentation Page

Form Approved
OMB No. 0704-0188

1. REPORT DATE	2. REPORT TYPE	3. DATES COVERED
15 NOV 2000	**N/A**	**-**

4. TITLE AND SUBTITLE	5a. CONTRACT NUMBER
The National Shipbuilding Research Program, A Shipyard Program for NPDES Compliance Appendix F - Bay/Estuary Model (B.E.S.T) Documentation	5b. GRANT NUMBER
	5c. PROGRAM ELEMENT NUMBER
6. AUTHOR(S)	5d. PROJECT NUMBER
	5e. TASK NUMBER
	5f. WORK UNIT NUMBER
7. PERFORMING ORGANIZATION NAME(S) AND ADDRESS(ES) **Naval Surface Warfare Center CD Code 2230-Design Integration Tower Bldg 192, Room 128 9500 MacArthur Blvd Bethesda, MD 20817-5000**	8. PERFORMING ORGANIZATION REPORT NUMBER
9. SPONSORING/MONITORING AGENCY NAME(S) AND ADDRESS(ES)	10. SPONSOR/MONITOR'S ACRONYM(S)
	11. SPONSOR/MONITOR'S REPORT NUMBER(S)

12. DISTRIBUTION/AVAILABILITY STATEMENT
Approved for public release, distribution unlimited

13. SUPPLEMENTARY NOTES

14. ABSTRACT

15. SUBJECT TERMS

16. SECURITY CLASSIFICATION OF:			17. LIMITATION OF ABSTRACT	18. NUMBER OF PAGES	19a. NAME OF RESPONSIBLE PERSON
a. REPORT	b. ABSTRACT	c. THIS PAGE			
unclassified	**unclassified**	**unclassified**	**SAR**	**127**	

DISCLAIMER

These reports were prepared as an account of government-sponsored work. Neither the United States, nor the United States Navy, nor any person acting on behalf of the United States Navy (A) makes any warranty or representation, expressed or implied, with respect to the accuracy, completeness or usefulness of the information contained in this report/ manual, or that the use of any information, apparatus, method, or process disclosed in this report may not infringe privately owned rights; or (B) assumes any liabilities with respect to the use of or for damages resulting from the use of any information, apparatus, method, or process disclosed in the report. As used in the above, “Persons acting on behalf of the United States Navy” includes any employee, contractor, or subcontractor to the contractor of the United States Navy to the extent that such employee, contractor, or subcontractor to the contractor prepares, handles, or distributes, or provides access to any information pursuant to his employment or contract or subcontract to the contractor with the United States Navy. ANY POSSIBLE IMPLIED WARRANTIES OF MERCHANTABILITY AND/OR FITNESS FOR PURPOSE ARE SPECIFICALLY DISCLAIMED.

APPENDIX F - BAY/ESTUARY MODEL (B.E.S.T.) DOCUMENTATION

APPENDIX F from *A Shipyard Program for NPDES Compliance*, NSRP Task N1-95-02, Applied Research Laboratory, State College, PA, July 2000

BEST: A Numerical Model of Bay/Estuary Hydrodynamics and Sediment/Contaminant Transport

by

Gour-Tsyh Yeh, Hwai-Ping Cheng, and Jing-Ru Cheng
Department of Civil and Environmental Engineering
The Pennsylvania State University
University Park, PA 16802
USA

ABSTRACT

This report presents a 2-D depth-averaged numerical model simulating water flow and reactive contaminant and sediment transport in bay/estuary systems. This model includes two computational modules: flow and transport. We use a splitting strategy to solve hydrodynamic equations where the method of characteristics (MOC) is employed first to compute circulation without taking into account eddy fluxes, and then the Galerkin finite element method is applied to deal with eddy fluxes. The computed flow results are used to compute the migration of sediments and contaminants in the transport module. Sediments can be either suspended in the water column or deposited on bed rock, and whose distributions are determined subject to advection, dispersion, and deposition/erosion processes. Contaminants, either organic or inorganic, may exist in the dissolved phase in the water column or in the interstitial water of the bed sediments. They may appear also as particulate chemicals on sediments through adsorption reactions. All chemical reactions, including aqueous complexation, adsorption/desorption, and volatilization, are assumed elementary and kinetic with reaction rates calculated based on the collision theory where forward and backward rate constants are determined experimentally. We employ a predictor-corrector strategy in the transport module where transport equations are computed in the predictor step with reaction rates estimated at the previous time, and rate correction is achieved node by node in the corrector step to obtain the concentration distributions at the present time. The Lagrangian-Eulerian approach is applied to solve the transport equations in the predictor step with a particle tracking technique used to handle advection. The Picard method and the Newton-Raphson method are used to solve the rate correction equations for sediment distribution and reactive chemistry, respectively, in the corrector step. Four examples are used to demonstrate the capability of this model.

TABLE OF CONTENTS

TABLE OF FIGURES

TABLE OF TABLES

Chapter 1. INTRODUCTION

For at least two decades, environmental issues have become major public concerns worldwide and have drawn scientists and engineers from a variety of disciplines to devote themselves to environmental impact analysis/assessment (EIA) studies. Along with the rapid development of computer technology and the advancement of knowledge in numerical methods, numerical simulation techniques have become extremely useful tools in today's EIA studies. Many numerical models have been presented to simulate circulation of fluid flow and/or mass transport of contaminants and sediments in order to deal with problems relating to both water quantity and quality in bay/estuary areas [Falconer and Lin, 1997; Paulsen and Owen, 1996; Blumberg et al., 1996; Falconer, 1990; Lai, 1977].

Many numerical strategies have been presented to handle the non-linear hydrodynamic flow equations that are used to describe the circulation of estuarine waters. The numerical strategies included total variation diminishing method [Tseng and Liang, 1997], two-step explicit method [Park et al., 1995], semi-implicit method [Cecchi et al., 1998], implicit method [Fennema and Chaudhry, 1989], high-order time integration schemes [Ozkan-Haller and Kirby, 1997], upwind/upstream numerical schemes [Shi and Toro, 1996; Anastasiou and Chan, 1997], filtered solution method [Laible and Lillys, 1997], least square method [Muccino et al, 1997; Tseng and Liang, 1997], the method ofcharacteristics [Lai, 1977; Hirsch et al., 1987], and hybrid Lagrangian-Eulerican (LE) approach [Hansen and Arneborg, 1997; Petera and Nassehi, 1996]. On the other hand, a variety of numerical strategies, such as splitting method [Falconer and Lin, 1997; Sommeijer and Kok, 1996], upwind fomulation [Falconer and Lin, 1997; Ors, 1997; Sommeijer and Kok, 1996]; LE approach [Spitaleri and Corinaldesi, 1997; Wood and Baptista, 1992], and decoupling scheme [Park and Kuo, 1996], have been introduced to handle contaminant and sediment transport equations.

In the past decade, the LE approach has attracted many numerical modelers' attention because it can avoid many types of numerical errors when advection/convection dominates [Yeh, 1990]. Casulli and Cheng have shown that the approach is unconditionally stable when it was used to solve 1-D shallow water equations [Casulli and Cheng, 1990]. Petera and Nassehi employed a particle tracking technique in the Lagrangian step and have demonstrated their approach would provide very stable results for the convection dominated very shallow depth computations in

estuaries [Petera and Nassehi, 1996]. Yeh and his colleagues have proposed adaptive local refinement numerical algorithms to accurately solve advection-diffusion transport equations on the LE framework [Cheng et al., 1996a; Yeh et al., 1992]. In our 2-D depth-averaged model presented here, we also used the LE approach to handle the advection and dispersion terms in both flow and transport equations.

The method of characteristics (MOC) might be considered the most adequate way to solve wave or hyperbolic-type equations because it approaches problems not only mathematically but physically also. Lai has developed comprehensive MOC models to solve 1-D shallow water equations [Lai, 1987] and has incorporated the MOC with the finite difference discretization to solve 2-D flow equations [Lai, 1977]. In this work, we apply the MOC to solve flow equations on the platform of finite element discretization. Diagonalization [Abbott, 1966] can be achieved easily when the MOC is used to solve 1-D equations. Its application to 2-D cases, however, is not straightforward [Hirsch et al., 1987]. The three characteristics associated with 2-D shallow water equations can be chosen in any direction [Lai, 1977]. Many iterations might be needed to reach convergence in the numerical simulation if the characteristic directions are not appropriately selected. To handle this, we perform local diagonalization for the 2-D characteristic equations. We also apply the Lagrangian approach to solve the characteristic equations, rather than the original governing equations, where a particle tracking technique [Cheng et al., 1996b] was employed to transport characteristic variables along characteristics.

Though many models have included updated numerical approaches to improve their computational performance, no existing water quality model, to our knowledge, has used a generic and mechanistic approach to simulate the reaction-migration behavior of non-conservative chemicals in bay/estuary areas. All existing models are either empirically-based or simulate systems containing specific reactions, and thus their applications are limited to specific systems. Unlike an empirically-based model whose model parameters might be system- or even environment-dependent, a generic and mechanistic model considers interactions among chemicals based on reaction mechanisms which are universal and can be applied to all systems. Based on our experience of modeling reactive contaminant transport in the subsurface [Cheng and Yeh, 1998; Yeh et al., 1998; Yeh and Tripathi, 1990], we use a generic, mechanistic approach to simulate reactive contaminant transport in

bay/estuary areas, desiring to enhance reactive contaminant transport modeling in this field. In our transport module, we take into account suspended sediments and bed sediments whose distributions are determined through hydrological transport and erosion/deposition processes. Any contaminant considered in our model is treated as a chemical species which can be either organic or inorganic. It may appear in the water column as a dissolved chemical, be adsorbed onto suspended or bed sediments to become particulate chemicals, or exist in the interstitial water of the bed sediments also in dissolved form. All reactions among chemicals are assumed elementary kinetic, and reaction rates are described based on the collision theory [Stumm and Morgan, 1981] where forward and backward rate constants can be measured experimentally. Figure 1.1 shows a schematic plot for the chemical reactions taken into account in our model.

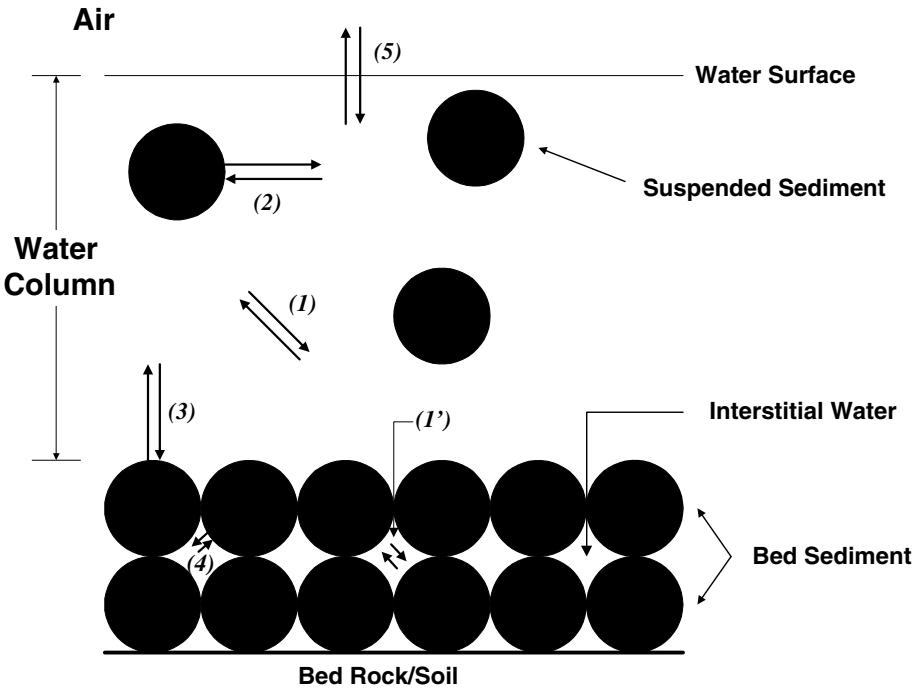

(1) (1') Aqueous complexation reations in the water column and in the interstitial water
(2) Adsorption/desorption between the water column and suspended sediments
(3) Adsorption/desorption reactions between the water column and bed sediments
(4) Adsorption/desorption reactions between the interstitial water and bed sediments
(5) Volatilization reactions between the water column and atmosphere

Figure 1.1. Schematic plot of chemical reactions taken into account in the transport module.

In developing this model, we have assumed (1) flow fields are not influenced by sediment

or contaminant distributions and (2) sediment distributions are not affected by contaminant distributions. The first assumption lets our model compute flow and transport module sequentially, which as a result demands much less computer time than that accounting for strong coupling between flow and transport modules due to density effect [Cheng and Yeh, 1998]. The second assumption allows us to calculate sediment transport prior to contaminant transport in our numerical approach as will be stated later on. Theoretically, strong coupling [Cheng and Yeh, 1998] must be used to couple chemical reactions with physical transport to provide accurate solutions. This may, however, require many coupling iterations to reach convergence, which might cause unaffordable computer effort for long-term simulation in surface systems where the time-step size is in the order of minute or second. To achieve efficient computations, most reactive contaminant transport models employ operator splitting strategies to decouple solute transport from chemical reactions [Salvage, 1998; Chilakapathi, 1995]. Rather than operator splitting, we use a predictor-corrector scheme to effectively solve reactive contaminant transport without surrendering much accuracy. We also employ the LE approach to deal with transport equations where backward particle tracking is applied in the Lagrangian step and the Galerkin finite element method is implemented in the Eulerian step.

To describe our model in detail in the following, we will first describe the governing equations and the associated initial and boundary conditions in Chapter 2. Then we will state the numerical approaches in Chapter 3, and use an example problems for demonstration in Chapter 4. Finally, we will summarize in Section 5.

Chapter 2. MATHEMATICAL BASIS

In this chapter, we are to give governing equations, initial conditions, and boundary conditions for simulating bay estuary circulation as well as contaminant and sediment transport.

2.1 Flow Equations

The governing equations of 2-D circulation flow in the bay/estuary area can be described by shallow water equations which are derived based on the conservation law of water mass and linear momentum and through the depth-averaging process [Wang and Connor, 1975]. The governing equations of a dynamic wave model, without taking into account Coriolis forces, can be written as follows.

The continuity equation:

$$\frac{\partial \eta}{\partial t} + \frac{\partial uh}{\partial x} + \frac{\partial vh}{\partial y} = S$$

where $\eta = \eta(x,y,t)$ is water surface elevation with respect to mean sea level; h(x,y,t) is water depth [L]; u is the x-velocity [L/T]; v is the y-velocity [L/T]; S represents the external source [L/T]. Here we also define sea bed elevation $Z_0 = -d(x,y)$, where d(x,y) is water depth at mean sea level (Figure 2.1). It is thus obvious that $\eta(x,y,t) = Z_0(x,y) + h(x,y,t)$.

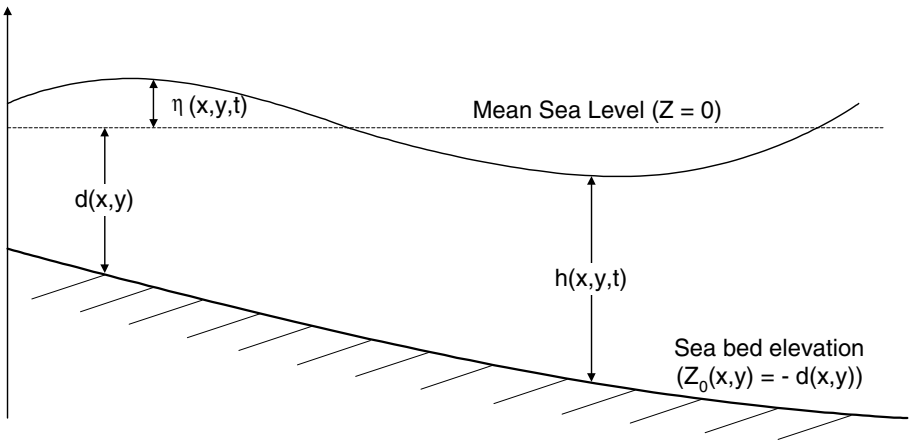

Figure 2.1. Schematic definitions of water stage $\eta(x,y,t)$, water depth h(x,y,t), and sea bed elevation $Z_0(x,y)$.

The momentum equations:

$$\underline{h} = -gh\frac{\partial \eta}{\partial x} + \frac{\partial F_{xx}}{\partial x} + \frac{\partial F_{xy}}{\partial y} + \frac{\tau_x^s}{\rho} - \frac{\tau_x^b}{\rho} + \frac{u^s}{\rho}$$

$$\underline{h} = -gh\frac{\partial \eta}{\partial y} + \frac{\partial F_{xy}}{\partial x} + \frac{\partial F_{yy}}{\partial y} + \frac{\tau_y^s}{\rho} - \frac{\tau_y^b}{\rho} + \frac{v^s}{\rho}$$

where (u^S,v^S) is projected velocity of the external source on the horizontal plane [L/T]; ρ is fluid density [M/L^3]; g is the acceleration due to gravity [L/T^2]; (τ_x^s,τ_y^s) is the surface shear stress per unit horizontal area [M/L/T^2]; (τ_x^b,τ_y^b) is the bottom shear stress per unit horizontal area [M/L/T^2] that can be estimated with Manning's formula [Chow, 1973]; F_{xx} and F_{yx} are the fluxes due to turbulence and diffusion along the x-direction, while F_{xy} and F_{yy} are along the y-direction [L^3/T^2]. F_{xx}, F_{yy}, F_{xy}, and F_{yx} are hypothesized to be proportional to both water depth and the derivatives of velocity, described as follows.

$$F_{xx} = h\epsilon_{xx}\frac{\partial u}{\partial x}$$

$$F_{yy} = h\epsilon_{yy}\frac{\partial v}{\partial y}$$

$$_{y} = F_{yx} = h\epsilon_{xy}\left[\frac{\partial u}{\partial y} + \frac{\partial}{\partial}\right.$$

where ϵ_{xx}, ϵ_{yy}, and ϵ_{xy} are eddy coefficients [L^2/T]. To perform transient simulations, water surface elevation and velocity must be given as the initial conditions. From a physical point of view, three types of boundary conditions may be taken into account, described as follows.

Water surface elevation-specified boundary condition:

This condition is applied when the water surface elevation at a boundary node can be prescribed through the simulation period. Such a condition can be expressed as

$$\eta(x_b,y_b,t) = \eta_b(t)$$

where (x_b, y_b) is the coordinate of a boundary node; $\eta_b(t)$ is a prescribed time-dependent water

surface elevation [L].

Normal flux-specified boundary condition:

This condition is employed when the time-dependent incoming normal flux at a boundary segment can be prescribed. It can be expressed as

$$) = -\mathbf{n}\cdot\mathbf{V}(x_b,y_b,t)\,h(x_b,$$

where **n** is the outward unit vector normal to the boundary segment; **q** is the flow flux vector [L_2/T]; **V** = (u, v); $q_b(t)$ is a time-dependent normal flux [L^2/T].

Impermeable boundary condition:

This condition is applied when the boundary segment is a closed boundary through which no water flow is allowed. It can be expressed as

$$,t) = -\mathbf{n}\cdot\mathbf{V}(x_b,y_b,t)\,h(x$$

2.2. Contaminant and Sediment Transport Equations

The 2-D depth-averaged governing equations of transport in bay/estuary areas can be derived according to the conservation law of material mass and through the averaging process over water depth [Wang and Connor, 1975]. In the model, suspended sediments, dissolved chemicals in the water column, and particulate chemicals on suspended sediments are subject to transport, while bed sediments, particulate chemicals on bed sediments, and dissolved chemicals in the interstitial water are taken as immobile. Their governing equations can be written as follows.

Continuity equations for suspended sediments: $n \in [1,N_s]$

$$\mathbf{q}\,S_n) = \nabla\cdot\left[h\mathbf{K}\cdot\nabla S_n\right] + M$$

where N_s is the number of sediment sizes; h is water depth [L]; t is time [T]; ∇ is the del operator; S_n is depth-averaged sediment concentration of the n-th fraction size in the water column [M/L^3]; **K** is dispersion coefficient tensor [L^2/T]; M_n^s is source of the n-th size fraction sediment [$M/L^2/T$]; R_n is erosion rate of the n-th size fraction sediment [$M/L^2/T$]; D_n is deposition rate of the n-th size

fraction sediment [$M/L^2/T$]. The determination of D_n and R_n can be found in sediment transport texts [Graf, 1984].

Continuity equations for bed sediments: $n \in [1,N_s]$

$$\frac{\partial M_n}{\partial t} = D_n - R_n$$

where M_n is sediment mass per unit horizontal bed area of the n-th size fraction [M/L^2].

Continuity equations for dissolved chemicals in the water column: $i \in [1,N_c]$

$$'hC_i^w + hk_i^{ab}(p_i - \frac{k_i^{af}}{k_i^{ab}}C_i$$

$$) + \sum_{m=1}^{N_{rx}} (a_{mj} - b_{mj})k_m^{rb}h\left[\prod_{j=}^{N}\right.$$

$$\theta_n\Big) C_i^w + \left(\sum_{n=1}^{N_s} \frac{R_n}{\rho_n}\theta_n\right) C$$

where N_c is the number of dissolved chemicals; C_i^w is depth-averaged concentration of the i-th dissolved chemical in the water column [M/L^3]; M_i^{cw} is source of the i-th dissolved chemical [$M/L^2/T$]; λ_i^w is combined first order degradation rate constant of the i-th dissolved chemical [1/T]; k_i^{ab} and k_i^{af} are backward and forward volatilization rate constants, respectively, associated with the i-th dissolved chemical in the atmosphere; p_i is the partial pressure in the atmosphere associated with the i-th dissolved chemical [atm]; k_{ni}^{sb} and k_{ni}^{sf} are backward and forward adsorption rate constants, respectively, associated with the i-th particulate chemical on suspended sediment of the n-th fraction size; C_{ni}^b is mass of particulate chemical on unit mass of bed sediment of the n-th fraction size [M/M]; k_{ni}^{bb} and k_{ni}^{bf} are backward and forward adsorption rate constants, respectively, associated with the i-th particulate chemical on bed sediment of the n-th fraction size; C_{ni}^s is mass of particulate chemical on unit mass of suspended sediment of the n-th fraction size [M/M]; N_{rx} is the number of

aqueous complexation reactions; k_m^{rb} and k_m^{rf} are backward and forward rate constants, respectively, of the m-th aqueous complexation reaction; a_{mj} (b_{mj}) is stoichiometric coefficient of the j-th dissolved chemical in the m-th aqueous complexation reaction when this dissolved chemical appears as a reactant (product) chemical; C_i^{bw} is the concentration of the i-th dissolved chemical in the interstitial water [M/L^3]; θ_n is porosity of the n-th size fraction bed sediment; ρ_n is bulk density of the n-th size bed sediment [M/L^3]; E is exchange coefficient due to diffusion between pore water and column water [L^3/L^2/T], which can be determined experimentally. In Eq. (2.12), the first term on the left side represents the mass increase rate of a dissolved chemical per unit horizontal area, while the second term on the left is the advection transport term. On the right hand side of Eq. (2.12), the first term is the dispersion transport term, the second is external source, the third represents an overall first order decay, the fourth is from the volatilization reactions, the fifth and the sixth are from the reactions of adsorption/desorption between the water column and suspended sediments and between the water column and bed sediments, respectively, the seventh is from the aqueous complexation reactions in the water column, the eighth is the exchange due to diffusion between the water column and the interstitial water, the ninth and tenth are the physical exchanges between the water column and the interstitial water due to deposition and erosion, respectively.

Continuity equations for particulate chemicals on suspended sediments: $n \in [1,N_s]$, $i \in [1,N_c]$

$$C_{ni}^{s})$$

$$)\Big] + M_{ni}^{cs} - \lambda_{ni}^{s} h S_n C_{ni}^{s} - k$$

where M_{ni}^{cs} is source of the i-th particulate chemical on suspended sediment of the n-th fraction size [M/L^2/T]; λ_{ni}^{s} is combined first order degradation rate constant of the i-th particulate chemical on suspended sediment of the n-th fraction size [1/T]. In Eq. (2.13), the first term on the left side represents the rate of mass increase of a suspended particulate chemical per unit horizontal area, while the second term on the left is the advection transport term. On the right hand side, the first

term is the dispersion transport term, the second is external source, the third represents an overall first order decay, the fourth is from the reactions of adsorption/desorption between the water column and suspended sediments, the fifth is due to erosion, and the last is due to deposition.

Continuity equations for particulate chemicals on bed sediments: $n \in [1,N_s]$, $i \in [1,N_c]$

$$- R_n C_{ni}^b) - \lambda_{ni}^b M_n C_{ni}^b - k$$

$$+ k_{ni}^{2f} M_n C_i^{bw} - k_{ni}^{2t}$$

where λ_{ni}^b is combined first order degradation rate constant of the i-th particulate chemical on bed sediment of the n-th fraction size [1/T]. In the above equation, the term on the left side represents the rate of mass increase of a bed particulate chemical per unit horizontal area. The first and second terms on the left of the equation are due to deposition and erosion, respectively, the third represents an overall first order decay, the fourth is from the reactions of adsorption/desorption between the water column and bed sediments, and the fifth and sixth are from the reactions of adsorption/ desorption between the interstitial water and bed sediments.

Continuity equations for dissolved chemicals in the interstitial water: $n \in [1,N_s]$, $i \in [1,N_c]$

$$\frac{D_n}{\rho_n} \theta_n (C_i^w - C_i^{bw}) - \sum_{n=1}^{N_s}$$

$$\iota_{mj} - b_{mj}) k_m^{rb} \left[\prod_{j=1}^{N_c} (C_j^{bw})^{b_m} \right.$$

where k_{ni}^{2b} and k_{ni}^{2f} are backward and forward adsorption rate constants, respectively, associated with the i-th particulate chemical in the interstitial water of bed sediment of the n-th fraction size. In Eq. (2.15), the term on the left side represents the mass increase rate of a dissolved chemical in the interstitial water per unit horizontal area. The first term on the left is due to diffusion between the

water column and the interstitial water, the second is from deposition, the third is from the reactions of adsorption/desorption between the water column and bed sediments, and the last is from the aqueous complexation reactions in the interstitial water.

In performing Eqs. (2.12) through (2.15), the following reactions are considered.

Aqueous complexation reactions in the water column and in the interstitial water: $m \in [1, N_{rx}]$

$$\sum_{i=1}^{N_c} a_{mi} C_i \rightleftarrows \sum_{i=1}^{N_c} b_{mi} C_i$$

$$k_m^{rf} \prod_{i=1}^{N_c} (C_i)^{a_{mi}} - k_m^{rb} \prod_{i=1}^{N_c}$$

where C_i can be either C_i^w or C_i^{bw}; R_a is defined as the rate of the aqueous complexation reaction.

Adsorption/desorption reactions between the water column and suspended sediments: $n \in [1, N_s]$, $i \in [1, N_c]$

$$C_i^w + S_n \rightleftarrows C_{ni}^s + S_n$$

$$_{ad}^{s} = k_{ni}^{sf} S_n C_i^w - k_{ni}^{sb} S_n C$$

where R_{ad}^s is defined as the rate of the adsorption reaction.

Adsorption/desorption reactions between the water column and bed sediments: $n \in [1, N_s]$, $i \in [1, N_c]$

$$C_i^w + M_n \rightleftarrows C_{ni}^b + M_n$$

$$_{i}^{b1} = k_{ni}^{bf} M_n C_i^w - k_{ni}^{bb} M_n$$

where R_{ad}^{b1} is defined as the rate of the adsorption reaction.

Adsorption/desorption reactions between interstitial water and bed sediments: $n \in [1, N_s]$, $i \in [1, N_c]$

$$C_i^{bw} + M_n \rightleftarrows C_{ni}^b + M_n$$

$$^{2} = k_{ni}^{2f} M_n C_i^{bw} - k_{ni}^{2b} M_n$$

where R_{ad}^{b2} is defined as the rate of the adsorption reaction.

Volatilization reactions between the water column and atmosphere: $i \in [1,N_c]$

$$\mathbf{C}_i^{w} \rightleftarrows \mathbf{p}_i$$

$$R_v = k_i^{af} C_i^{w} - k_i^{ab} p_i$$

where R_v is defined as the rate of the volatilization reaction. In Eqs. (2.16), (2.18), (2.20), (2.22), and (2.24) the bold form is used to present the chemical formula of a contaminant or a sediment. To achieve transient simulations, the concentrations of contaminants and sediments must be provided initially. Five types of boundary conditions can be used for mobile substances, i.e., suspended sediments, dissolved chemicals, and particulate chemicals on suspended sediments. They are

Dirichlet boundary condition:

This condition is applied when concentration is given at the boundary. That is,

$$C(x_b,y_b,t) = C_b(t)$$

where C can be the S_n, C_i^{w}, or $S_n C_{ni}^{s}$; $C_b(t)$ is a time-dependent concentration on the boundary [M/L^3].

Variable boundary condition:

This boundary condition is employed when the flow direction would change with time during simulations. Two cases are considered, regarding to the flow direction on the boundary segment.

< Case 1 > Flow is coming in from outside:

$$_b,t) - h\mathbf{K}\cdot\nabla C(x_b,y_b,t)\Big| =$$

< Case 2 > Flow is going out from inside:

$$\cdot\left(-h\mathbf{K}\cdot\nabla C(x_b,y_b,t)\right) =$$

where **n** is the outward unit normal vector of the boundary segment; $C_{in}(t)$ is a time-dependent concentration [M/L^3], which is associated with the incoming flow.

Ocean boundary condition:

This boundary condition is employed when the flow is controlled by tides. Two cases are considered, regarding to the flow direction on the boundary segment.

< Case 1 > Flow is coming in from outside:

$$\left. {}_{b},t) - h\mathbf{K}\cdot\nabla C(x_b,y_b,t)\right| =$$

< Case 2 > Flow is going out from inside:

$$\cdot\left(-h\mathbf{K}\cdot\nabla C(x_b,y_b,t)\right) =$$

where $C_o(t)$, a time-dependent concentration [M/L^3] at the ocean boundary during the incoming flow, will be specified as

$$C_o(t) = C_{max}e^{-ft}$$

where C_{max} is the maximum concentration at the end of the last outgoing flow and f is a flushing decay constant, which is estimated to match the specific flushing rate obtained from field data.

Cauchy boundary condition:

This condition is applied when the total incoming material flux is prescribed as a function of time on a boundary segment. It can be written as

$$_{b},y_b,t) - h\mathbf{K}\cdot\nabla C(x_b,y_b,t$$

where $q_b^c(t)$ is a time-dependent Cauchy flux [M/T/L].

Neumann boundary condition:

This condition is employed when the incoming diffusive material flux can be prescribed on a boundary segment. It is written as

$$\left(-h\mathbf{K}\cdot\nabla C(x_b,y_b,t)\right) = ($$

where $q_b^n(t)$ is a time-dependent Neumann flux [M/T/L].

Chapter 3. NUMERICAL APPROACHES

In this chapter, we are to present the numerical approaches employed to solve the governing equations of flow and transport given in the previous chapter.

3.1. Numerical Approaches for Solving the Flow Equations

A splitting strategy is employed in our approach to solve 2-D depth-averaged shallow water equations. After mathematical manipulation Eqs. (2.1) through (2.3) can be written in matrix form as

$$\frac{\partial E}{\partial t} + A_x \frac{\partial E}{\partial x} + A_y \frac{\partial E}{\partial y} = R \tag{3.1}$$

where

$$E = \{\eta \quad u \quad v\}^T \tag{3.2}$$

$$A_x = \begin{bmatrix} u & h & 0 \\ g & u & 0 \\ 0 & 0 & u \end{bmatrix} \qquad A_y = \begin{bmatrix} v & 0 & h \\ 0 & v & 0 \\ g & 0 & v \end{bmatrix} \tag{3.3}$$

$$R = \begin{Bmatrix} R_1 \\ R_2 \\ R_3 \end{Bmatrix} = \begin{Bmatrix} S + u\dfrac{\partial Z_0}{\partial x} + v\dfrac{\partial Z_0}{\partial y} \\ \dfrac{1}{h}\left[\dfrac{\partial F_{xx}}{\partial x} + \dfrac{\partial F_{yx}}{\partial y}\right] + \dfrac{(u^S - u)S}{h} + \dfrac{\tau_x^s - \tau_x^b}{h\rho} \\ \dfrac{1}{h}\left[\dfrac{\partial F_{xy}}{\partial x} + \dfrac{\partial F_{yy}}{\partial y}\right] + \dfrac{(v^S - v)S}{h} + \dfrac{\tau_y^s - \tau_y^b}{h\rho} \end{Bmatrix} \tag{3.4}$$

Eq. (3.1) can be written as

$$\frac{\partial E}{\partial t} + A_x^d \frac{\partial E}{\partial x} + A_y^d \frac{\partial E}{\partial y} = RJ + RD \tag{3.5}$$

where

$$A_x^d = \begin{bmatrix} u & 0 & 0 \\ 0 & u & 0 \\ 0 & 0 & u \end{bmatrix} \qquad A_y^d = \begin{bmatrix} v & 0 & 0 \\ 0 & v & 0 \\ 0 & 0 & v \end{bmatrix} \tag{3.6}$$

$$RJ = \begin{Bmatrix} RJ_1 \\ RJ_2 \\ RJ_3 \end{Bmatrix} = \begin{Bmatrix} R_1 - h\dfrac{\partial u}{\partial x} - h\dfrac{\partial v}{\partial y} \\ R_2 - RD_2 - g\dfrac{\partial \eta}{\partial x} \\ R_3 - RD_3 - g\dfrac{\partial \eta}{\partial y} \end{Bmatrix} \tag{3.7}$$

$$RD = \begin{Bmatrix} RD_1 \\ RD_2 \\ RD_3 \end{Bmatrix} = \begin{Bmatrix} 0 \\ \dfrac{1}{h}\left[\dfrac{\partial F_{xx}}{\partial x} + \dfrac{\partial F_{yx}}{\partial y}\right] \\ \dfrac{1}{h}\left[\dfrac{\partial F_{xy}}{\partial x} + \dfrac{\partial F_{yy}}{\partial y}\right] \end{Bmatrix} \tag{3.8}$$

With the Lagrangian approach, Eq. (3.5) can be further written as

$$\frac{DE}{Dt} = RJ + RD \tag{3.9}$$

where

$$\frac{DE}{Dt} = \frac{\partial E}{\partial t} + A_x^d \frac{\partial E}{\partial x} + A_y^d \frac{\partial E}{\partial y} \tag{3.10}$$

Eq. (3.9) can be approximated as

$$\frac{E - E^p}{\Delta t} = RJ + RD \tag{3.11}$$

where E^p represents the Lagrangian value of E. If we let $E^{\#}$ be the solution of

$$\frac{DE}{Dt} = RJ \tag{3.12}$$

we have

$$\frac{E^{\#} - E^{p}}{\Delta t} = RJ \tag{3.13}$$

then substituting Eq. (3.13) into Eq. (3.11) yields

$$\frac{E - E^{\#}}{\Delta t} = RD \tag{3.14}$$

With the above splitting strategy, we solve Eq. (3.13) for $E^{\#}$ first and then solve Eq. (3.14) to obtain E based on $E^{\#}$. We also employ the Picard method in the iteration loop that deals with the coupling of Eqs. (3.13) and (3.14) due to non-linearity. Eq. (3.13) is solved by the method of characteristics as detailed in the following.

Method of Characteristics

Eq. (3.13) can be written as

$$\frac{\partial E}{\partial t} + A_x \frac{\partial E}{\partial x} + A_y \frac{\partial E}{\partial y} = RI \tag{3.15}$$

where

$$RI = \begin{Bmatrix} RI_1 \\ RI_2 \\ RI_3 \end{Bmatrix} = \begin{Bmatrix} R_1 \\ R_2 - RD_2 \\ R_3 - RD_3 \end{Bmatrix} \tag{3.16}$$

Let

$$\mathbf{A}\cdot\mathbf{k} = A_x k_x + A_y k_y = \begin{bmatrix} uk_x + vk_y & hk_x & hk_y \\ gk_x & uk_x + vk_y & 0 \\ gk_y & 0 & uk_x + vk_y \end{bmatrix} \tag{3.17}$$

where **k** is the unit vector of the characteristic direction. Then the associated eigenvalues and eigenvectors are

$$\lambda_1 = uk_x + vk_y \qquad e_1 = \{0 \quad k_y \quad -k_x\}^T \tag{3.18}$$

$$\lambda_2 = uk_x + vk_y + \sqrt{gh} \qquad e_2 = \left\{ \frac{\sqrt{gh}}{2} \quad \frac{gk_x}{2} \quad \frac{gk_y}{2} \right\}^T \tag{3.19}$$

$$\lambda_3 = uk_x + vk_y - \sqrt{gh} \qquad e_3 = \left\{ -\frac{\sqrt{gh}}{2} \quad \frac{gk_x}{2} \quad \frac{gk_y}{2} \right\}^T \tag{3.20}$$

We define

$$L = \begin{bmatrix} 0 & \frac{\sqrt{gh}}{2} & -\frac{\sqrt{gh}}{2} \\ k_y & \frac{gk_x}{2} & \frac{gk_x}{2} \\ -k_x & \frac{gk_y}{2} & \frac{gk_y}{2} \end{bmatrix} \tag{3.21}$$

The inverse of matrix L is

$$L^{-1} = \begin{bmatrix} 0 & k_y & -k_x \\ \frac{1}{\sqrt{gh}} & \frac{k_x}{g} & \frac{k_y}{g} \\ -\frac{1}{\sqrt{gh}} & \frac{k_x}{g} & \frac{k_y}{g} \end{bmatrix} \tag{3.22}$$

Define the following transformation

$$\partial W = L^{-1}\partial E = \begin{bmatrix} 0 & k_y & -k_x \\ \frac{1}{\sqrt{gh}} & \frac{k_x}{g} & \frac{k_y}{g} \\ -\frac{1}{\sqrt{gh}} & \frac{k_x}{g} & \frac{k_y}{g} \end{bmatrix} \begin{Bmatrix} \partial\eta \\ \partial u \\ \partial v \end{Bmatrix} \tag{3.23}$$

Multiplying Eq. (3.15) by L^{-1} yields

$$\frac{\partial W}{\partial t} + L^{-1}A_x L\frac{\partial W}{\partial x} + L^{-1}A_y L\frac{\partial W}{\partial y} = L^{-1}RI \tag{3.24}$$

or

$$\frac{\partial W}{\partial t} + \begin{bmatrix} u & \frac{gck_y}{2} & -\frac{gck_y}{2} \\ \frac{hk_y}{c} & u+ck_x & 0 \\ -\frac{hk_y}{c} & 0 & u-ck_x \end{bmatrix} \frac{\partial W}{\partial x} + \begin{bmatrix} v & -\frac{gck_x}{2} & \frac{gck_x}{2} \\ -\frac{hk_x}{c} & v+ck_y & 0 \\ \frac{hk_x}{c} & 0 & v-ck_y \end{bmatrix} \frac{\partial W}{\partial y} = L^{-1}RI \tag{3.25}$$

where

$$c = \sqrt{gh} \tag{3.26}$$

Eq. (3.25) can be further written as follows.

$$\frac{\partial W}{\partial t}+\begin{bmatrix} u & 0 & 0 \\ 0 & u+ck_x & 0 \\ 0 & 0 & u-ck_x \end{bmatrix}\frac{\partial W}{\partial x}+\begin{bmatrix} v & 0 & 0 \\ 0 & v+ck_y & 0 \\ 0 & 0 & v-ck_y \end{bmatrix}\frac{\partial W}{\partial y}$$

$$+\begin{Bmatrix} g\left(k_y\frac{\partial \eta}{\partial x}-k_x\frac{\partial \eta}{\partial y}\right) \\ \frac{h}{c}\left[k_yk_y\frac{\partial u}{\partial x}+k_xk_x\frac{\partial v}{\partial y}-k_xk_y\left(\frac{\partial u}{\partial y}+\frac{\partial v}{\partial x}\right)\right] \\ \frac{-h}{c}\left[k_yk_y\frac{\partial u}{\partial x}+k_xk_x\frac{\partial v}{\partial y}-k_xk_y\left(\frac{\partial u}{\partial y}+\frac{\partial v}{\partial x}\right)\right] \end{Bmatrix} = L^{-1}RI \tag{3.27}$$

Local Diagonalization

As we can see from Eq. (3.27) which displays the characteristic form of the shallow water equations, the last term on the left plays the role of a non-linear source/sink and may increase difficulty in reaching convergence. The method we are taking to handle this is to make the term zero using diagonalization. To achieve local diagonalization, we first define a new L^{-1} which performs the following transformation.

$$\partial W = L^{-1}\partial E = \begin{bmatrix} 0 & k_y^{(1)} & -k_x^{(1)} \\ \frac{1}{c} & \frac{k_x^{(2)}}{g} & \frac{k_y^{(2)}}{g} \\ -\frac{1}{c} & \frac{k_x^{(2)}}{g} & \frac{k_y^{(2)}}{g} \end{bmatrix}\begin{Bmatrix} \partial \eta \\ \partial u \\ \partial v \end{Bmatrix} \tag{3.28}$$

Multiplying Eq. (3.15) by this new L^{-1} will yield

$$\begin{Bmatrix} \frac{DW_1}{Dt} \\ \frac{DW_2}{Dt} \\ \frac{DW_3}{Dt} \end{Bmatrix} + \begin{Bmatrix} S_1 \\ S_2 \\ S_3 \end{Bmatrix} = \begin{Bmatrix} k_y^{(1)} RI_2 - k_x^{(1)} RI_3 \\ \frac{1}{c} RI_1 + \frac{k_x^{(2)}}{g} RI_2 + \frac{k_y^{(2)}}{g} RI_3 \\ \frac{-1}{c} RI_1 + \frac{k_x^{(2)}}{g} RI_2 + \frac{k_y^{(2)}}{g} RI_3 \end{Bmatrix} \tag{3.29}$$

where

$$\frac{DW_1}{Dt} = \frac{\partial W_1}{\partial t} + u\frac{\partial W_1}{\partial x} + v\frac{\partial W_1}{\partial y} \tag{3.30}$$

$$\frac{DW_2}{Dt} = \frac{\partial W_2}{\partial t} + \left(u + ck_x^{(2)}\right)\frac{\partial W_2}{\partial x} + \left(v + ck_y^{(2)}\right)\frac{\partial W_2}{\partial y} \tag{3.31}$$

$$\frac{DW_3}{Dt} = \frac{\partial W_3}{\partial t} + \left(u - ck_x^{(2)}\right)\frac{\partial W_3}{\partial x} + \left(v - ck_y^{(2)}\right)\frac{\partial W_3}{\partial y} \tag{3.32}$$

$$S_1 = g\left(k_y^{(1)}\frac{\partial \eta}{\partial x} - k_x^{(1)}\frac{\partial \eta}{\partial y} \right) \tag{3.33}$$

$$S_2 = \frac{h}{c}\left[k_y^{(2)}k_y^{(2)}\frac{\partial u}{\partial x} + k_x^{(2)}k_x^{(2)}\frac{\partial v}{\partial y} - k_x^{(2)}k_y^{(2)}\left(\frac{\partial u}{\partial y} + \frac{\partial v}{\partial x} \right) \right] \tag{3.34}$$

$$S_3 = \frac{-h}{c}\left[k_y^{(2)}k_y^{(2)}\frac{\partial u}{\partial x} + k_x^{(2)}k_x^{(2)}\frac{\partial v}{\partial y} - k_x^{(2)}k_y^{(2)}\left(\frac{\partial u}{\partial y} + \frac{\partial v}{\partial x} \right) \right] \tag{3.35}$$

It is clear that when we choose ($k_x^{(1)}$, $k_y^{(1)}$) as the direction for the first characteristic and ($k_x^{(2)}$, $k_y^{(2)}$) for the second and third by satisfying the following conditions, we can set S1, S2, and S3 to zero and thus achieve local diagonalization.

$$k_y^{(1)}\frac{\partial \eta}{\partial x} - k_x^{(1)}\frac{\partial \eta}{\partial y} = 0 \tag{3.36}$$

$$k_y^{(2)} k_y^{(2)} \frac{\partial u}{\partial x} + k_x^{(2)} k_x^{(2)} \frac{\partial v}{\partial y} - k_x^{(2)} k_y^{(2)} \left(\frac{\partial u}{\partial y} + \frac{\partial v}{\partial x} \right) = 0 \qquad (3.37)$$

We can always find $k_x^{(1)}$ and $k_y^{(1)}$ to satisfy Eq. (3.36), i.e., wave direction that is tangential to the gradient of water surface elevation can always be found, but we will not be able to find any real solutions of $k_x^{(2)}$ and $k_y^{(2)}$ in solving Eq. (3.37) when the discriminant of the quadratic equation, i.e., $(\partial u/\partial y + \partial v/\partial x)^2 - 4(\partial u/\partial x)(\partial v/\partial y)$, is less than zero. In this case, Hirsh et al. have suggested to select directions which minimize the coupling terms [Hirsh et al, 1987], e.g., S_2 and S_3 in our case here. Therefore, we calculate $k_x^{(2)}$ and $k_y^{(2)}$ through the following equation [Hirsh et al, 1987] if there exists no real $(k_x^{(2)}, k_y^{(2)})$ satisfying Eq. (3.37).

$$\tan\left[\frac{2k_y^{(2)}}{k_x^{(2)}} \right] = \frac{\dfrac{\partial u}{\partial y} + \dfrac{\partial v}{\partial x}}{\dfrac{\partial u}{\partial x} - \dfrac{\partial v}{\partial y}} \qquad (3.38)$$

Backward Tracking Along Characteristics

Eqs. (3.30) through (3.32) can be discretized, in time, as follows.

$$k_y^{(1)} \frac{u^{n+1} - u_1^*}{\Delta t} - k_x^{(1)} \frac{v^{n+1} - v_1^*}{\Delta t} + S_1 = k_y^{(1)} RI_2 - k_x^{(1)} RI_3 \qquad (3.39)$$

$$\frac{1}{c} \frac{\eta^{n+1} - \eta_2^*}{\Delta t} + \frac{k_x^{(2)}}{g} \frac{u^{n+1} - u_2^*}{\Delta t} + \frac{k_y^{(2)}}{g} \frac{v^{n+1} - v_2^*}{\Delta t} + S_2 = \frac{1}{c} RI_1 + \frac{k_x^{(2)}}{g} RI_2 + \frac{k_y^{(2)}}{g} RI_3 \qquad (3.40)$$

$$\frac{-1}{c} \frac{\eta^{n+1} - \eta_3^*}{\Delta t} + \frac{k_x^{(2)}}{g} \frac{u^{n+1} - u_3^*}{\Delta t} + \frac{k_y^{(2)}}{g} \frac{v^{n+1} - v_3^*}{\Delta t} + S_3 = \frac{-1}{c} RI_1 + \frac{k_x^{(2)}}{g} RI_2 + \frac{k_y^{(2)}}{g} RI_3 \qquad (3.41)$$

where u_1^* and v_1^* are determined through backward tracking along the first characteristic, while η_2^*, u_2^*, and v_2^* are associated with the second characteristic and η_3^*, u_3^*, and v_3^* are associated with the third characteristic. Figure 3.1 demonstrates this backward tracking along characteristics. In general, we have

$$u_1^* = a_1 u_{k1}^n + a_2 u_{k2}^n + a_3 u_{k3}^n + a_4 u_{k4}^n \quad (3.42)$$

$$v_1^* = a_1 v_{k1}^n + a_2 v_{k2}^n + a_3 v_{k3}^n + a_4 v_{k4}^n \quad (3.43)$$

$$\eta_2^* = b_1 \eta_{j1}^n + b_2 \eta_{j2}^n + b_3 \eta_{j3}^n + b_4 \eta_{j4}^n \quad (3.44)$$

$$u_2^* = b_1 u_{j1}^n + b_2 u_{j2}^n + b_3 u_{j3}^n + b_4 u_{j4}^n \quad (3.45)$$

$$v_2^* = b_1 v_{j1}^n + b_2 v_{j2}^n + b_3 v_{j3}^n + b_4 v_{j4}^n \quad (3.46)$$

$$\eta_3^* = d_1 \eta_{m1}^n + d_2 \eta_{m2}^n + d_3 \eta_{m3}^n + d_4 \eta_{m4}^n \quad (3.47)$$

$$u_3^* = d_1 u_{m1}^n + d_2 u_{m2}^n + d_3 u_{m3}^n + d_4 u_{m4}^n \quad (3.48)$$

$$v_3^* = d_1 v_{m1}^n + d_2 v_{m2}^n + d_3 v_{m3}^n + d_4 v_{m4}^n \quad (3.49)$$

where η_i^n, u_i^n, v_i^n represent the water surface elevation, x-velocity, and y-velocity at node i (i = k1 through k4, j1 through j4, and m1 through m4) at $t = t^n$ (Figure 3.1); coefficients a_1 through a_4 are interpolation factors at nodes k1 through k4, respectively, while b_1 through b_4 are corresponding to nodes j1 through j4 and d_1 through d_4 are for nodes m1 through m4.

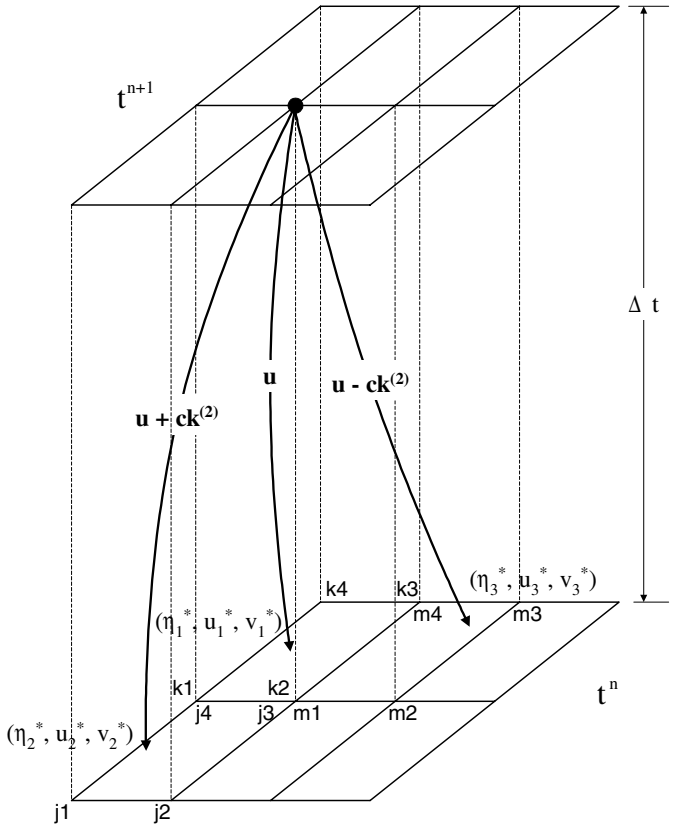

Figure 3.1. Backward tracking along characteristics in solving 2-D hydrodynamic equations.

By using the spatial reachout scheme [Lai, 1987] in backward tracking, u_1^*, v_1^*, η_2^*, u_2^*, v_2^*, η_3^*, u_3^*, and v_3^* can be determined explicitly as described by Eqs. (3.42) through (3.49). Hence, we can solve Eqs. (3.39) through (3.41) for ($\eta^\#$, $u^\#$, $v^\#$) node by node as stated below.

After being multiplied by water depth (i.e., h), Eqs. (3.39) through (3.41) can be written as

$$a_{12}u + a_{13}v = b_1 \tag{3.50}$$

$$a_{21}\eta + a_{22}u + a_{23}v = b_2 \tag{3.51}$$

$$a_{31}\eta + a_{32}u + a_{33}v = b_3 \tag{3.52}$$

where

$$a_{12} = k_y^{(1)}\left[\frac{h}{\Delta t} + h\kappa + S\right] \tag{3.53}$$

$$a_{13} = -k_x^{(1)}\left[\frac{h}{\Delta t} + h\kappa + S\right] \tag{3.54}$$

$$\begin{aligned} b_1 = {} & \frac{hk_y^{(1)}}{\Delta t}u_1^* - \frac{hk_x^{(1)}}{\Delta t}v_1^* - gh\left(k_y^{(1)}\frac{\partial \eta}{\partial x} - k_x^{(1)}\frac{\partial \eta}{\partial y}\right) \\ & + k_y^{(1)}u^S S - k_x^{(1)}v^S S + k_y^{(1)}\frac{\tau_x^s}{\rho} - k_x^{(1)}\frac{\tau_y^s}{\rho} \end{aligned} \tag{3.55}$$

$$a_{21} = \frac{h}{c\Delta t} \tag{3.56}$$

$$a_{22} = k_x^{(2)}\left[\frac{h}{g\Delta t} + \frac{1}{g}(h\kappa + S)\right] - \frac{h}{c}\frac{\partial Z_0}{\partial x} \tag{3.57}$$

$$a_{23} = k_y^{(2)}\left[\frac{h}{g\Delta t} + \frac{1}{g}(h\kappa + S)\right] - \frac{h}{c}\frac{\partial Z_0}{\partial y} \tag{3.58}$$

$$\begin{aligned} b_2 = {} & \frac{h}{c\Delta t}\eta_2^* + \frac{hk_x^{(2)}}{g\Delta t}u_2^* + \frac{hk_y^{(2)}}{g\Delta t}v_2^* + \frac{h}{c}SS + \frac{k_x^{(2)}}{g}u^S S + \frac{k_y^{(2)}}{g}v^S S \\ & + \frac{k_x^{(2)}}{g}\frac{\tau_x^s}{\rho} + \frac{k_y^{(2)}}{g}\frac{\tau_y^s}{\rho} - \frac{h^2}{c}\left[k_y^{(2)}k_y^{(2)}\frac{\partial u}{\partial x} + k_x^{(2)}k_x^{(2)}\frac{\partial v}{\partial y} - k_x^{(2)}k_y^{(2)}\left(\frac{\partial u}{\partial y} + \frac{\partial v}{\partial x}\right)\right] \end{aligned} \tag{3.59}$$

$$a_{31} = \frac{-h}{c\Delta t} \tag{3.60}$$

$$a_{32} = k_x^{(2)}\left[\frac{h}{g\Delta t} + \frac{1}{g}(h\kappa + S)\right] + \frac{h}{c}\frac{\partial Z_0}{\partial x} \tag{3.61}$$

$$a_{33} = k_y^{(2)}\left[\frac{h}{g\Delta t} + \frac{1}{g}(h\kappa + S)\right] + \frac{h}{c}\frac{\partial Z_0}{\partial y} \tag{3.62}$$

$$b_3 = \frac{-h}{c\Delta t}\eta_3^* + \frac{hk_x^{(2)}}{g\Delta t}u_3^* + \frac{hk_y^{(2)}}{g\Delta t}v_3^* - \frac{h}{c}S + \frac{k_x^{(2)}}{g}u\,{}^sS + \frac{k_y^{(2)}}{g}v\,{}^sS + \frac{k_x^{(2)}}{g}\frac{\tau_x^s}{\rho} + \frac{k_y^{(2)}}{g}\frac{\tau_y^s}{\rho} + \frac{h^2}{c}\left[k_y^{(2)}k_y^{(2)}\frac{\partial u}{\partial x} + k_x^{(2)}k_x^{(2)}\frac{\partial v}{\partial y} - k_x^{(2)}k_y^{(2)}\left(\frac{\partial u}{\partial y} + \frac{\partial v}{\partial x}\right)\right] \tag{3.63}$$

With the coefficients, a_{ij}, and the right hand side, b_i, evaluated using the updated iterate, we solve Eqs. (3.50) through (3.52) for $\eta^{\#}$, $u^{\#}$, $v^{\#}$ arithmetically.

Finite Element Approximation

Now, we can solve Eq. (3.14) as follows. Eq. (3.14) can be written in detail as

$$\frac{\eta - \eta^{\#}}{\Delta t} = 0 \tag{3.64}$$

$$\frac{h(u - u^{\#})}{\Delta t} = \left[\frac{\partial F_{xx}}{\partial x} + \frac{\partial F_{yx}}{\partial y}\right] \tag{3.65}$$

$$\frac{h(v - v^{\#})}{\Delta t} = \left[\frac{\partial F_{xy}}{\partial x} + \frac{\partial F_{yy}}{\partial y}\right] \tag{3.66}$$

Eq. (3.64) yields that $\eta = \eta^{\#}$, while Eqs. (3.65) and (3.66), in the form of diffusive transport equations, can be discretized with the Galerkin finite element method as

$$\frac{1}{\Delta t}[QA]\{u\} + [QD^1]\{u\} + [QD^4]\{v\} = \{QR^1\} + \{BQ^1\} \tag{3.67}$$

$$\frac{1}{\Delta t}[QA]\{v\} + [QD^2]\{u\} + [QD^3]\{v\} = \{QR^2\} + \{BQ^2\} \tag{3.68}$$

where [QA] is the mass matrix; [QD1] and [QD3] are stiffness matrices involving only the diagonal terms of eddy diffusion; [QD2] and [QD4] are stiffness matrices involving only the off-diagonal terms of eddy diffusion; {QR1} and {QR2} are load vectors generated from $u^{\#}$ and $v^{\#}$; {BQ1} and {BQ2} are load vectors representing diffusive fluxes through the boundary. They can be written in detail as

$$QA_{i,j} = \sum_{e \in M_e} \int_{R_e} N_\alpha^e \, h \, N_\beta^e \, dR_e \tag{3.69}$$

$$QD_{i,j}^1 = \sum_{e \in M_e} \int_{R_e} \nabla N_\alpha^e \cdot \begin{bmatrix} h\epsilon_{xx} & 0 \\ 0 & h\epsilon_{xy} \end{bmatrix} \cdot \nabla N_\beta^e \, dR_e \tag{3.70}$$

$$QD_{i,j}^2 = \sum_{e \in M_e} \int_{R_e} \nabla N_\alpha^e \cdot \begin{bmatrix} 0 & h\epsilon_{xy} \\ 0 & 0 \end{bmatrix} \cdot \nabla N_\beta^e \, dR_e \tag{3.71}$$

$$QD_{i,j}^3 = \sum_{e \in M_e} \int_{R_e} \nabla N_\alpha^e \cdot \begin{bmatrix} h\epsilon_{xy} & 0 \\ 0 & h\epsilon_{yy} \end{bmatrix} \cdot \nabla N_\beta^e \, dR_e \tag{3.72}$$

$$QD_{i,j}^4 = \sum_{e \in M_e} \int_{R_e} \nabla N_\alpha^e \cdot \begin{bmatrix} 0 & 0 \\ h\epsilon_{xy} & 0 \end{bmatrix} \cdot \nabla N_\beta^e \, dR_e \tag{3.73}$$

$$QR_i^1 = \sum_{e \in M_e} \int_{R_e} N_\alpha^e \, \frac{hu^\#}{\Delta t} \, dR_e \tag{3.74}$$

$$QR_i^2 = \sum_{e \in M_e} \int_{R_e} N_\alpha^e \, \frac{hv^\#}{\Delta t} \, dR_e \tag{3.75}$$

$$BQ_i^1 = \sum_{e \in M_e} \int_{B_e} \left\{ N_\alpha^e \mathbf{n} \cdot \begin{bmatrix} h\epsilon_{xx} & 0 \\ 0 & h\epsilon_{xy} \end{bmatrix} \cdot \nabla u + N_\alpha^e \mathbf{n} \cdot \begin{bmatrix} 0 & 0 \\ h\epsilon_{xy} & 0 \end{bmatrix} \cdot \nabla v \right\} dB_e \tag{3.76}$$

$$BQ_i^2 = \sum_{e \in M_e} \int_{B_e} \left\{ N_\alpha^e \mathbf{n} \cdot \begin{bmatrix} 0 & h\epsilon_{xy} \\ 0 & 0 \end{bmatrix} \cdot \nabla u + N_\alpha^e \mathbf{n} \cdot \begin{bmatrix} h\epsilon_{xy} & 0 \\ 0 & h\epsilon_{yy} \end{bmatrix} \cdot \nabla v \right\} dB_e \tag{3.77}$$

where M_e represents all elements composing the domain of interest; R_e represent the domain of element e; B_e represents the boundary of element e.

Implementation of Boundary Conditions

A boundary segment can be either a closed (impermeable) or an open (flow-through) boundary. To perform numerical simulations, no boundary condition needs to be specified on the closed boundary, while η, u, and v of the approaching flow, with respect to the characteristic ongoing direction, must be given on the open boundary. In solving Eq. (3.13), we implement boundary conditions after using backward tracking to construct Eqs. (3.39) through (3.41) as follows.

For the case of a closed boundary node:

The first characteristic equation is replaced by the following equation, representing a zero normal flux on the boundary.

$$\mathbf{n} \cdot \mathbf{V} = 0 \tag{3.78}$$

Tracking along the impermeable boundary will be used for the second and third characteristics if necessary.

For the case of a open boundary node:

In this case we assume a zero lateral flux on the boundary, and the first characteristic equation is replaced by the following equation.

$$\mathbf{n}_{\perp} \cdot \mathbf{V} = 0 \tag{3.79}$$

where $\mathbf{n}_{\perp}$ is the unit vector parallel to the boundary. Either the second or the third characteristic equation, depending on the propagation direction, will be replaced by the boundary condition specified on the boundary where sub-critical flow is presumed. Only when the propagation direction is inward to the domain of interest, will the replacement be employed. There are two types of boundary conditions considered here.

(1) Given time-dependent normal flux, $q_b(t, x_b, y_b)$:

$$\mathbf{n} \cdot \mathbf{V} = \frac{q_b}{h} \tag{3.80}$$

(2) Given time-dependent water surface elevation, $\eta_b(t, x_b, y_b)$:

$$\eta = \eta_b \tag{3.81}$$

Based on the fact that diffusive fluxes are negligible when compared with advective fluxes in bay/estuary areas, we have assumed zero diffusive fluxes through open boundaries in using the Galerkin finite element method to solve Eq. (3.14). This assumption will lead to both {BQ1} and {BQ2} being zero, which consequently eases the construction of the matrix equations corresponding to Eqs. (3.65) and (3.66).

3.2. Numerical Approaches for Solving the Transport Equations

In bay/estuary areas where advection dominates dispersion, the LE approach [Wood and Baptista, 1992] has been considered an appropriate way to compute material transport because it may greatly reduce many types of numerical errors [Yeh, 1990]. This approach can always provide non-negative computed concentration in solving solute transport equations when linear or bi-linear elements are used for discretization, which is required in computing concentration distributions subject to chemical reactions [Cheng and Yeh, 1998]. Therefore we can write the governing equations of mobile substances in the LE form as follows.

For suspended sediments: $n \in [1, N_s]$

$$h\frac{dS_n}{dt} - \nabla\cdot\left[h\mathbf{K}\cdot\nabla S_n\right] = \left[M_n^s + R_n - D_n\right] - S\,S_n \qquad (3.82)$$

where d/dt represents the material or total derivative with respect to time; S is external fluid source [L/T].

For dissolved chemicals in the water column: $i \in [1, N_c]$

$$
\begin{aligned}
&h\frac{dC_i^{\,w}}{dt} - \nabla\cdot\left[h\mathbf{K}\cdot\nabla C_i^{\,w}\right] \\
&= \sum_{m=1}^{N_{rx}} (a_{mj} - b_{mj}) k_m^{rb} h \left[\prod_{j=1}^{N_c} (C_j^{\,w})^{b_{mj}} - \frac{k_m^{rf}}{k_m^{rb}} \prod_{j=1}^{N_c} (C_j^{\,w})^{a_{mj}}\right] \\
&+ \left[M_i^{cw} + h k_i^{ab} p_i + \sum_{n=1}^{N_s} k_{ni}^{sb} h (S_n C_{ni}^{\,s}) + \sum_{n=1}^{N_s} k_{ni}^{bb} (M_n C_{ni}^{\,b}) + M_i^{crw} + E C_i^{\,bw} + \sum_n \frac{R_n}{\rho_n} \theta_n C_i^{\,bw}\right] \\
&- \left[\lambda_i^w h + h k_i^{af} + \sum_{n=1}^{N_s} S_n h k_{ni}^{sf} + \sum_{n=1}^{N_s} M_n k_{ni}^{bf} + E + \sum_n \frac{D_n}{\rho_n} \theta_n + S\right] C_i^{\,w}
\end{aligned}
\tag{3.83}
$$

For particulate chemicals on suspended sediments: $n \in [1,N_s]$, $i \in [1,N_c]$

$$
\begin{aligned}
&h\frac{d(S_n C_{ni}^{\,s})}{dt} - \nabla\cdot\left[h\mathbf{K}\cdot\nabla(S_n C_{ni}^{\,s})\right] \\
&= \left[M_{ni}^{cs} + k_{ni}^{sf} h S_n C_i^{\,w} + \frac{R_n}{M_n}(M_n C_{ni}^{\,b}) - \frac{D_n}{S_n}(S_n C_{ni}^{\,s})\right] - \left[\lambda_{ni}^{s} h + k_{ni}^{sb} h + S\right](S_n C_{ni}^{\,s})
\end{aligned}
\tag{3.84}
$$

In obtaining Eqs. (3.82) through (3.84), we have substituted the flow continuity equation into Eqs. (2.10), (2.12), and (2.13). The flow continuity equation is the balance equation of water mass and can be written as follows.

$$
\frac{\partial \eta}{\partial t} + \frac{\partial uh}{\partial x} + \frac{\partial vh}{\partial y} = S \tag{3.85}
$$

where $\eta = \eta(x,y,t)$ is water surface elevation; u is the x-velocity [L/T]; v is the y-velocity [L/T]; Here we also define sea bed elevation $Z_0 = -d(x,y)$, where d(x,y) is water depth at mean sea level. It is thus obvious that $\eta(x,y,t) = Z_0(x,y) + h(x,y,t)$ and $\partial\eta/\partial t = \partial h/\partial t$.

In solving Eqs. (3.82) through (3.84), we compute advection in the Lagrangian step where backward particle tracking is applied to determine the Lagrangian concentrations at all global nodes. We then use the Lagrangian concentrations as the initial conditions to solve the transport equations

in the Eulerian step where the Galerkin finite element is applied.

The 2-D transport equations presented above are a set of non-linear partial differential equations where non-linearity is introduced through the deposition/erosion and reaction terms. To perform efficient computation without sacrificing much computational accuracy, we employ a predictor-corrector strategy to solve the governing equations. Here we give a brief description of this strategy. The governing equations of mobile substances (i.e., Eqs. (3.82) through (3.84)) can be expressed in the following form.

$$h\frac{dC}{dt} = L(C) + RHS \tag{3.86}$$

where C can be S_n, C_i^w, or $S_nC_{ni}^s$, L is the dispersion operator, and RHS represents other terms. With the predictor-corrector strategy, we solve Eq. (3.86) with the following two steps. First, we solve

$$h\frac{C^{N+1/2} - C^*}{\Delta\tau} = L(C^{N+1/2}) + (RHS)^N \tag{3.87}$$

where $\Delta\tau$ represents the time period consumed in backward particle tracking [T]; C^* is the Lagrangian concentration [M/L^3]; $(RHS)^N$ represents RHS evaluated at the previous time [$M/L^2/T$]; $C^{N+1/2}$ is the intermediate concentration which we solve for with RHS evaluated at the previous time [M/L^3]. It is noted that $\Delta\tau$ is the real time period for a fictitious particle to travel through advection from a upstream location to the global node being considered, $\Delta\tau$ is location-dependent [Yeh et al, 1992]. This time period is also what we use to calculate dispersion and reactions in the Eulerian step. Second, we solve

$$h\frac{C^{N+1} - C^*}{\Delta\tau} = L(C^{N+1/2}) + (RHS)^{N+1} \tag{3.88}$$

where C^{N+1} is the concentration of the present time [M/L^3]; $(RHS)^{N+1}$ represents RHS evaluated at the present time [$M/L^2/T$]. We can subtract Eq. (3.88) by Eq. (3.87) to yield

$$h\frac{C^{N+1} - C^{N+1/2}}{\Delta\tau} = (RHS)^{N+1} - (RHS)^N \tag{3.89}$$

To save computer effort, it is better to solve Eq. (3.89) than Eq. (3.88) because Eq. (3.89) does not involve the dispersion operator and thus can be solved node by node. To summarize, we first solve Eq. (30) for $C^{N+1/2}$ in the predictor step and perform the corrector step by solving Eq. (3.89) to obtain C^{N+1}.

We employ an adaptive explicit-implicit scheme to avoid negative numerical results in solving Eq. (3.87). With this scheme, the following equation is actually solved when $(RHS)^N$ is negative.

$$h\frac{C^{N+1/2}-C^{*}}{\Delta\tau}-\frac{(RHS)^{N}}{C^{N}}C^{N+1/2} = L(C^{N+1/2}) \tag{3.90}$$

Consequently, we are solving the following correction equation in the corrector step.

$$h\frac{C^{N+1}-C^{N+1/2}}{\Delta\tau} = (RHS)^{N+1}-\frac{(RHS)^{N}}{C^{N}}C^{N+1/2} \tag{3.91}$$

With the Galerkin finite element approximation, Eq. (3.87) can be discretized as follows.

$$\left(\frac{[QA]}{\Delta\tau}+w[QD]\right)\{C\} = \frac{[QA]}{\Delta\tau}\{C^{*}\}+\{QR\}+(1-w)[QD]\{C^{N}\}+\{QB\} \tag{3.92}$$

where w is time weighting factor; [QA] is the mass matrix, [QD] is the stiffness matrix due to dispersion; {QR} is the load vector contributed from $(RHS)^N$; {QB} is the load vector accounting for dispersive boundary fluxes. The associated element matrices and column vectors are defined as follows.

$$[QA]^{e} = \int_{R_e} N_i h N_j \, dR_e \tag{3.93}$$

$$[QD]^{e} = \int_{R_e} \nabla N_i \cdot \left(h\mathbf{K}\cdot\nabla N_j\right) dR_e \tag{3.94}$$

$$\{QR\}^{e} = \int_{R_e} N_i (RHS)^{N} \, dR_e \tag{3.95}$$

$$\{QB\}^e = -\int_{B_e} \left(-h\mathbf{K}\cdot\nabla C\right) dB_e \tag{3.96}$$

where R_e and B_e represent the domain and the boundary, respectively, of element e; N_i and N_j are element shape functions at the i-th and j-th element nodes, respectively, of element e. It is noted that $\{QR\}^e$ must be evaluated using nodal quadratures such that Eqs. (3.87) and (3.89) are solved consistently. Also, boundary conditions for mobile substances are implemented in this predictor step. If $(RHS)^N$ is negative, Eq. (3.90) is solved in the predictor step. It can be discretized as

$$\left(\frac{[QA]}{\Delta\tau} + w\,[QD] - [QC] \right) \{C\} = \frac{[QA]}{\Delta\tau}\{C^*\} + (1-w)\,[QD]\{C^N\} + \{QB\} \tag{3.97}$$

where [QC] is the stiffness matrix due to source/sink terms evaluated at the previous time. The element matrix of [QC] is defined as

$$[QC]^e = \int_{R_e} N_i \frac{(RHS)^N}{C^N} N_j \, dR_e \tag{3.98}$$

where $[QC]^e$ must be lumped to maintain consistency in solving Eqs. (3.90) and (3.91).

With the predictor-corrector strategy, we solve the entire transport system by completing the following steps.

Step 1 We determine the Lagrangian concentrations for suspended sediments, dissolved chemicals in the water column, and particulate chemicals on suspend sediments, respectively.

Step 2 We solve Eqs. (3.82) and (2.11) for S_n and M_n, respectively. In this step, we first solve Eq. (3.82) with all source/sink terms evaluated at the previous time to obtain the intermediate value for suspended sediments. Then we prepare the corrector form of Eq. (3.82) as follows.

$$
\begin{aligned}
& h\frac{(S_n)^{N+1}-(S_n)^{N+1/2}}{\Delta\tau} \\
&\quad = (RHS_n^{\,s})^{N+1}-(RHS_n^{\,s})^{N} \qquad \left(\text{if } (RHS_n^{\,s})^{N}\geq 0\right) \\
&\quad = (RHS_n^{\,s})^{N+1}-\frac{(RHS_n^{\,s})^{N}}{(S_n)^{N}}(S_n)^{N+1/2} \qquad \left(\text{if } (RHS_n^{\,s})^{N}<0\right)
\end{aligned}
\tag{3.99}
$$

where

$$
(RHS_n^{\,s}) = \left[M_n^{\,s}+R_n-D_n\right]-S\,S_n \tag{3.100}
$$

At last, we solve Eqs. (3.99) and (2) node by node with the Picard method to obtain the solutions for suspended and bed sediments.

Step 3 We solve Eqs. (3.83), (3.84), (2.14), and (2.15) for $C_i^{\,w}$, $S_nC_{ni}^{\,s}$, $M_nC_{ni}^{\,b}$, and $C_{ni}^{\,bw}$, respectively. In this step, we solve Eqs. (3.83) and (3.84) with all source/sink terms evaluated at the previous time to determine the intermediate concentrations of $C_i^{\,w}$ and $S_nC_{ni}^{\,s}$, followed by preparing the corrector form of Eqs. (3.83) and (3.84) as given below.

For dissolved chemicals:

$$
\begin{aligned}
& h\frac{(C_i^{\,w})^{N+1}-(C_i^{\,w})^{N+1/2}}{\Delta\tau} \\
&\quad = (RHS_i^{\,c})^{N+1}-(RHS_i^{\,c})^{N} \qquad \left(\text{if } (RHS_i^{\,c})^{N}\geq 0\right) \\
&\quad = (RHS_i^{\,c})^{N+1}-\frac{(RHS_i^{\,c})^{N}}{(C_i^{\,w})^{N}}(C_i^{\,w})^{N+1/2} \qquad \left(\text{if } (RHS_i^{\,c})^{N}<0\right)
\end{aligned}
\tag{3.101}
$$

where

$$(RHS_i^c) = \sum_{m=1}^{N_{rx}} (a_{mj} - b_{mj}) k_m^{rb} h \left[\prod_{j=1}^{N_c} (C_j^w)^{b_{mj}} - \frac{k_m^{rf}}{k_m^{rb}} \prod_{j=1}^{N_c} (C_j^w)^{a_{mj}} \right]$$

$$+ \left[M_i^{cw} + h k_i^{ab} p_i + \sum_{n=1}^{N_s} k_{ni}^{sb} h (S_n C_{ni}^s) + \sum_{n=1}^{N_s} k_{ni}^{bb} (M_n C_{ni}^b) + M_i^{crw} + E C_i^{bw} + \sum_{n=1}^{N_s} \frac{R_n}{\rho_n} \theta_n C_i^{bw} \right] \quad (3.102)$$

$$- \left[\lambda_i^w h + h k_i^{af} + \sum_{n=1}^{N_s} S_n h k_{ni}^{sf} + \sum_{n=1}^{N_s} M_n k_{ni}^{bf} + S + E + \sum_{n=1}^{N_s} \frac{D_n}{\rho_n} \theta_n \right] C_i^w$$

For particulate chemicals on suspended sediments:

$$h \frac{(S_n C_{ni}^s)^{N+1} - (S_n C_{ni}^s)^{N+1/2}}{\Delta \tau}$$

$$= (RHS_{ni}^s)^{N+1} - (RHS_{ni}^s)^N \qquad \left(\text{if } (RHS_{ni}^s)^N \geq 0 \right) \quad (3.103)$$

$$= (RHS_{ni}^s)^{N+1} - \frac{(RHS_{ni}^s)^N}{(C_{ni}^s)^N} (C_{ni}^s)^{N+1/2} \qquad \left(\text{if } (RHS_{ni}^s)^N < 0 \right)$$

where

$$(RHS_{ni}^s) = \left[M_{ni}^{cs} + k_{ni}^{sf} h S_n C_i^w + \frac{R_n}{M_n} (M_n C_{ni}^b) - \frac{D_n}{S_n} (S_n C_{ni}^s) \right] \quad (3.104)$$

$$- \left[\lambda_{ni}^s h + k_{ni}^{sb} h + S \right] (S_n C_{ni}^s)$$

Eqs. (2.14) and (2.15) can be written as follows.

For particulate chemicals on bed sediments:

$$\frac{(M_n C_{ni}^b)^{N+1} - (M_n C_{ni}^b)^N}{\Delta t} = (RHS_{ni}^b)^{N+1} \quad (3.105)$$

where

$$(RHS_{ni}^{b}) = \left[\frac{D_n}{S_n}(S_n C_{ni}^{s}) - \frac{R_n}{M_n}(M_n C_{ni}^{b}) + k_{ni}^{bf} M_n C_i^{w} + k_{ni}^{2f} M_n C_i^{bw}\right] - \left[\lambda_{ni}^{b} + k_{ni}^{bb} + k_{ni}^{2b}\right](M_n C_{ni}^{b}) \quad (3.106)$$

For dissolved chemicals in interstitial water of bed sediments:

$$\frac{\left(\sum_{n=1}^{N_s} \frac{\theta_n}{\rho_n} M_n C_i^{bw}\right)^{N+1} - \left(\sum_{n=1}^{N_s} \frac{\theta_n}{\rho_n} M_n C_i^{bw}\right)^{N}}{\Delta t} = (RHS_i^{bw})^{N+1} \quad (3.107)$$

where

$$(RHS_i^{bw}) = \sum_{n=1}^{N_s} k_{ni}^{2b} M_n C_{ni}^{b} - \left(E + \sum_{n=1}^{N_s} \frac{D_n}{\rho_n}\theta_n + \sum_{n=1}^{N_s} k_{ni}^{2f} M_n\right) C_i^{bw} + \left(E + \sum_{n=1}^{N_s} \frac{D_n}{\rho_n}\theta_n C_i^{w}\right) + \left(\sum_{n=1}^{N_s} \frac{\theta_n}{\rho_n} M_n\right) \sum_{m=1}^{N_{rx}} (a_{mj} - b_{mj}) k_m^{rb} \left[\prod_{j=1}^{N_c} (C_j^{bw})^{b_{mj}} - \frac{k_m^{rf}}{k_m^{rb}} \prod_{j=1}^{N_c} (C_j^{bw})^{a_{mj}}\right] \quad (3.108)$$

Finally, we solve Eqs. (3.101), (3.103), (3.105), and (3.107) node by node with the Newton-Raphson method. When the chemistry system is highly non-linear, we may have Jacobian entries vary many order of magnitude, which will introduce numerical difficulty in reaching correct solutions [Press et al., 1992]. To overcome this, we incorporate full pivoting with a direct solver to correctly solve the Jacobian matrix equation resulting from the Newton-Raphson method [Yeh et al., 1998]. The details of the residual equations and the associated Jacobian matrix for the Newton-Raphson method are given below.

To achieve Step 3 above, the following residual equations are constructed, where we have $i \in [1, N_c]$ and $n \in [1, N_s]$ for the ranges of subscripts i and n.

For dissolved chemicals in the water column:

$$
\begin{aligned}
&(RES_i^{\,c}) \\
&= h\left[(C_i^{\,w})^{N+1} - (C_i^{\,w})^{N+1/2}\right] - \Delta\tau\left[(RHS_i^{\,c})^{N+1} - (RHS_i^{\,c})^{N}\right] \quad \left(\text{if } (RHS_i^{\,c})^{N} \geq 0\right) \\
&= h\left[(C_i^{\,w})^{N+1} - (C_i^{\,w})^{N+1/2}\right] - \Delta\tau\left[(RHS_i^{\,c})^{N+1} - \frac{(RHS_i^{\,c})^{N}}{(C_i^{\,w})^{N}}(C_i^{\,w})^{N+1/2}\right] \quad \left(\text{if } (RHS_i^{\,c})^{N} < 0\right)
\end{aligned}
\tag{3.109}
$$

For particulate chemicals on suspended sediments:

$$
\begin{aligned}
&(RES_{ni}^{\,s}) \\
&= h\left[(S_n C_{ni}^{\,s})^{N+1} - (S_n C_{ni}^{\,s})^{N+1/2}\right] - \Delta\tau\left[(RHS_{ni}^{\,s})^{N+1} - (RHS_{ni}^{\,s})^{N}\right] \\
&\qquad\qquad \left(\text{if } (RHS_{ni}^{\,s})^{N} \geq 0\right) \\
&= h\left[(S_n C_{ni}^{\,s})^{N+1} - (S_n C_{ni}^{\,s})^{N+1/2}\right] - \Delta\tau\left[(RHS_{ni}^{\,s})^{N+1} - \frac{(RHS_{ni}^{\,s})^{N}}{(S_n C_{ni}^{\,s})^{N}}(S_n C_{ni}^{\,s})^{N+1/2}\right] \\
&\qquad\qquad \left(\text{if } (RHS_{ni}^{\,s})^{N} < 0\right)
\end{aligned}
\tag{3.110}
$$

For particulate chemicals on bed sediments:

$$
(RES_{ni}^{\,b}) = (M_n C_{ni}^{\,b})^{N+1} - (M_n C_{ni}^{\,b})^{N} - \Delta t\,(RHS_{ni}^{\,b})^{N+1} \tag{3.111}
$$

For dissolved chemicals in the interstitial water of the bed sediments:

$$
(RES_i^{\,bw}) = \left(\sum_{n=1}^{N_s} \frac{\theta_n}{\rho_n} M_n C_i^{\,bw}\right)^{N+1} - \left(\sum_{n=1}^{N_s} \frac{\theta_n}{\rho_n} M_n C_i^{\,bw}\right)^{N} - \Delta t\,(RHS_i^{\,bw})^{N+1} \tag{3.112}
$$

The entries of the associated Jacobian matrix are evaluated as follows.

For dissolved chemicals in the water column:

$$\frac{(RES_i^c)}{(C_1^w)^{N+1}} = \delta_{il}h + \delta_{il}\Delta\tau\left(\lambda_i^w h + SS + R + hk_i^{af} + \sum_{n=1}^{N_s} S_n h k_{ni}^{sf} + \sum_{n=1}^{N_s} M_n k_{ni}^{bf} + E + \sum_{n=1}^{N_s}\frac{D_n}{\rho_n}\theta_n\right) \tag{3.113}$$

$$\Delta\tau\left[\sum_{m=1}^{N_{rx}}(a_{mi}-b_{mi})h\left(k_m^{rb}b_{ml}(C_1^w)^{b_{ml}-1}\prod_{j=1,j\neq 1}^{N_c}(C_j^w)^{b_{mj}} - k_m^{rf}a_{ml}(C_1^w)^{a_{ml}-1}\prod_{j=1,j\neq 1}^{N_c}(C_j^w)^{a_{mj}}\right)\right]$$

$$\frac{\partial(RES_i^c)}{\partial(S_n C_{nl}^s)^{N+1}} = -\delta_{il}\Delta\tau\, k_{ni}^{sb} h \tag{3.114}$$

$$\frac{\partial(RES_i^c)}{\partial(M_n C_{nl}^b)^{N+1}} = -\delta_{il}\Delta\tau\, k_{ni}^{bb} \tag{3.115}$$

$$\frac{\partial(RES_i^c)}{\partial(C_1^{bw})^{N+1}} = -\delta_{il}\Delta\tau\left(E + \sum_{n=1}^{N_s}\frac{\theta_n}{\rho_n}R_n\right) \tag{3.116}$$

For particulate chemicals on suspended sediments:

$$\frac{\partial(RES_{ni}^s)}{\partial(C_1^w)^{N+1}} = -\delta_{il}\Delta\tau\, k_{ni}^{sf} S_n h \tag{3.117}$$

$$\frac{\partial(RES_{ni}^s)}{\partial(S_n C_{nl}^s)^{N+1}} = \delta_{il}h + \delta_{il}\Delta\tau\frac{D_n}{S_n} + \delta_{il}\Delta\tau\left(\lambda_{ni}^s h + k_{ni}^{sb}h + SS + R\right) \tag{3.118}$$

$$\frac{\partial(RES_{ni}^s)}{\partial(M_n C_{nl}^b)^{N+1}} = -\delta_{il}\Delta\tau\frac{R_n}{M_n} \tag{3.119}$$

$$\frac{\partial(RES_{ni}^s)}{\partial(C_1^{bw})^{N+1}} = 0 \tag{3.120}$$

For particulate chemicals on bed sediments:

$$\frac{\partial(RES_{ni}^{\ b})}{\partial(C_1^{\ w})^{N+1}} = -\delta_{il}\,\Delta t\,k_{ni}^{\ bf}M_n \tag{3.121}$$

$$\frac{\partial(RES_{ni}^{\ b})}{\partial(S_n C_{nl}^{\ s})^{N+1}} = -\delta_{il}\,\Delta t\,\frac{D_n}{S_n} \tag{3.122}$$

$$\frac{\partial(RES_{ni}^{\ b})}{\partial(M_n C_{nl}^{\ b})^{N+1}} = \delta_{il} + \delta_{il}\,\Delta t\,\frac{R_n}{M_n} + \delta_{il}\,\Delta t\left(\lambda_{ni}^{\ b} + k_{ni}^{\ bb} + k_{ni}^{\ 2b}\right) \tag{3.123}$$

$$\frac{\partial(RES_{ni}^{\ b})}{\partial(C_1^{\ bw})^{N+1}} = -\delta_{il}\,\Delta t\,k_{ni}^{\ 2f}M_n \tag{3.124}$$

For dissolved chemicals in the interstitial water of the bed sediments:

$$\frac{\partial(RES_i^{\ bw})}{\partial(C_1^{\ w})^{N+1}} = -\delta_{il}\,\Delta t\left(E + \sum_{n=1}^{N_s}\frac{D_n}{\rho_n}\theta_n\right) \tag{3.125}$$

$$\frac{\partial(RES_i^{\ bw})}{\partial(S_n C_{nl}^{\ s})^{N+1}} = 0 \tag{3.126}$$

$$\frac{\partial(RES_i^{\ bw})}{\partial(M_n C_{nl}^{\ b})^{N+1}} = -\delta_{il}\,\Delta t\,k_{ni}^{\ 2b} \tag{3.127}$$

$$\begin{aligned}\frac{\partial(RES_i^{\ bw})}{\partial(C_1^{\ bw})^{N+1}} = {} & \delta_{il}\left(\sum_{n=1}^{N_s}\frac{\theta_n}{\rho_n}M_n\right) + \delta_{il}\,\Delta t\left(E + \sum_{n=1}^{N_s}\frac{D_n}{\rho_n}\theta_n + \sum_{n=1}^{N_s}k_{ni}^{\ 2f}M_n\right) - \Delta t\left(\sum_{n=1}^{N_s}\frac{\theta_n}{\rho_n}M_n\right) \\ & \left[\sum_{m=1}^{N_{rx}}(a_{mi}-b_{mi})\left(k_m^{\ rb}b_{ml}(C_1^{\ bw})^{b_{ml}-1}\prod_{j=1,j\neq 1}^{N_c}(C_j^{\ bw})^{b_{mj}} - k_m^{\ rf}a_{ml}(C_1^{\ bw})^{a_{ml}-1}\prod_{j=1,j\neq 1}^{N_c}(C_j^{\ bw})^{a_{mj}}\right)\right]\end{aligned} \tag{3.128}$$

3.3 Estimation of Deposition and Erosion

We estimate the deposition and erosion rates by using the following equations.

< Case 1 > Cohesive sediments: (e.g., silt and clay)

$$D_n = V_{sn} S_n \left[1 - \frac{\tau_b}{\tau_{cDn}} \right] \tag{3.129}$$

$$R_n = E_n \left[\frac{\tau_b}{\tau_{cRn}} - 1 \right] \tag{3.130}$$

where V_{sn} is the settling velocity of the n-th size fraction sediment [L/T]; τ_b is the bottom shear stress or the bottom friction stress [M/L/T^2]; τ_{cDn} is the critical shear stress for the deposition of the n-th size fraction sediment [M/L/T^2]; τ_{cRn} is the critical shear stress for the erosion of the n-th size fraction sediment [M/L/T^2]; E_n is the erodibility of the n-th size fraction sediment [M/L^2]. In the computer code, V_{sn}, τ_{cDn}, τ_{cRn}, and E_n are input parameters, while τ_b is computed in the flow module.

< Case 2 > Non-cohesive sediments: (e.g., sand)

$$D_n = \frac{G_{sAn} - G_{sn}}{\Delta L} \tag{3.131}$$

$$R_n = \frac{G_{sn} - G_{sAn}}{\Delta L} \tag{3.132}$$

where G_{sAn} is the actual load rate of the n-th size fraction sediment per unit width at a upstream location [M/L/T]; G_{sn} is the maximum load rate (capacity) of the n-th size fraction sediment per unit width at a downstream location [M/L/T]; ΔL is the distance between the upstream and the downstream locations. In the computer code, ΔL can be determined based on the coordinates, while G_{sAn} and G_{sn} are computed based on the following equations.

$$G_{sAn} = S_n * u * r \tag{3.133}$$

$$G_{sn} = 10 \frac{\rho^2 u r S (\tau_b - \tau_{crn})}{g d_n (\rho_{sn} - \rho)^2} \tag{3.134}$$

where ρ is the fluid density [M/L^3]; ρ_{sn} is the density of the n-th size fraction sediment [M/L^3]; u is

channel flow velocity [L/T]; r is hydraulic radius [L]; S the friction slope, d_n is the median diameter of the n-th size fraction sediment particle [L]; g is gravity [L/T^2]; τ_{crn} is the critical bottom shear stress of the n-th size fraction sediment at which sediment movement begins [$M/L/T^2$]. Among these parameters, ρ, ρ_{sn}, d_n, and τ_{crn} are input by users, while u, r, and S are estimated in the flow module.

Note: Eq. (3.134) is from "Hydraulics of Sediment Transport" by Walter Hans Graf (1984), Water Resources Publication, Eq. (7.14) on page 128. Eqs. (3.129) through (3.132) can be found from "CHNTRN: A Channel Transport Model for Simulating Sediment and Chemical Distribution in a Stream/River Network" by Yeh (1983), ORNL-5882 Report, Eqs. (29) and (30) on page 12.

Chapter 4. EXAMPLES

4.1 Example 1 --- 1-D Standing Wave Problem

We used a one-dimensional standing wave example [Wang and Connor, 1975] to verify our approach. This problem was governed by the wave equations as follows.

$$\frac{\partial^2 u}{\partial t^2} = c^2 \frac{\partial^2 u}{\partial x^2}$$

$$\frac{\partial^2 \eta}{\partial t^2} = c^2 \frac{\partial^2 \eta}{\partial x^2}$$

$$c^2 = gh$$

where u is the velocity along the flow direction [L/T]; c is the wave speed [L/T]; h is water depth [L]; η is the deviation of water surface elevation [L]; g is gravity [L/T^2]. The domain of interest was 200 m long in the x-direction and 50 m wide in the y-direction. It was discretized with 20 elements: 10 m $\times$ 50 m each. The mean water depth was 4 meters. The boundary end at X = 200 m was closed, while the other one at X = 0 m was open and the water surface elevation fluctuated up and down according to

$$\eta|_{X=0m} = \eta_0 \sin\frac{2\pi t}{200}$$

where η_0 represents the amplitude of the sinusoidal surface deviation applied to the boundary X = 0 m. Therefore, we set u = 0 m/s at X = 200 m to settle the boundary condition for achieving the simulation. The analytical solution of this linear wave problem is as follows.

$$\frac{\pi}{\sqrt{c}} \sin\left[\frac{2\pi}{\sqrt{c}}\left(\frac{x}{200} - 1\right)\right]$$

$$\cos\left[\frac{2\pi}{\sqrt{c}}\left(\frac{x}{200} - 1\right)\right]$$

Given initial condition at t = 50 s according to Eqs. (4.5) and (4.6), we first chose $\eta_0 = 0.1$ in this example to perform a simulation of 400 seconds, i.e., from t = 50 s to 450 s. We found the numerical solution is essentially unchanged for time step size less than 2.5 seconds and element number more than 20, which means we have obtained a convergent solution to the hydrodynamic flow equations (i.e., Eqs. (2.1) through (2.3)). The differences between the numerical result and the analytical solution of Eqs. (4.1) through (4.3) ((Figures 4.1(a) and 4.2(a)) was caused by the nonlinear terms accounted for in Eq. (2.2). To prove this, we reduced η_0 to 0.05 and 0.025 to diminish the nonlinear effect. Figures 4.1 and 4.2 compare the numerical results and the analytical solutions of the deviation of water surface elevation at x = 100 m and 200 m, respectively for η_0 = 0.1, 0.05, and 0.025. It is obvious that the difference decreases with the reduction of η_0. When η_0 is reduced to 0.025, we have the computational result and the analytical solution match precisely (Figures 3(c) and 4(c)). An excellent agreement was also obtained in comparison of the velocity at time = 100 s, 200 s, 300 s, and 400 s for the case of $\eta_0 = 0.025$ (Figure 4.3). It is thus verified that our MOC numerical model can solve standing wave problems accurately.

(a)

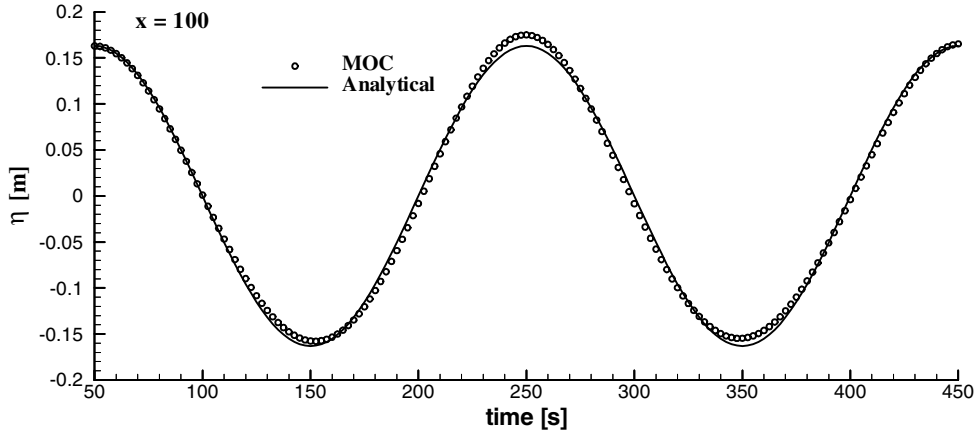

(b)

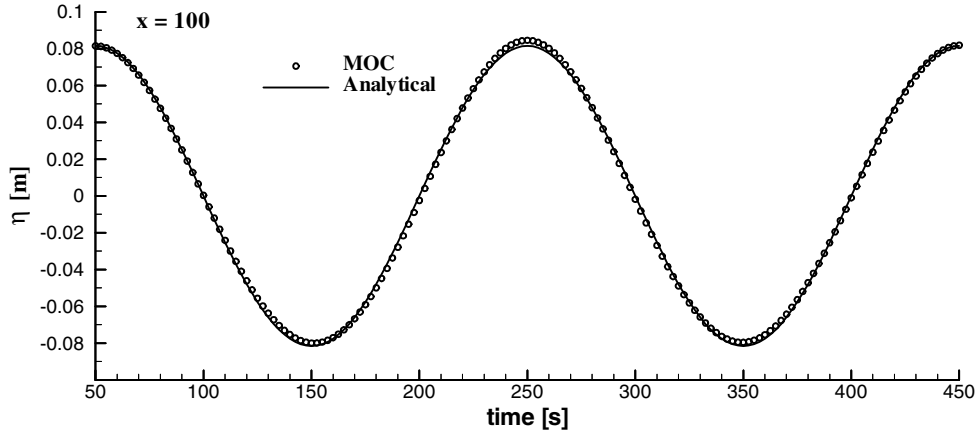

(c)

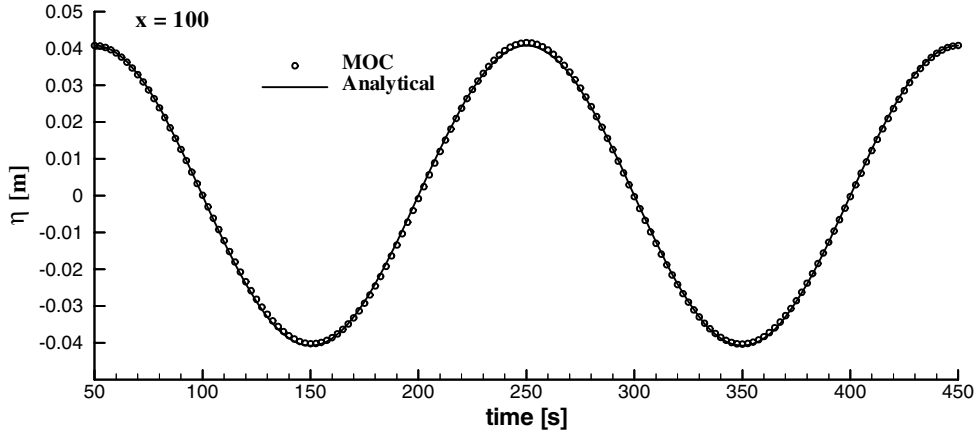

Figure 4.1. The deviation of water surface elevation at x = 100 for (a) η_0 = 0.1 m, (b) η_0 = 0.05 m, and (c) η_0 = 0.025 m during the simulation of Example 1.

(a)

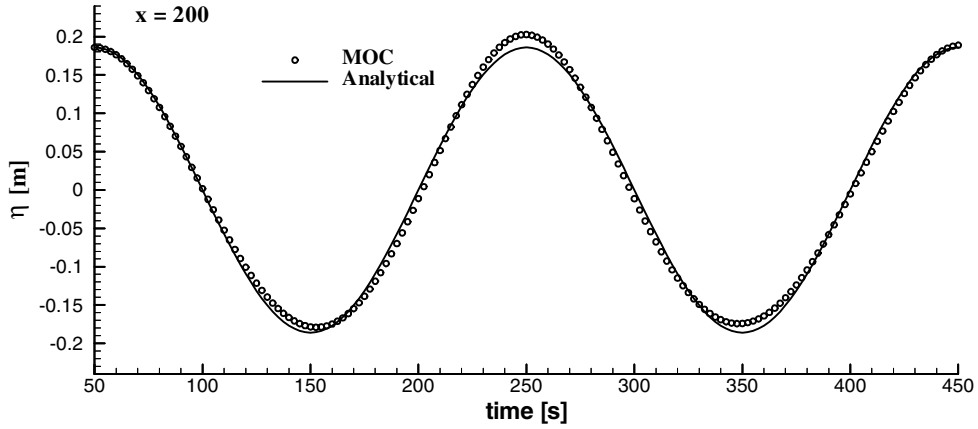

(b)

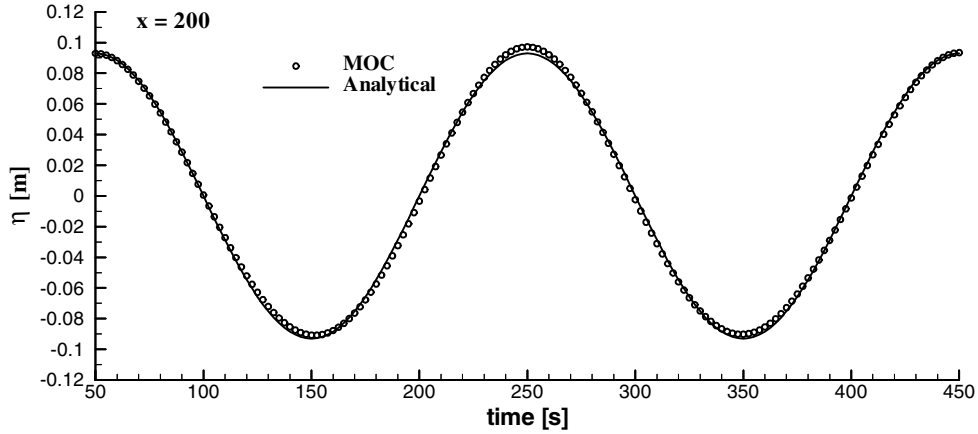

(c)

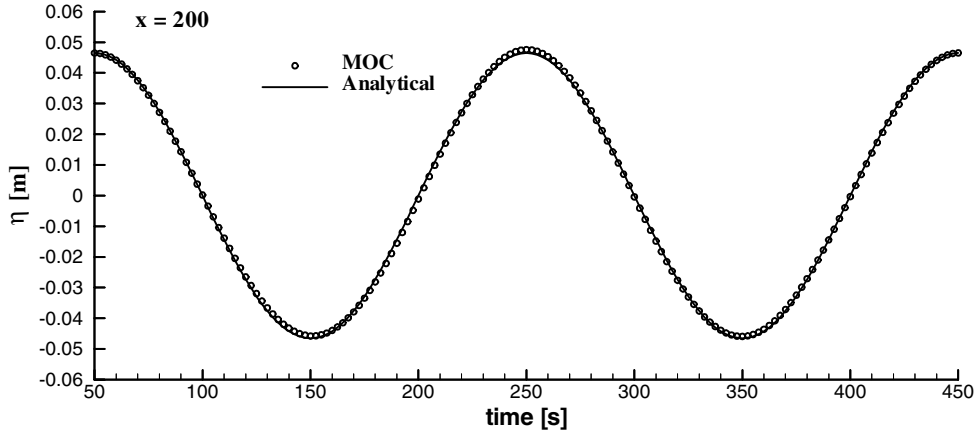

Figure 4.2. The deviation of water surface elevation at x = 200 for (a) η_0 = 0.1 m, (b) η_0 = 0.05 m, and (c) η_0 = 0.025 m during the simulation of Example 1.

(a)

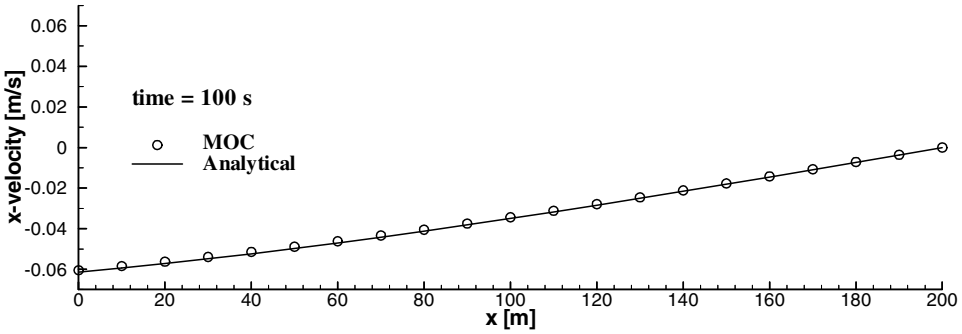

(b)

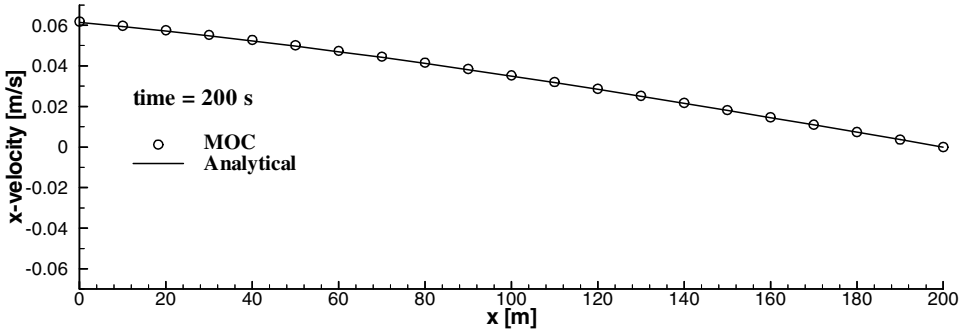

(c)

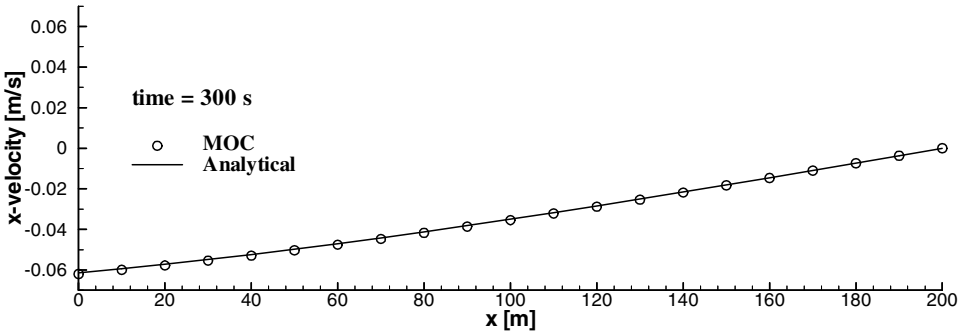

(d)

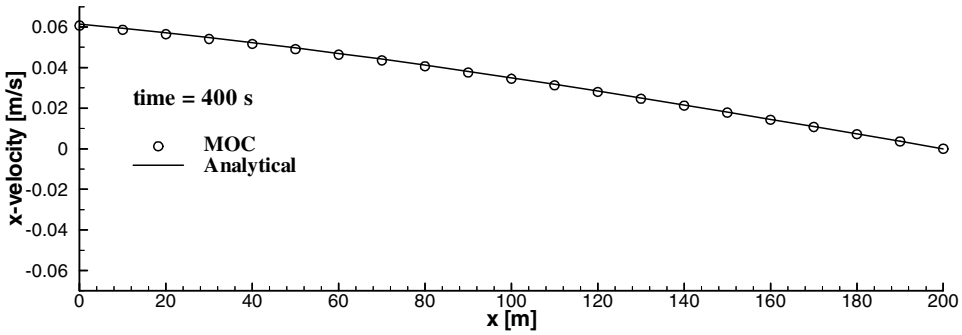

Figure 4.3. Comparison of analytical and computed x-velocity at time = (a) 100 s, (b) 200 s, (c) 300 s, and (d) 400 s for $\eta_0 = 0.025$ m in Example 1.

4.2 Example 2 --- Salem Harbor Problem

In this example, we used the model to simulate hypothetical contaminant and sediment transport at Salem harbor where the mean sea level water depth varies from 1.4 m to 8.4 m [Yeh and Kalasinsky, 1977]. We first used the flow module to compute a quasi-steady flow pattern controlled by an assumed semidiurnal tide. Then we took the flow result at the end of a tidal cycle as the initial condition to start a transient simulation where a dissolved chemical was introduced into the domain through point source injection. Twenty semidiurnal tidal cycles were applied to perform a 10 day simulation. The time step sizes were set constant at 20 seconds for the flow computation and 60 seconds for the transport computation.

As shown in Figure 4.4 for the flow simulation, we had a tidal boundary condition given on the ocean boundary side with a maximum tide amplitude of 1.4 m and the closed boundary condition applied to the rest of the boundary. When the transient simulation began, we had 10 point sources of 1 m^3/s taken into account to simulate man-induced injection (e.g., outfall). Convergence was considered reached when either the maximum relative error of water depth was less than 10^{-4} or the root mean square error was less than 10^{-8}.

The transport system contained (1) 3 suspended sediments (**SS1**, **SS2**, and **SS3**) and 3 corresponding bed sediments (**BS1**, **BS2**, and **BS3**), (2) 1 dissolved chemical species in the water column (**C**), (3) 3 particulate chemical species adsorbed on suspended sediments (**PS1**, **PS2**, and **PS3**; one for each sediment) and 3 particulate chemical species on bed sediments (**PB1**, **PB2**, and **PB3**), and (4) 1 dissolved chemical species in the interstitial water (**CB**). The following adsorption reactions were taken into account.

SS1 $k_f = 0.001$,
SS2 $k_f = 0.0005$
SS3 $k_f = 0.0001$
· **BS1** $k_f = 0.0001$
· **BS2** $k_f = 0.0000$
· **BS3** $k_f = 0.0000$
+ **BS1** $k_f = 0.0001$
+ **BS2** $k_f = 0.0000$
+ **BS3** $k_f = 0.0000$

where k_f and k_b represent forward and backward reaction rate constants, respectively. We assumed

all sediments were of cohesive type and deposition and erosion rates were estimated by the following equations [Yeh, 1983].

$$S_n\left[1 - \frac{\tau_b}{\tau_{cDn}}\right] \qquad \text{if}$$

$$\text{if}$$

$$\left[\frac{\tau_b}{\tau_{cRn}} - 1\right] \qquad \text{if}$$

$$\text{if } \tau$$

where V_{sn} is the settling velocity of the n-th size fraction sediment [L/T]; τ_{cDn} is the critical shear stress for the deposition of the n-th size fraction sediment [M/L/T^2]; τ_{cRn} is the critical shear stress for the erosion of the n-th size fraction sediment [M/L/T^2]; E_n is the erodibility of the n-th size fraction sediment [M/L^2]; and τ_b is the bottom shear stress or the bottom friction stress [M/L/T^2] that can be estimated with Manning's formula [Chow, 1973]. Table 4.1 lists the characteristics of the three sizes of sediments, where the bulk density and porosity are for bed sediments.

Initially, there was no chemical nor bed sediment in the domain. Only the three suspended sediments with 100 kg/m^3 of each size existed throughout the region of interest. The water volume exchange rate was 0.002 m^3/m^2/s between the column and the interstitial waters. The flushing decay rate was 0.1 s^{-1} for the ocean boundary condition. The dispersion coefficient was 5.2 m^2/s. Neither radioactive decay nor volatilization existed. Each point source injected the dissolved chemical with a rate of 1 kg/s. The allowed maximum relative error of concentration was set to 10^{-4} for determining convergence.

Figure 4.5 plots the velocity change during the twentieth tidal cycle of the transient simulation, which represents a quasi-steady flow pattern. Based on the computational results, this quasi-steady flow pattern, determined subject to both tides and point sources, has been reached after three tidal cycles. Figures 4.6 and 4.7 plot the distributions at time = 5 and 10 days for BS1 and SS1, respectively. Figure 4.7 shows the trend to settle **SS1** in the bay area subject to the periodic tide. The decrease of SS1 with time (Figure 4.7) was the result of both deposition (Figure 4.6) and the

flushing process from the ocean boundary side. Figures 4.8 and 4.9 show the distributions of BS2 and SS2, respectively, at time = 5 and 10 days. The concentration contours at time = 5 and 10 days are barely differentiable, suggesting that a quasi-steady distribution pattern between BS2 and SS2 may be reached in 5 days. An examination of the computational results revealed that a quasi-steady distribution pattern can be considered reached after 5 tidal cycles (i.e., 2.5 days). Figure 4.10 depicts the contour of BS3 at time = 10 days, which presents a steady state concentration distribution that has been reached in this 10 day simulation. By checking the numerical results, it took almost no time to turn all **SS3** into **BS3** due to its large settling speed.

Figure 4.11 depicts the distributions of C at various times. It is obvious that the periodic flow pattern could effectively transport chemicals from the injection locations to the northwestern corner of the bay through advection. Figure 4.12 plots the contour of CB at time = 10 days, which matches that of C (Figure 4.11) because of the diffusive exchange of chemicals between the column and the interstitial waters as well as the identical adsorption reactions onto bed sediments for **C** and **CB** (the last six reactions in Eq. (4.7)). Figure 4.13 shows the distributions of PS1 and PS2, presented as mass of particulate chemicals included in a unit volume of fluid in the water column [kg/m^3], at time = 10 days. The contour patterns are also consistent with that of C because the distributions of SS1 and SS2 were basically smooth over the bay area (Figures 4.7 and 4.9). On the other hand, however, the distributions of particulate chemicals on bed sediments, presented as mass of particulate chemicals per unit horizontal bed area [kg/m^2], are ragged (Figure 4.14) due mainly to the rough distributions of bed sediments (Figures 4.6, 4.8, and 4.10).

Table 4.1. List of sediment parameters in example 2.

	SS1 and BS1	SS2 and BS2	SS3 and BS3
Settling Speed (m/s)	1.2×10^{-6}	1.5×10^{-4}	6.5×10^{-2}
Critical shear stress for deposition ($kg/m/s^2$)	0.5	0.5	0.6
Critical shear stress for erosion ($kg/m/s^2$)	0.4	0.4	0.5
Erodibility (kg/m^2)	1.0	1.0	1.0
Specific weight (kg/m^3)	1307.7	1500	1727.3
Bulk density (kg/m^3)	1200	1300	1400
Porosity (m^3/m^3)	0.35	0.4	0.45

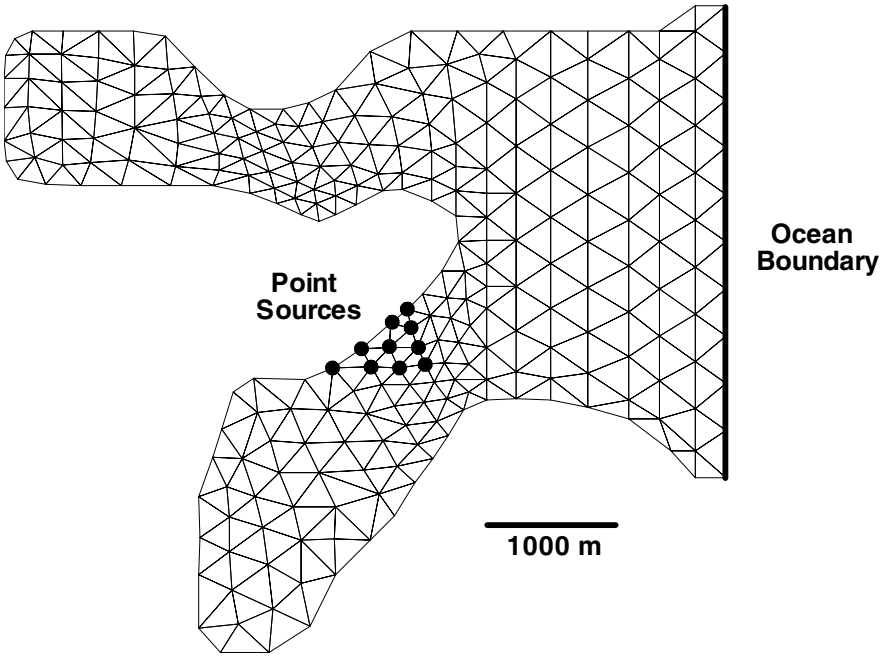

Figure 4.4. Discretization, ocean boundary, and point sources of Salem harbor in the demonstrative example.

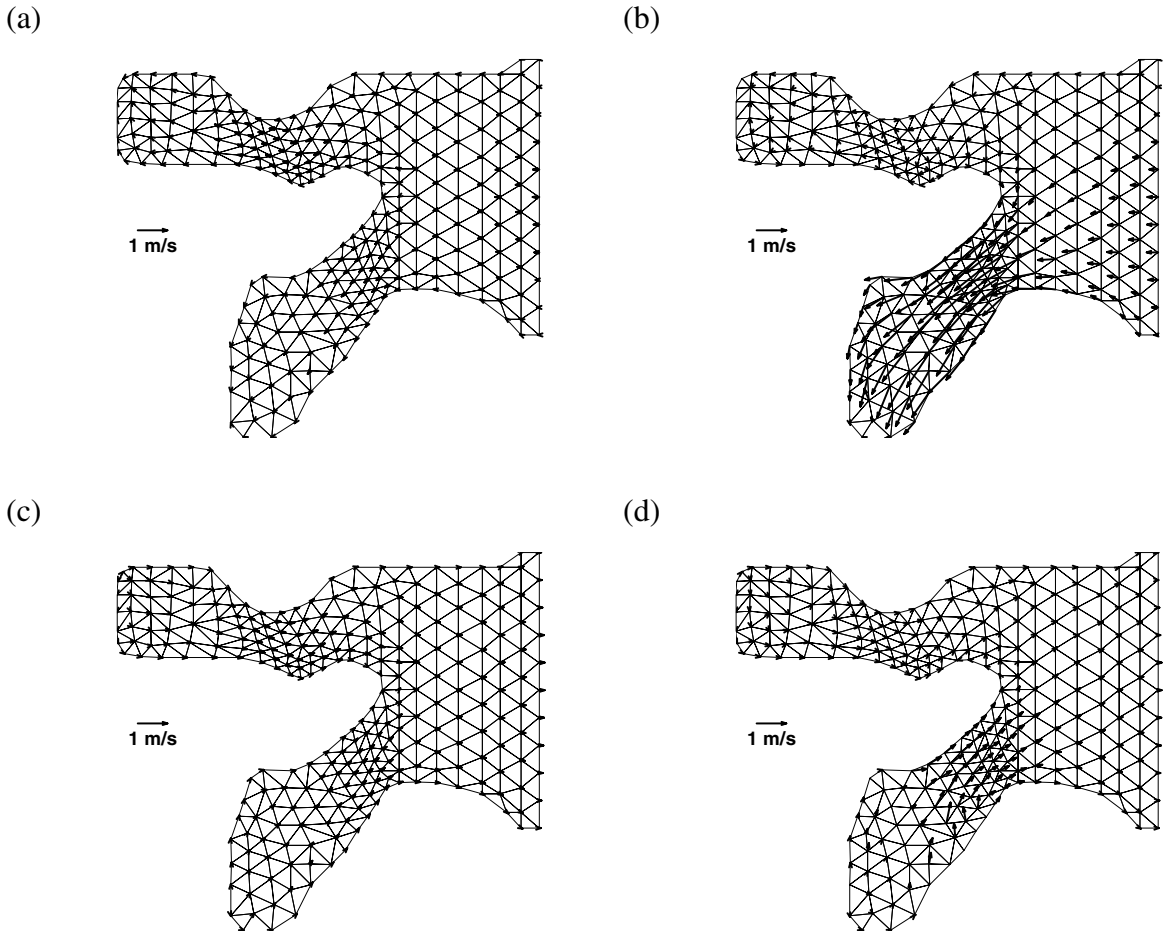

Figure 4.5. Velocity at (a) 0.25T, (b) 0.5T, (c) 0.75T, and (d) T of the twentieth tidal cycle.

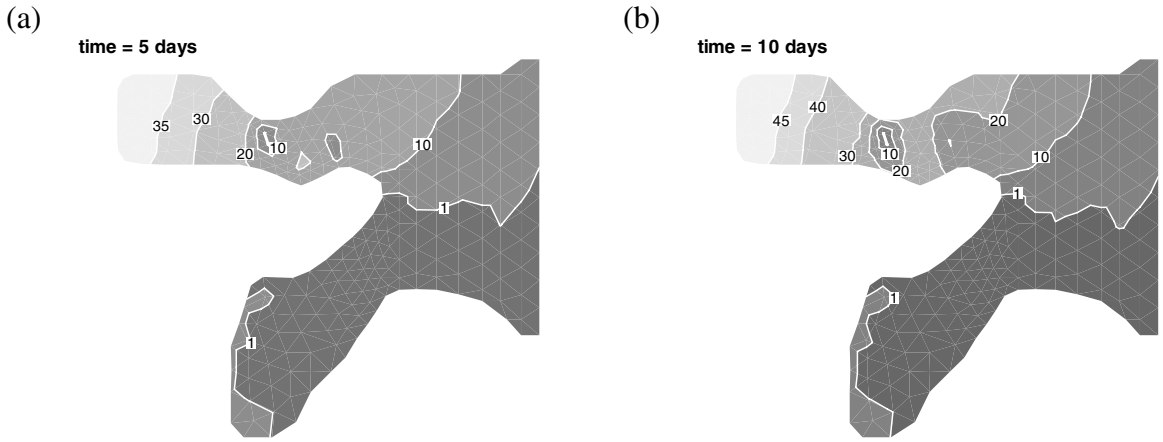

Figure 4.6. Numerical results of BS1 [kg/m^2] at time = (a) 5 days and (b) 10 days.

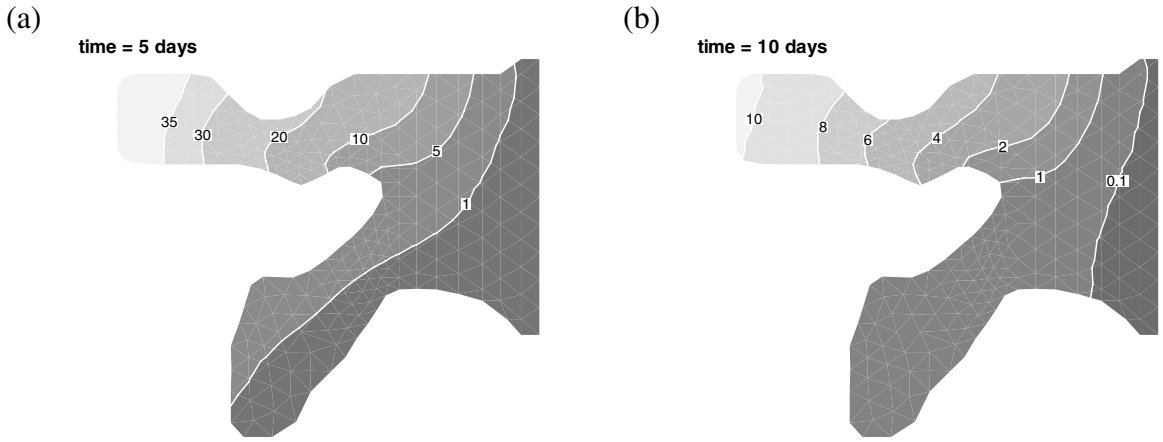

Figure 4.7. Numerical results of SS1 [kg/m^3] at time = (a) 5 days and (b) 10 days .

(a)

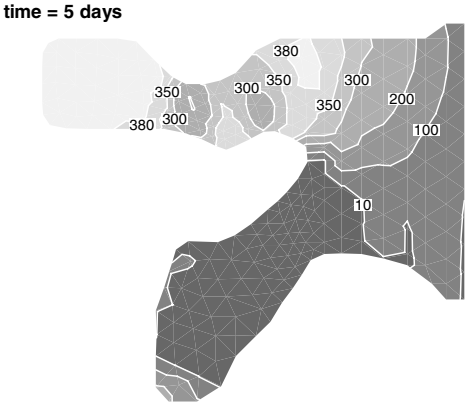

(b)

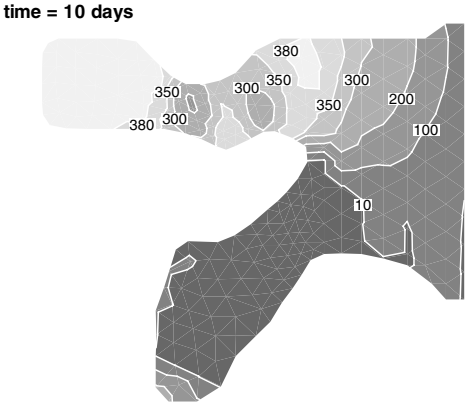

Figure 4.8. Numerical results of BS2 [kg/m^2] at time = (a) 5 days and (b) 10 days.

(a)

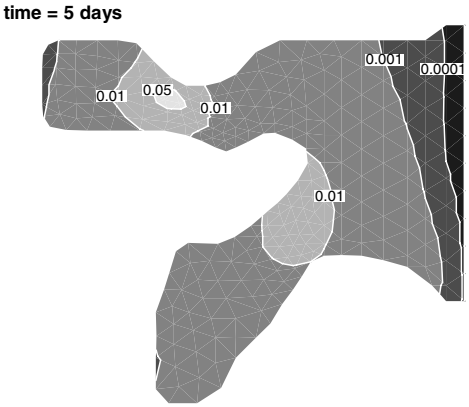

(b)

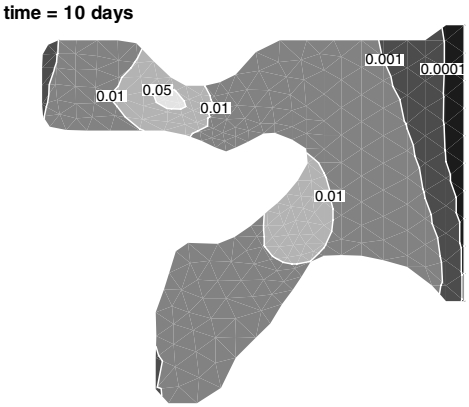

Figure 4.9. Numerical results of SS2 [kg/m^3] at time = (a) 5 days and (b) 10 days.

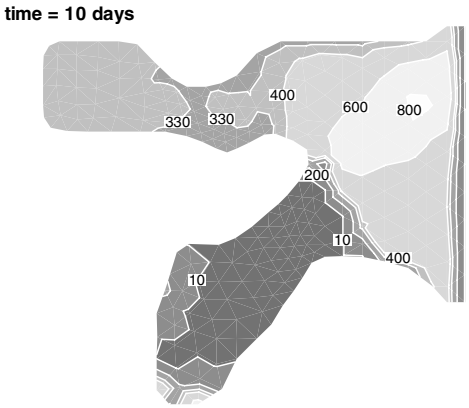

Figure 4.10. Numerical results of BS3 [kg/m^2] at time = 10 days.

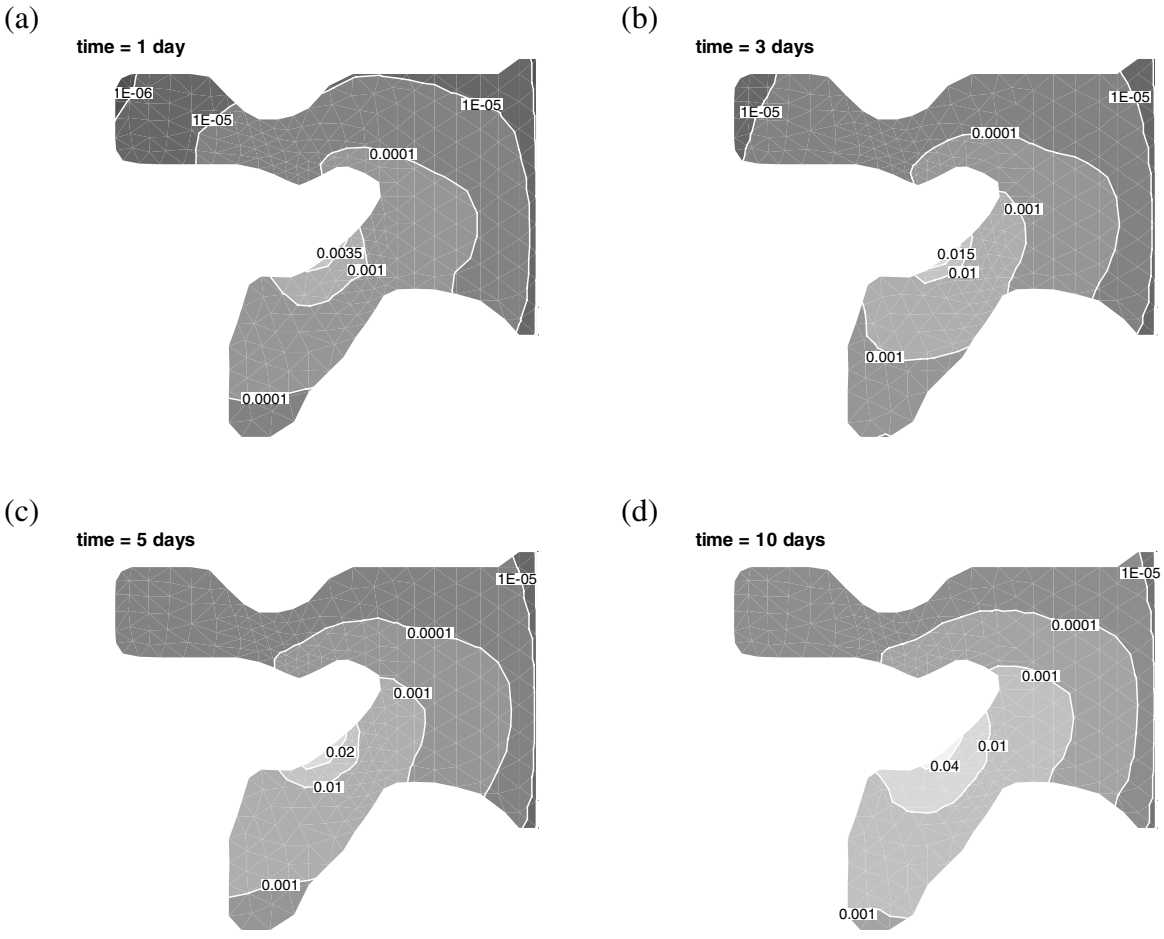

Figure 4.11. Numerical results of C [kg/m^3] at time = (a) 1 day, (b) 3 days, (c) 5 days, and (d) 10 days.

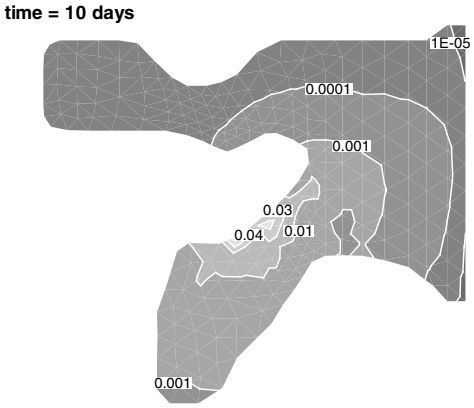

Figure 4.12. Numerical results of CB [kg/m^3] at time = 10 days.

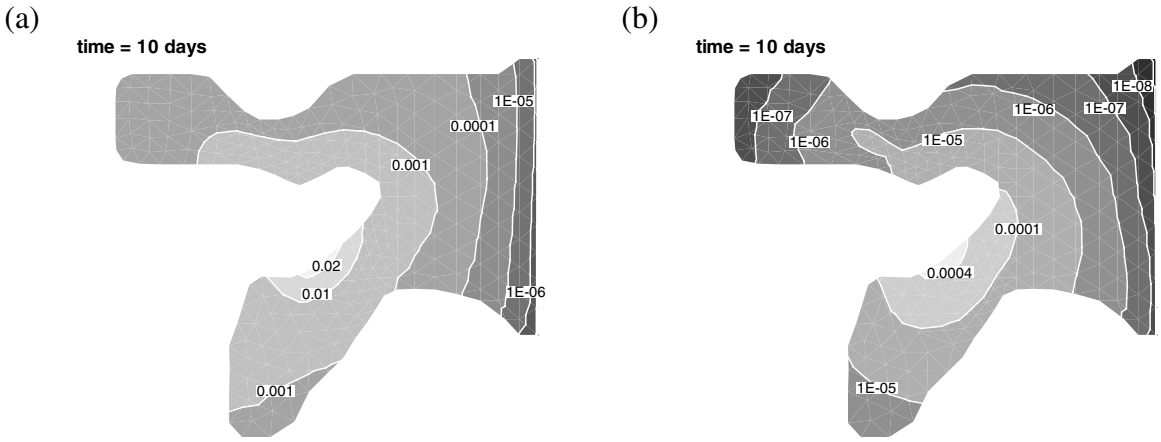

Figure 4.13. Numerical results of (a) PS1 [kg/m^3] and (b) PS2 [kg/m^3]at time = 10 days.

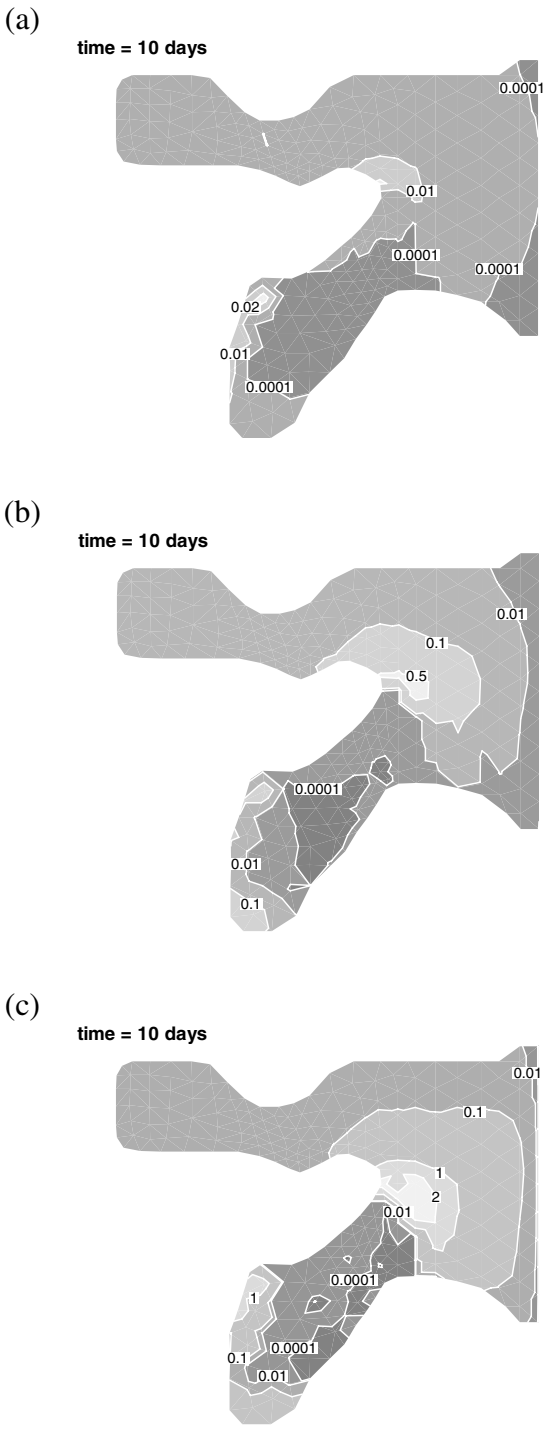

Figure 4.14. Numerical results of (a) PB1 [kg/m^2], (b) PB2 [kg/m^2], and (c) PB3 [kg/m^2] at time = 10 days.

4.3 Example 3 --- San Diego Bay Problem (I)

In this example, we used our model to simulate a hypothetical sediment and contaminant transport at San Diego South bay under a quasi-steady flow pattern determined according to an assumed semidiurnal tide. This quasi-steady flow pattern was computed by a hydrodynamic flow model which solved shallow water equations with our flow module. The domain was discretized with 1415 elements and 1567 nodes (Figure 4.15). The mean depth varied from 20 meters near the ocean boundary to about 0.4 meter toward the south end of the bay. The flow pattern was determined with a tidal boundary condition implemented on the ocean boundary side where the maximum tidal amplitude was 1.2 m and with the rest of the boundary treated as closed (Figure 4.15). It was also assumed subject to 8 point sources (Figure 4.15) each with an injection rate of 1 m^3/s. Manning's n was assumed 0.01 throughout the entire bay. Figure 4.16 depicts the contours of water surface elevation in the bay area at various times during one tidal cycle.

The hypothetic transport system contained 2 sizes of cohesive sediments and 1 dissolved chemical. The deposition and erosion rate were computed with Eqs. (4.8) and (4.9). Table 4.2 lists the characteristics of the two sizes of sediments, where the bulk density and porosity were used for their corresponding bed sediments. Through reactions, we can have a total of 4 sediments (2 suspended, **SS1** and **SS2**, and 2 bed, **BS1** and **BS2**) and 6 chemical species (one dissolved in the water column, **C**, one dissolved in the interstitial water, **CB**, and one particulate adsorbed onto each sediment, **PS1**, **PS2**, **PB1**, and **PB2**) included in our transport system. The following adsorption reactions were considered.

- **SS1** k_f = 0.0001
- **SS2** k_f = 0.0005
+ **BS1** k_f = 0.0001
+ **BS2** k_f = 0.0005
+ **BS1** k_f = 0.0001
+ **BS2** k_f = 0.0005

Initially, there was no dissolved chemical nor suspended sediments anywhere in the domain. It was assumed only the two bed sediments of 100 kg/m^2 were uniformly distributed throughout the region of interest. As the simulation began, the dissolved chemical was released into the domain

through point sources with a rate of 1 kg/s at each point source. The water volume exchange rate was 0.002 $m^3/m^2/s$ between the column and the interstitial waters. The flushing decay rate was 0.1 s^{-1} for the ocean boundary condition. The dispersion coefficient was 5.2 m^2/s. Chemicals were neither radioactive nor volatile. The allowed maximum relative error of concentration was 10^{-4}. A 10 day simulation was performed with a constant time step size of 20 seconds.

Figures 4.17 and 4.18 show the distributions of BS1 and BS2, respectively, at time = 5 and 10 days. It is observed that after 5 days almost all bed sediments in zone A were washed out, while sediments which were eroded from zone A were pushed into zone B by tides and then deposited due to the reduction of flow velocities along the bay's longitudinal direction from the ocean boundary to its south end. In zone C where the flow velocity was too small to resuspend bed sediments, bed sediment concentrations did not change much. The increase of bed sediments in this zone was due to deposition of suspended sediments which were transported by tides from nearby areas. As one can see from Figure 4.19 that only minor amounts of suspended sediments were transported into zone C.

Figures 4.20 and 4.21 present concentration distributions of the dissolved chemical in the water column (i.e., C) and the interstitial water (i.e., CB), respectively, at both time = 5 days and time = 10 days. Through the comparison of these two figures, C and CB had approximately the same distribution pattern. In addition, their distributions did not change drastically from time = 5 days to time = 10 days. This was because the semidiurnal tide was not strong enough to overcome the bay's long-strip geometry to bring out chemicals through advection. In other words, dispersion was the main process to bring chemicals away from the injection sources.

Figures 4.22 and 4.23 plot particulate chemical concentrations on suspended sediments and bed sediments, respectively, at time = 10 days. It is observed that there existed more PB2 than PB1 because more adsorption was allowed for dissolved chemicals to be adsorbed onto BS2 by comparing the last four reactions in Eq. (4.10). On the other hand, we observed more PS1 than PS2 even though the system should allow more PS2 to be formed according to the first two adsorption reactions in Eq. (4.10). This was because SS1 was at least one order of magnitude larger than SS2 and we present PS1 and PS2 in Figure 4.23 as the mass of particulate chemicals on bed sediments per unit bed area.

Table 4.2. List of sediment parameters in Example 3.

	Sediment 1 (**SS1** and **BS1**)	Sediment 2 (**SS2** and **BS2**)
Settling Speed (m/s)	1.2×10^{-6}	1.5×10^{-4}
Critical shear stress for deposition ($kg/m/s^2$)	0.5	0.5
Critical shear stress for erosion ($kg/m/s^2$)	0.4	0.4
Erodibility (kg/m^2)	1.0	1.0
Specific weight (kg/m^3)	1500	1285.7
Bulk density (k/m^3)	1300	1200
Porosity (m^3/m^3)	0.4	0.3

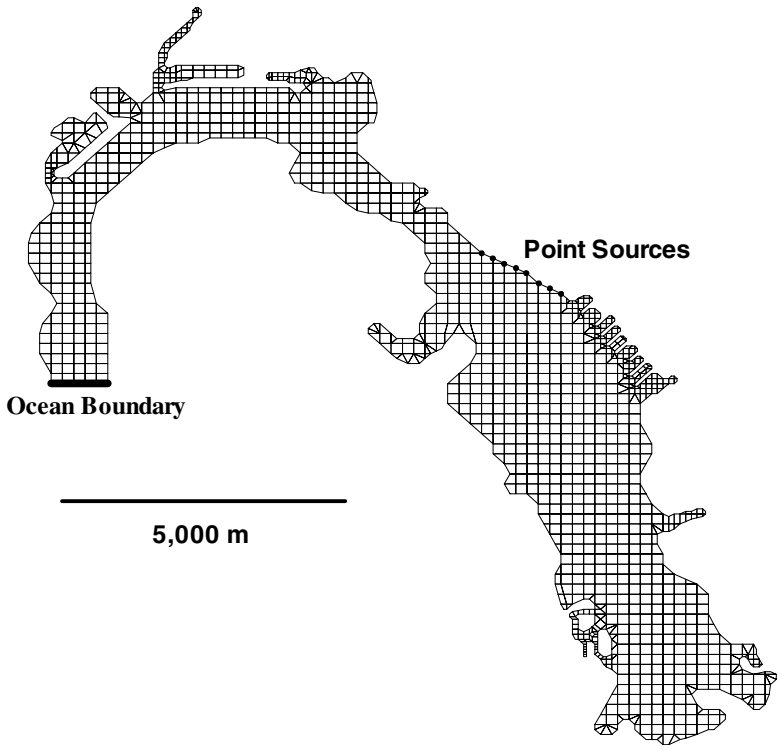

Figure 4.15. The domain and its discretization of Example 3.

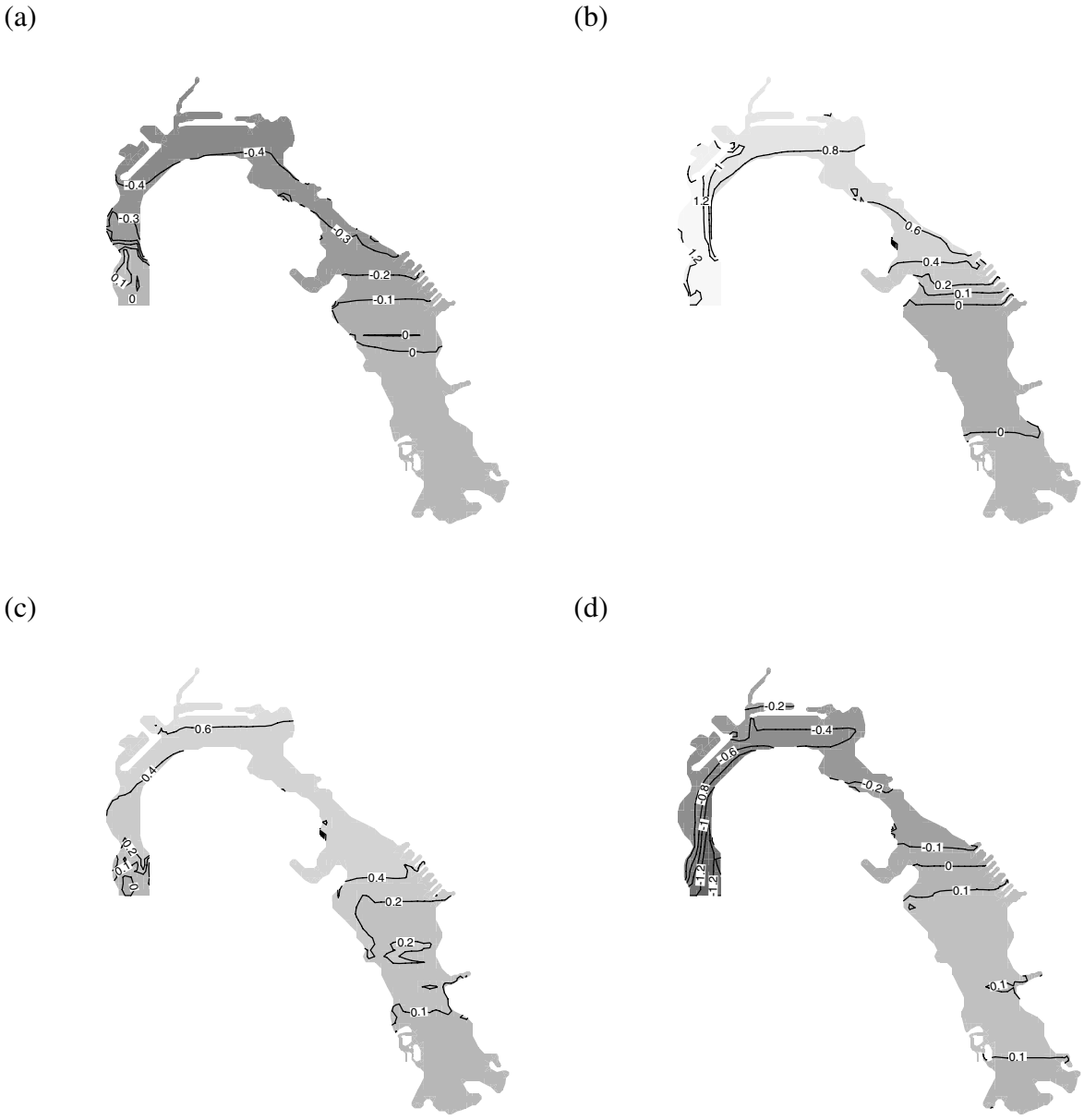

Figure 4.16. Surface elevation at (a) 0 or T, (b) 0.25T, (c) 0.5T, and (d) 0.75T in the bay area during a tidal cycle where T = 12 hours.

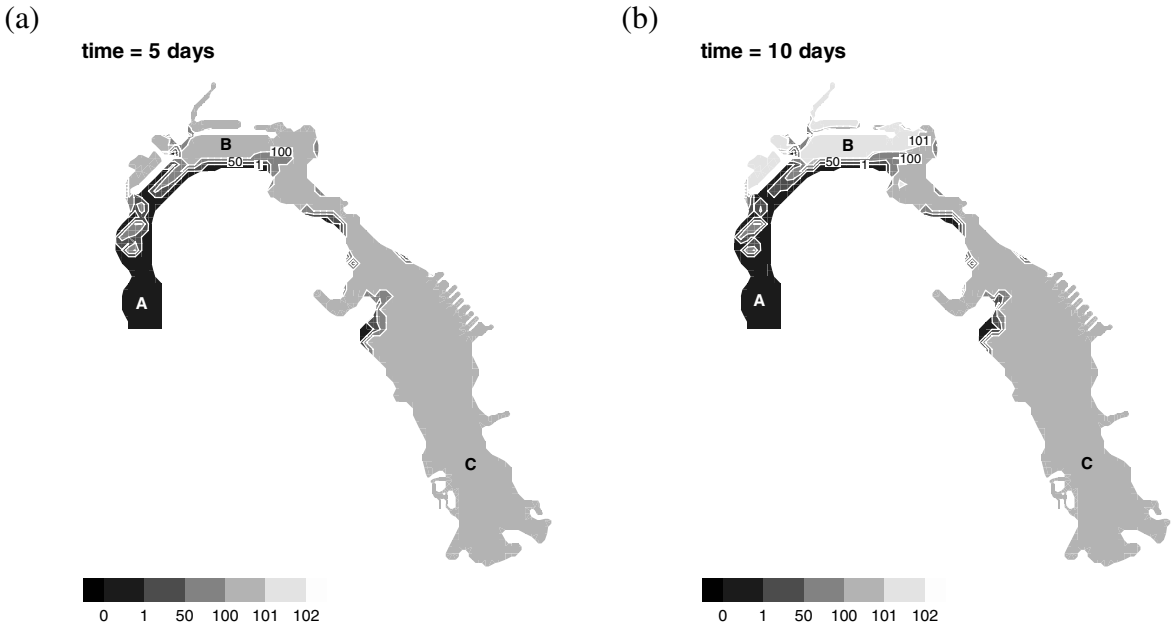

Figure 4.17. Numerical results of BS1 [kg/m^2] at time = (a) 5 days and (b) 10 days in the bay of Example 4.

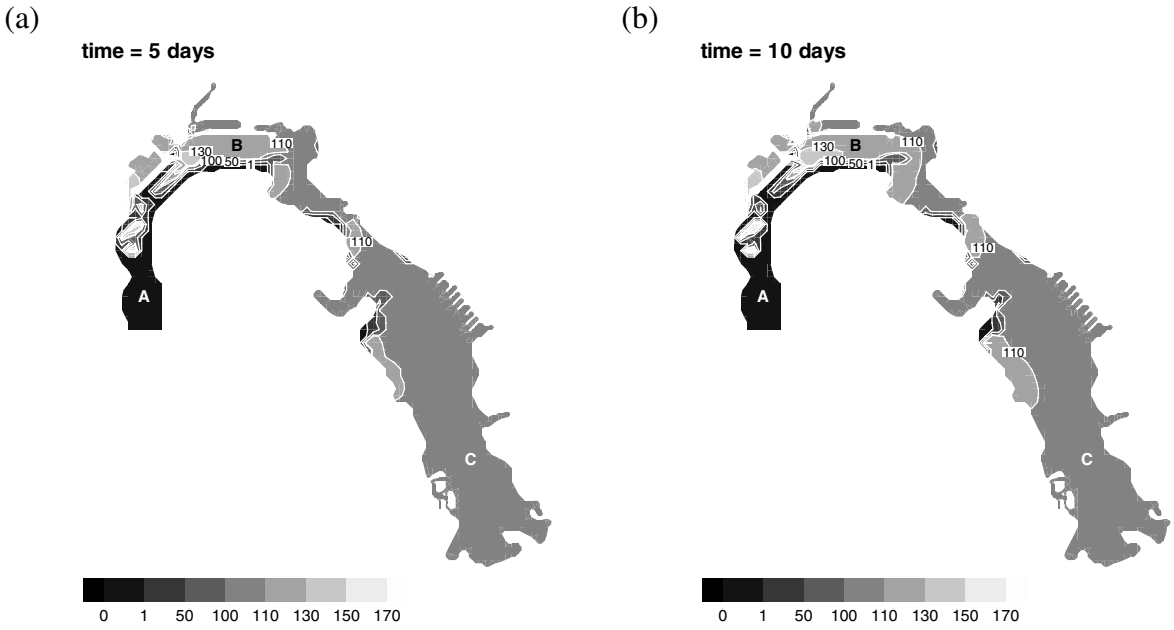

Figure 4.18. Numerical results of BS2 [kg/m^2] at time = (a) 5 days and (b) 10 days in the bay of Example 3.

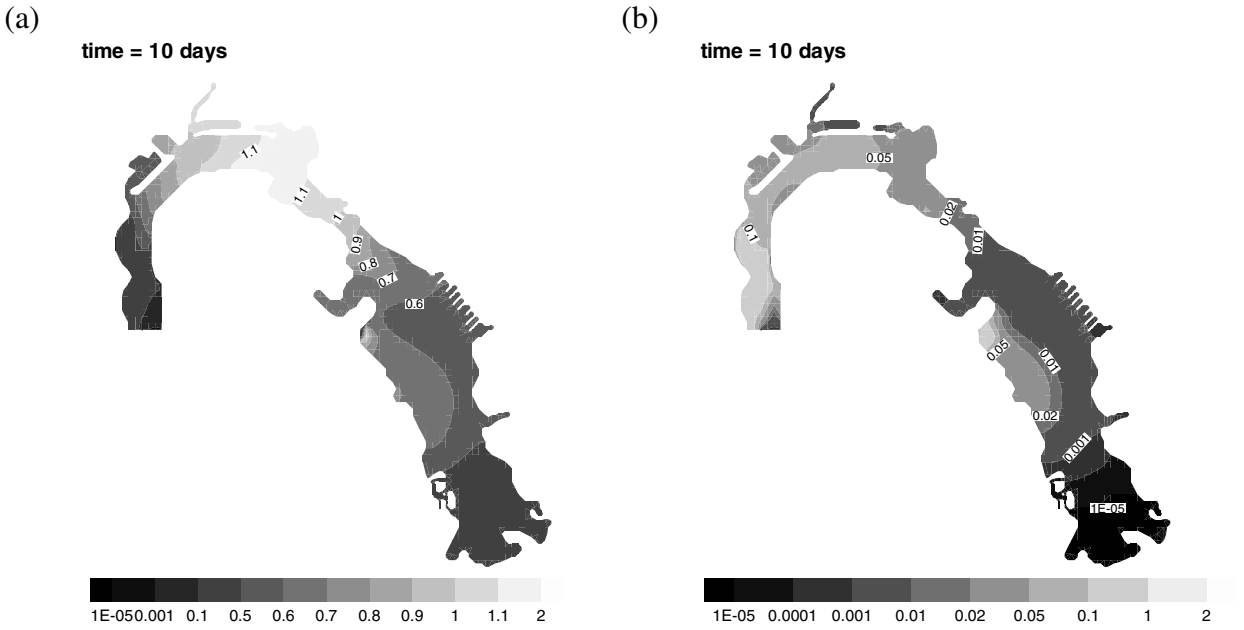

Figure 4.19. Numerical results of (a) SS1 [kg/m^3] and (b) SS2 [kg/m^3] at time = 10 days in the bay of Example 3.

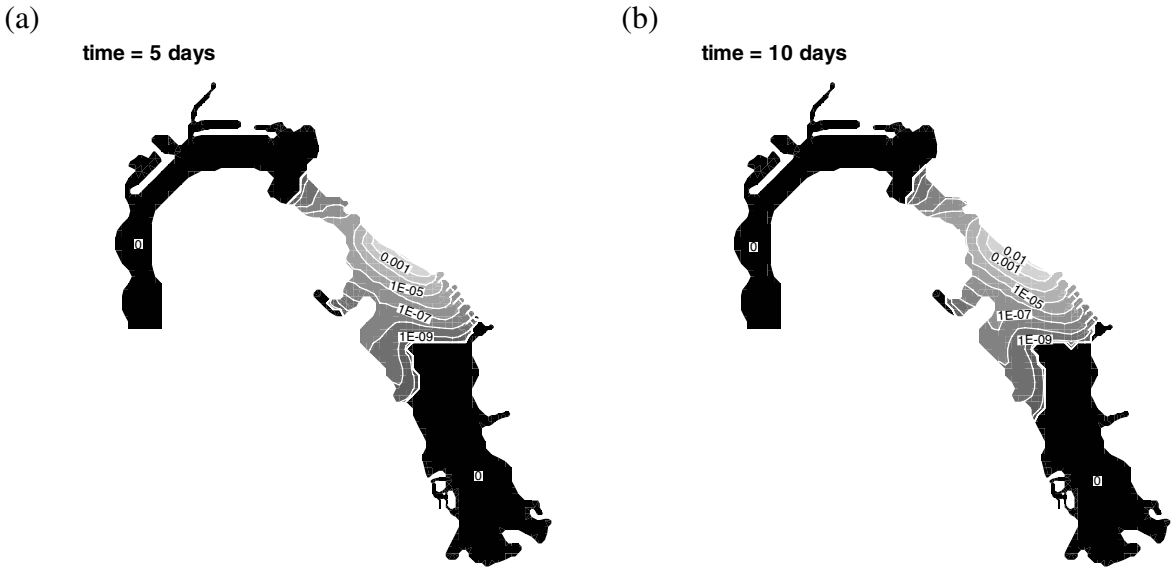

Figure 4.20. Numerical results of C [kg/m^3] at time = (a) 5 days and (b) 10 days in the bay of Example 3.

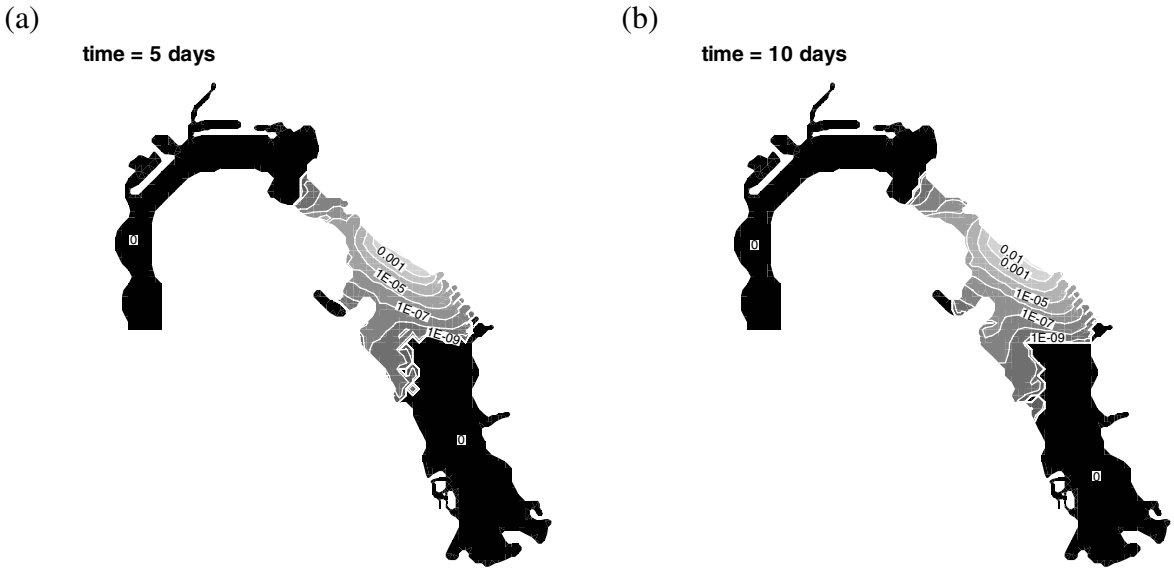

Figure 4.21. Numerical results of CB [kg/m^3] at time = (a) 5 days and (b) 10 days in the bay of Example 3.

(a) (b)

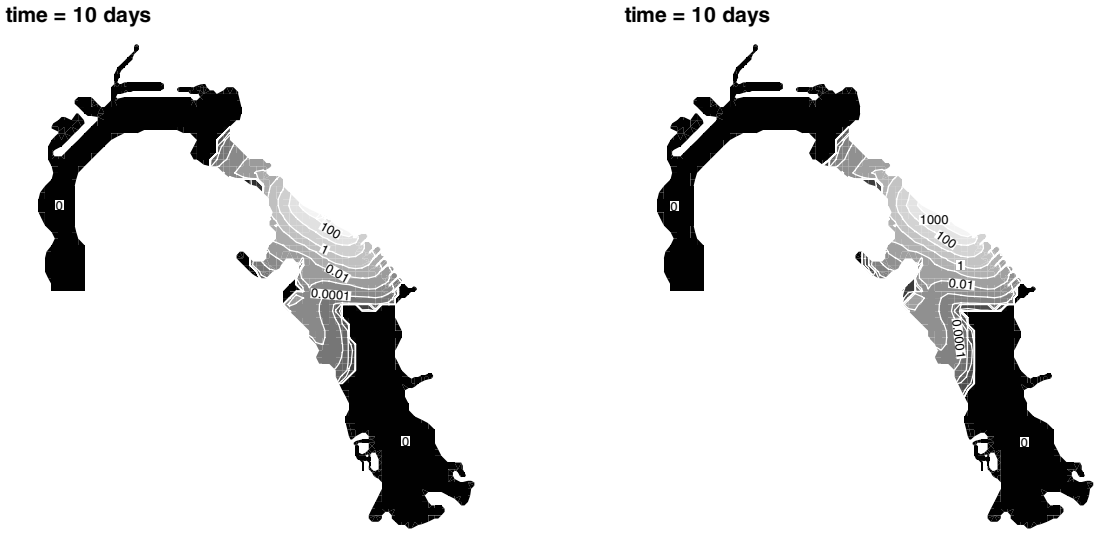

Figure 4.22. Numerical results of (a) PB1 [kg/m^2] and (b) PB2 [kg/m^2] at time = 10 days in the bay of Example 3.

(a) (b)

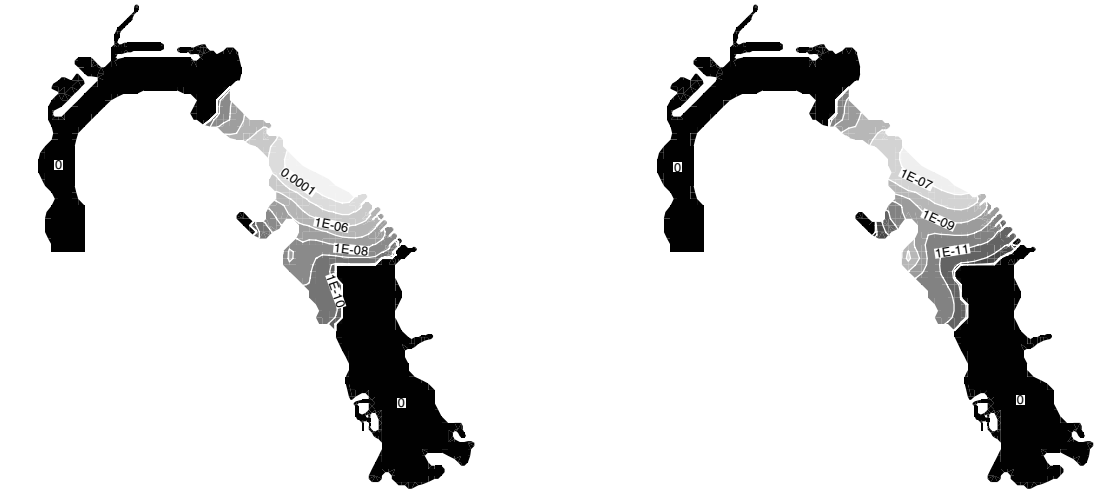

Figure 4.23. Numerical results of (a) PS1 [kg/m^3] and (b) PS2 [kg/m^3] at time = 10 days in the bay of Example 3.

4.4 Example 4 --- San Diego Bay Problem (II)

This example differed from Example 3 only in the size of the simulated region and the application of open boundary conditions. As shown in Figure 4.24 (a), the domain was discretized with 2467 elements and 2566 nodes where the grids used to discretize the bay area were identical to those used in Example 3. The mean depth varied from about 85 meters close to the Point C on the ocean boundary to about 0.4 meter toward the south end of the bay (Figure 4.24(b)). A tidal boundary condition with the maximum tidal amplitude of 2.0 m was applied to the ocean boundary where a wave lead of 4 s per every 100 m was assumed from Point A to B, A to C, and C to D, i.e., the wave came from northeast and arrived at Point A first, then Point B, Point C, and finally Point D. The rest of the boundary was treated as closed as that in Example 3(Figure 4.24).

Figure 4.25 depicts the contours of water surface elevation at various times during one tidal cycle. It is observed that Figures 4.25 and 4.16 show similar elevation distributions in the bay at various times. Therefore, we also expected similar concentration distributions of the dissolved chemical in the water column (i.e., C) and the interstitial water (i.e., CB) in both Examples 3 and 4 because the sources were injected in the middle of the bay and the tide could not transport the chemical to the Pacific Ocean through the exit of the bay in 10 days. Figures 4.26 and 4.27 present concentration distributions of C and CB, respectively, at both time = 5 days and time = 10 days. Through the comparison of these two figures with Figures 4.20 and 4.21, we verified our expectation.

Figures 4.28 and 4.29 show the distributions of BS1 and BS2, respectively, at time = 5 and 10 days. Like the chemical concentrations mentioned above, similar numerical results were obtained in the bay, except for the throat part that suspended sediments may enter the bay from or exit to the Pacific Ocean. Figure 4.30 helps to demonstrate this by showing the distribution of suspended sediments at time = 10 days where suspended sediments in the throat area were more than those in Example 3 (Figure 4.19).

Figures 4.31 and 4.32 plot the distribution of particulate chemicals at time = 10 days. Again, the distributions similar to those in Example 3 (Figures 4.22 and 4.23). It is thus suggested a simulated domain that includes only the bay can be used to save computer time when the injection is placed far enough from the throat of the bay.

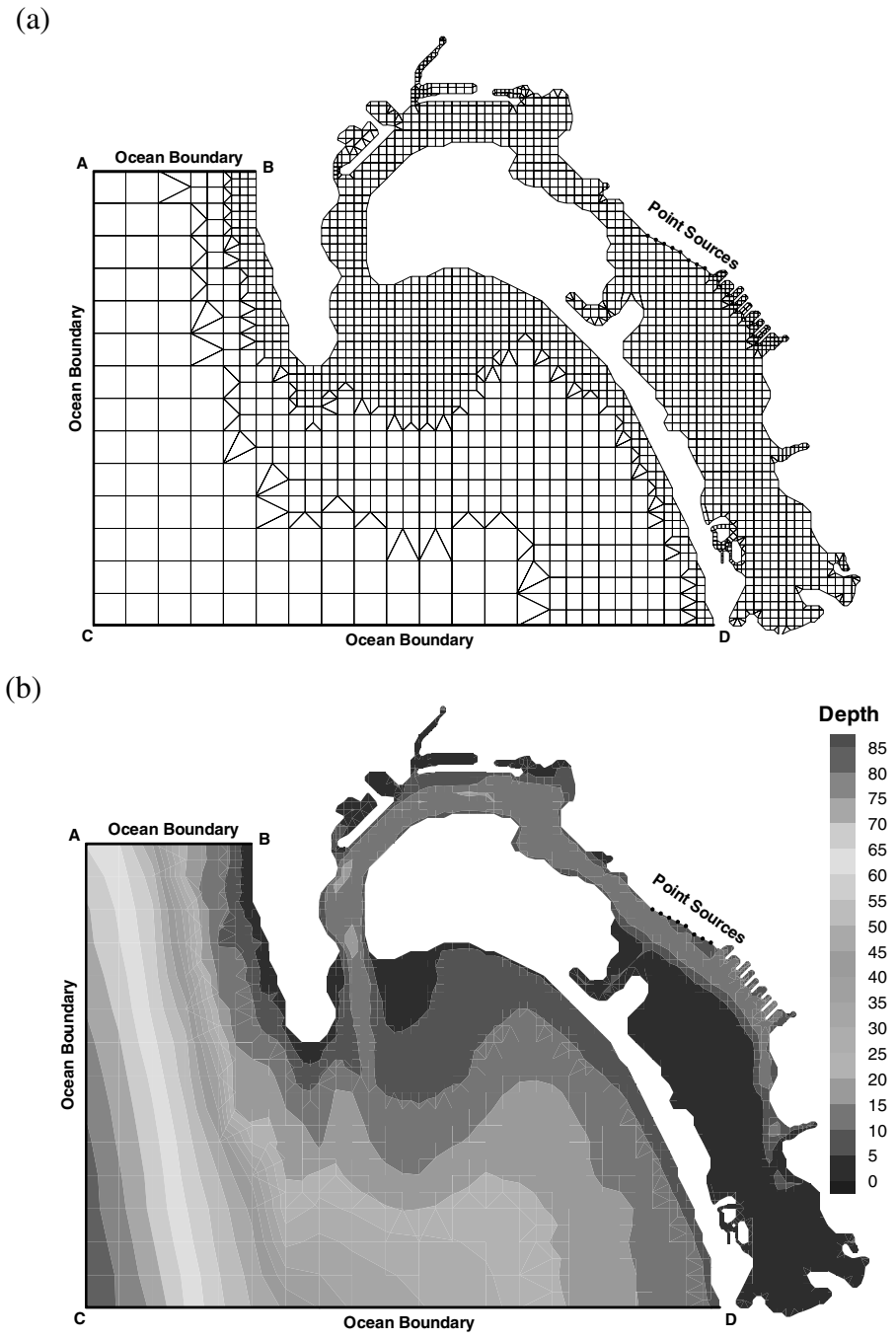

Figure 4.24. (a) The discretization and (b) the mean sea level water depth [m] of the simulation region in Example 4.

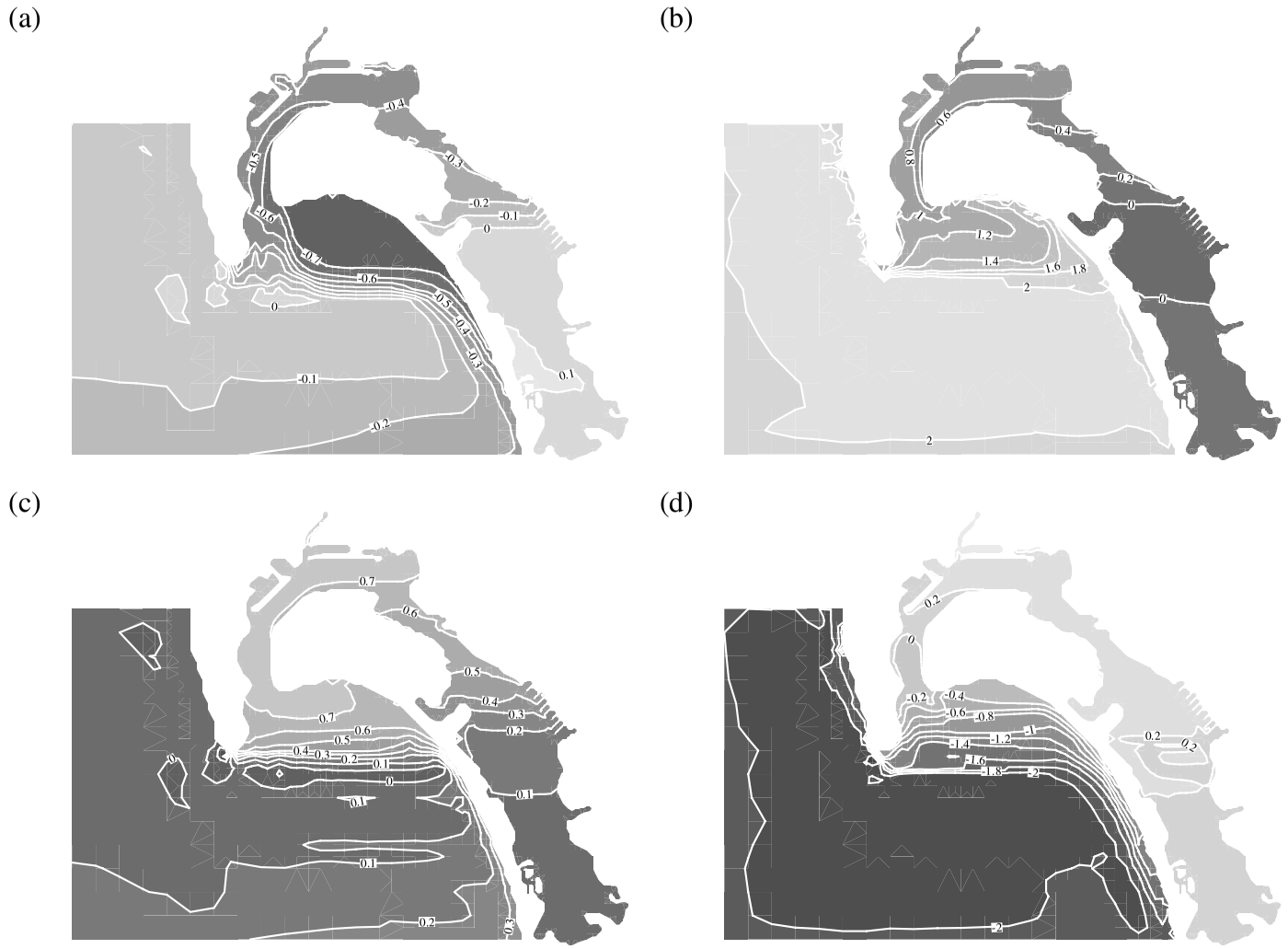

Figure 4.25. Surface elevation at (a) 0 or T, (b) 0.25T, (c) 0.5T, and (d) 0.75T during a tidal cycle in Example 4 where T = 12 hours.

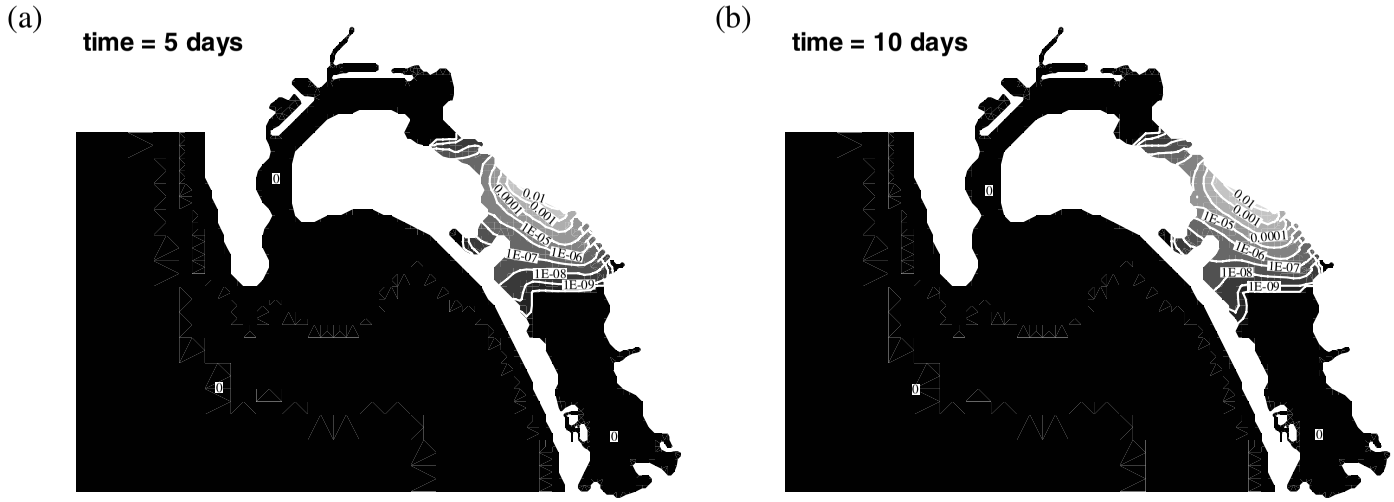

Figure 4.26. Numerical results of C [kg/m^3] at time = (a) 5 days and (b) 10 days in Example 4.

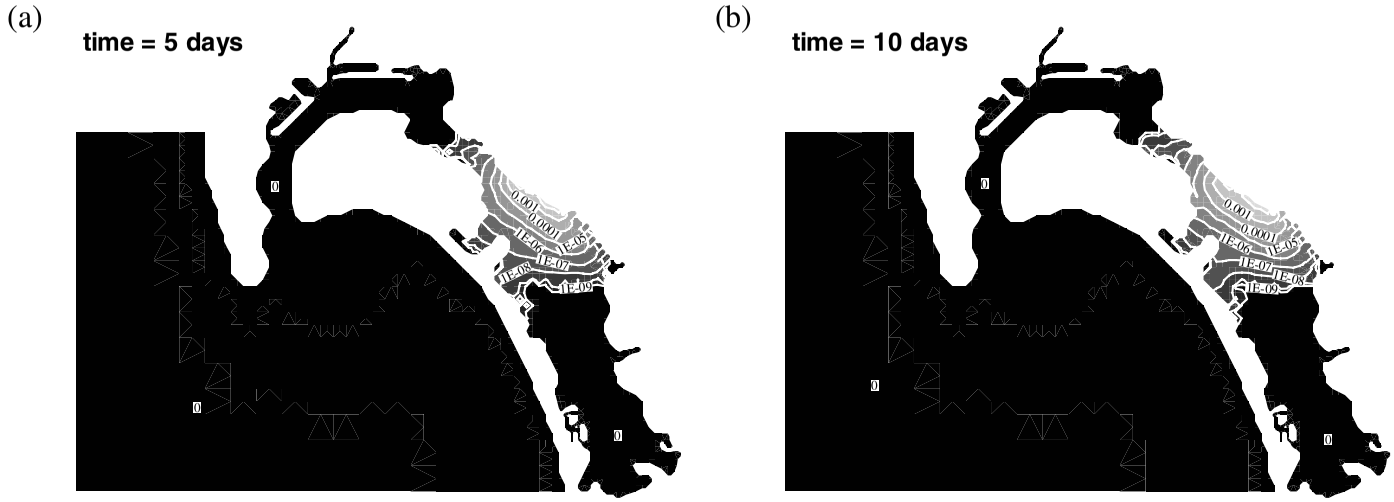

Figure 4.27. Numerical results of CB [kg/m^3] at time = (a) 5 days and (b) 10 days in Example 4.

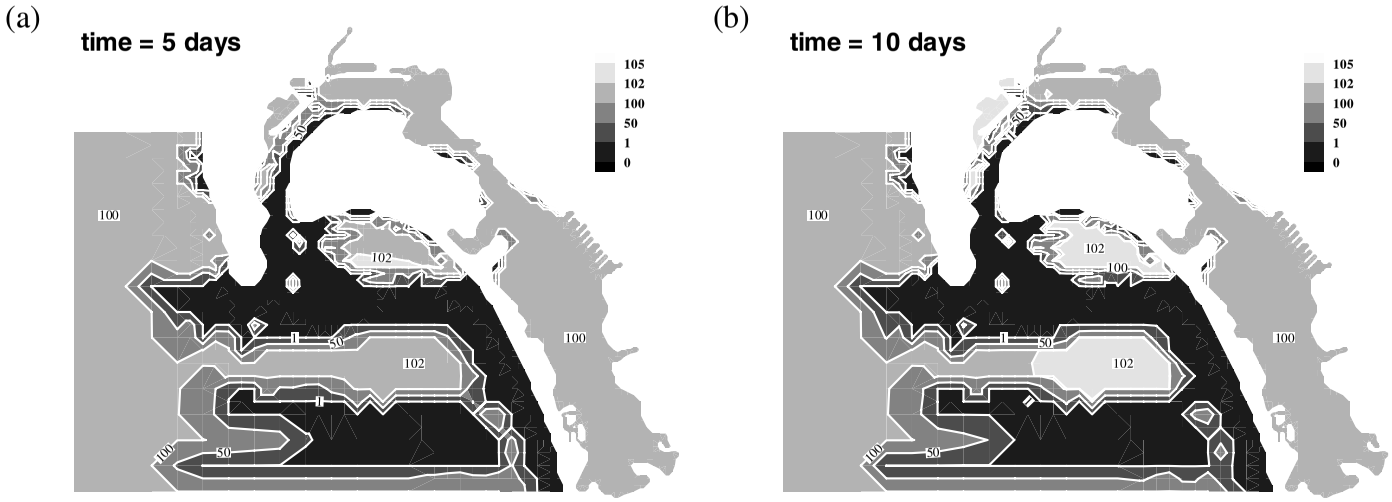

Figure 4.28. Numerical results of BS1 [kg/m^2] at time = (a) 5 days and (b) 10 days in Example 4.

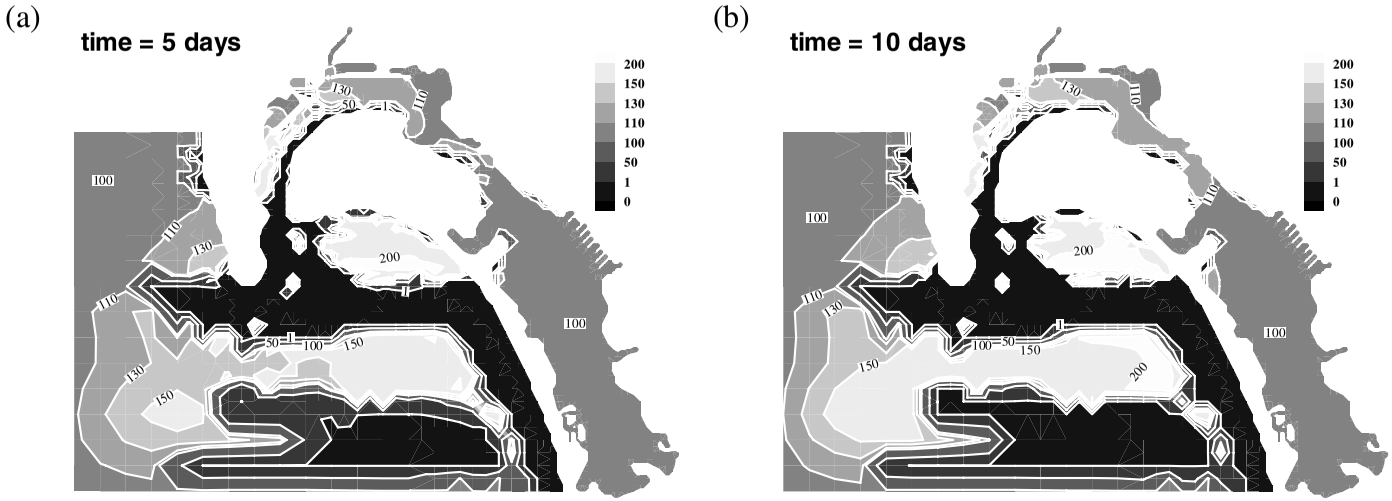

Figure 4.29. Numerical results of BS2 [kg/m^2] at time = (a) 5 days and (b) 10 days in Example 4.

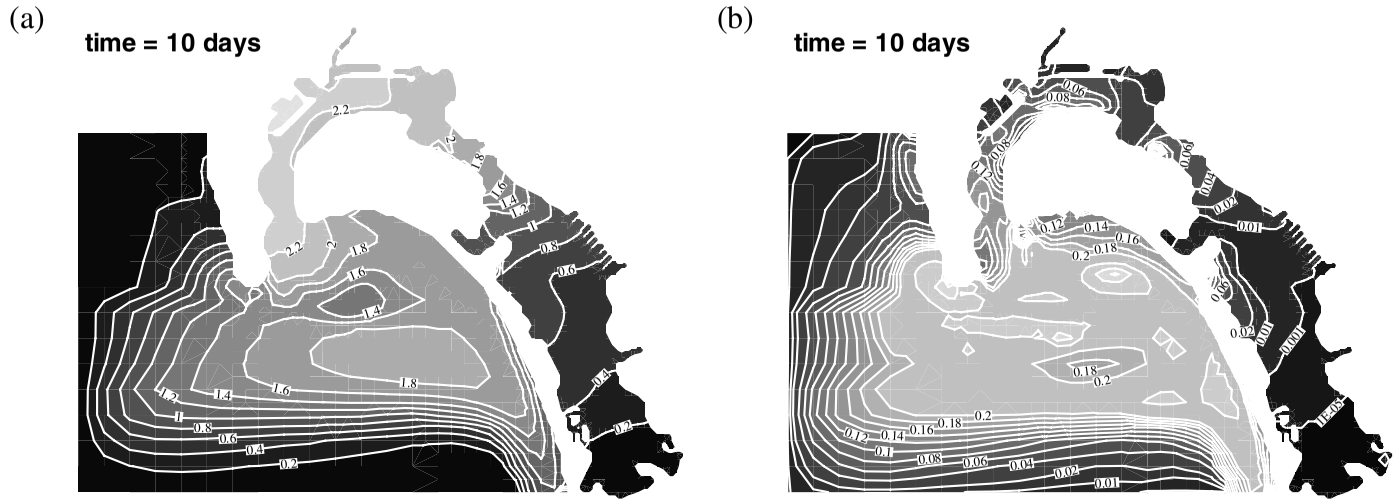

Figure 4.30. Numerical results of (a) SS1 [kg/m^3] and (b) SS2 [kg/m^3] at time = 10 days in Example 4.

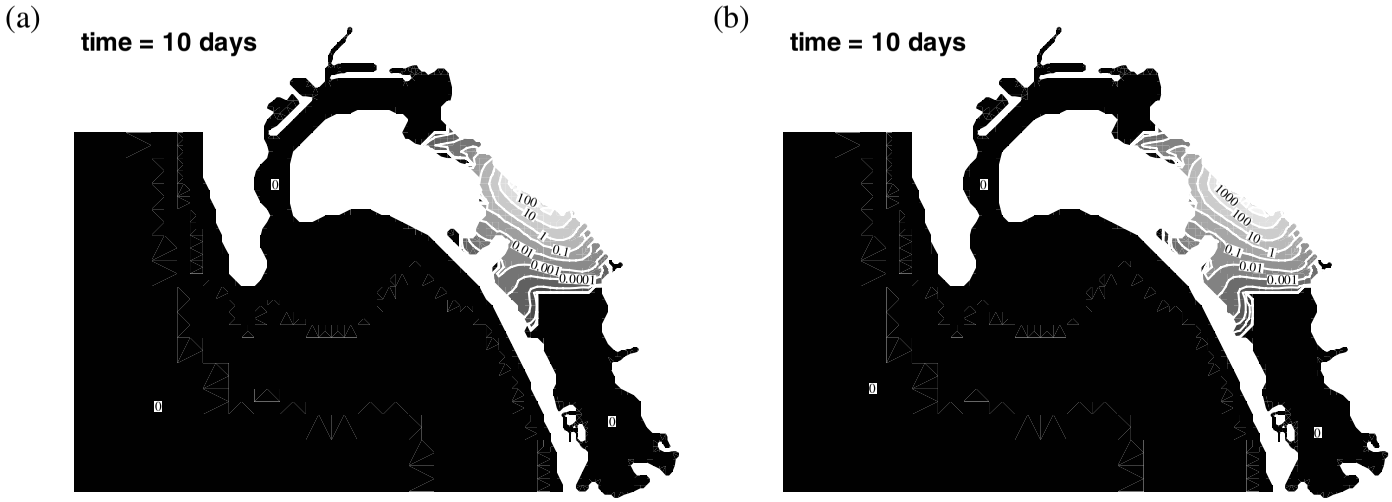

Figure 4.31. Numerical results of (a) PB1 [kg/m^2] and (b) PB2 [kg/m^2] at time = 10 days in Example 4.

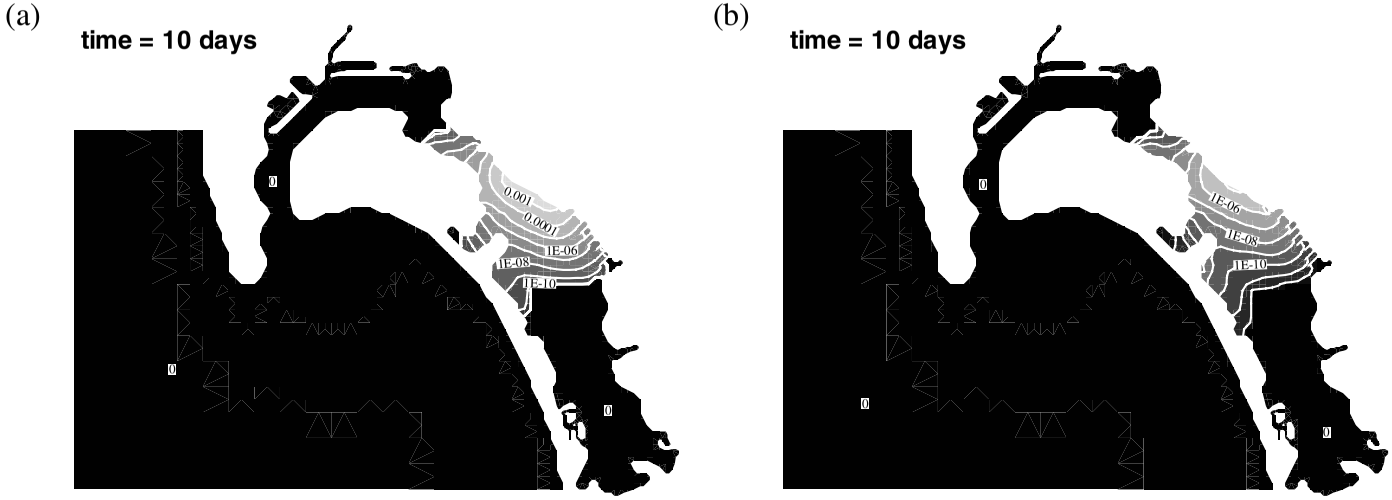

Figure 4.32. Numerical results of (a) PS1 [kg/m^3] and (b) PS2 [kg/m^3] at time = 10 days in Example 4.

Chapter 5. SUMMARY

We have presented a 2-D depth-averaged model simulating hydrodynamics and reactive contaminant and sediment transport in bay/estuary areas. A splitting strategy was employed in the flow module to solve shallow water equations. We used the method of characteristics first to solve the equations without including eddy flux terms where local diagonalization was achieved, and then we accounted for these terms with the Galerkin finite element method. Zero normal flux was applied to the closed boundary, while zero lateral flux was assumed on the open boundary. Both were to replace the first characteristic equations of boundary nodes. Either normal flux- or water surface-driven boundary conditions can be used on the open boundary where sub-critical flow exists. The open boundary condition was to replace the equation of the incoming characteristic, either the second or the third, of boundary nodes. We employed a generic, mechanistic approach to model reactive contaminant and sediment migration in the transport module, desiring to promote reactive contaminant transport modeling in this field so that practical systems can be more accurately simulated. Chemical reactions, including aqueous complexation, adsorption/desorption, and volatilization, were assumed elementary and kinetic where reaction rates were computed through forward and backward reaction rate constants based on the collision theory. Suspended sediments, dissolved chemicals in the water column, and particulate chemicals on suspended sediments were subject to transport and thus were mobile. Bed sediments, dissolved chemicals in the interstitial water, and particulate chemicals on bed sediments were considered immobile. The set of governing equations were solved with a predictor-corrector strategy. In the predictor step, the physical transport terms were solved by using the Lagrangian-Eulerian finite element method with all source/sink terms evaluated at the previous time. In the corrector step where non-linearity was handled, the Picard method was used to solve for sediment distributions, and the Newton-Raphson method was employed to solve the correction equations of reactive contaminants. An adaptive explicit-implicit scheme was also applied to avoid negative numerical results. Four example problems accounting for 1-D standing wave problem and the transports of both sediments and contaminants in the Salem harbor as well as in the Sandiego South bay with semidiurnal tides applied on the ocean boundary were used to demonstrate the capability of the model.

Appendix I. DATA INPUT GUIDE

This data input guide describe the following files: geometry file, flow model file, chemical/sediment and reaction information file, transport model file, initial water surface elevation file, initial velocity file, initial dissolved chemical concentration file, initial particulate chemical concentration file, and initial sediment concentration file.

I.1. File 1: geometry file (GEOM file)

T1-T3 Cards		**Job title**	
		Only one T1, T2, and T3 card can be used.	
GE Card		Element information	
Field	Variable	Value	Description
C 1-2	IC1	GE	Card group identifier.
C 3	IC3		Identification of element.
		3	A triangular element is being input.
		4	A quadrilateral element is being input.
1	M	+	id of global element.
2	IE1(M,1)	+	id of the global node that serves as the 1-st element node of the global element.
3	IE2(M,2)	+	id of the global node that serves as the 2-nd element node of the global element..
4	IE2(M,3)	+	id of the global node that serves as the 3-rd element node of the global element.
5	IE2(M,4)	+	id of the global node that serves as the 4-th element node of the global element. It is zero for a triangular element.
6	IE2(M,5)	+	id of the material type of the global element.
GN Card		Node information	
Field	Variable	Value	Description
C 1-2	IC1	GN	Card group identifier.
C 3	IC3		blank .
1	N	+	id of global node..
2	X2(N,1)	+	The x-coordinate of the global node.
3	X2(N,2)	+	The y-coordinate of the global node.
4	X2(N,3)	+	The mean water surface elevation of the global node.
EN Card		End of data control	
Field	Variable	Value	Description
C1-2	IC1	EN	Card group identifier.
C 3	IC3	D	End of input data.

I.2. File 2: flow file (BCFT file)

T1-T3 Cards	Job title
	Only one T1, T2, and T3 card can be used.

OP Card		Run option parameters	
Field	Variable	Value	Description
C 1-2	IC1	OP	Card group identifier.
C 3	IC3	1	Simulation selection.
1	KMOD		Index of flow/transport simulation.
		0	Neither flow nor transport simulation will proceed. Only data are read for testing purpose.
		1	Only flow is simulated.
		2	Only transport is simulated.
		12	Both flow and transport are simulated.
2	IRUN		Index of flow simulation run.
		-2	Quasi-steady flow is input from the file "STEADY.STO" for executing transient transport simulations.
		-1	Initial flow conditions are given for transient simulations.
		0	Quasi-steady flow will be compute under given boundary conditions.
		1	Quasi-steady flow will be computed first and then be used to simulate transient transport.
		2	Quasi-steady flow will be computed first and the final result will be used as the initial condition for transient simulations.

KMOD	IRUN	Simulation
0	any	Only input data are read
1	-1	Transient flow
1	0	Quasi-steady flow
1	2	Quasi-steady flow & transient flow
2	-2	Transient transport
12 or 2	1	Quasi-steady flow and transient transport
12	-1	Transient flow and transport
12	2	Quasi-steady flow & transient flow and transport

* (1,0) + (2,-2) = (12,1) or (2,1)

Field	Variable	Value	Description
C 1-2	IC1	OP	Card group identifier.
C 3	IC3	2	Solver specification.
1	ILUMP		Index of using mass lumping.
		0	No mass lumping.
		1	Mass lumping.
2	IPNTS		Index of using linear matrix solver for flow simulations.
		1	The pointwise iterative matrix solver.
		2	Preconditioned Conjugate Gradient Method (polynomial),
		3	Preconditioned Conjugate Gradient Method (Incomplete Cholesky).
3	IQUAR		Index of using quadrature for numerical integration.
		11	Nodal quadrature for both line and element integrations.
		12	Nodal quadarature for line integration and Gaussian quadrature for element integration.
		21	Gaussian quadarature for line integration and nodal quadrature for element integration.
		22	Gaussian quadrature for both line and element integrations.
4	IDIFF		Index of taking into account the eddy viscosity terms.
		1	Yes.
		0	No, the eddy viscosity terms are neglected.
5	IALLOW		Index of allowing the simulation to continue when there is no convergence reached for the non-linear iteration.
		1	Yes.
		0	No.
6	IMODEL		Index of simulating flow.
		1	Using MOC to solve the dynamic model only.
		-10	Specifying water depth and flow velocity with the initial condition. The flow equation is not solved.
7	IQUASI		Index of quasi-steady state check.
		0	No check.
		1	Performing the quasi-steady check

Field	Variable	Value	Description
C 1-2	IC1	OP	Card group identifier.
C 3	IC3	3	Weighting factor for simulations.
1	W		Time derivative weighting factor for flow simulation.
		0.5	Crank-Nicolson central.
		1.0	Backward difference.
2	OME		Relaxation parameter for solving nonlinear matrix equations.
		0.0-1.0	Under relaxation.
		1.0	Exact relaxation.
		1.0-2.0	Over relaxation.
3	OMI		Relaxation parameter for solving linearized matrix equation.
		0.0-1.0	Under relaxation.
		1.0	Exact relaxation.
		1.0-2.0	Over relaxation.

Field	Variable	Value	Description
C 1-2	IC1	OP	Card group identifier.
C 3	IC3	4	Preconditioned Conjugate Gradient method.
1	IEIGEN	0	GG will not be read.
		1	GG will be read.
2	GG	+	Upper bound of the maximum eigenvalue of the coefficient matrix used in the Preconditioned Conjugate Gradient method.

Field	Variable	Value	Description
C 1-2	IC1	OP	Card group identifier.
C 3	IC3	5	Method of characteristics.
1	ISK		Index of choosing the directions of characteristics.
		-1	Using the velocity direction as the direction of characteristics.
		0	Solve the diagonalization equations for the directions.
		1	Specify directions by users.
2	ANGLE1	+	User specified angle for the direction of the first characteristic. (COS(ANGLE1), SIN(ANGLE1)) is the direction.
3	ANGLE2	+	User specified direction for the second and third characteristics. (COS(ANGLE2), SIN(ANGLE2)) is the direction.

IP Card — Iteration Parameters

Field	Variable	Value	Description
C 1-2	IC1	IP	Card group identifier.
C 3	IC3	1	Total simulation time.
1	NNITER	+	Allowed number for the non-linear iteration in the flow simulation.
2	NPITER	+	Allowed number for the linearized iteration in the flow simulation.
3	TOLBH	+	Allowed relative error for water depth.
4	TOLBV	+	Allowed relative error for velocity components.
5	V_CUT	+	Cut-off of velocity. If the computed velocity is smaller than this value, it is set to zero.
6	FMSR	+	Multiplication factor to set the allowed mean square root errors, BHMSR for water depth and BVMSR for velocity, where BHMSR = TOLBH*FMSR; BVMSR = TOLBV*FMSR.
7	ACCU	+	The allowed absolute error between two tidal cycles to reach quasi-steady state.

PT Card — Time marching parameters

Field	Variable	Value	Description
C 1-2	IC1	PT	Card group identifier.
C 3	IC3	1	Total simulation time.
1	NXW	+	Subelement number in one direction that is used in the "in-element" particle tracking. The total subelement number included in one global element is NXW*NXW.
2	IDETQ		Index of particle tracking approach.
		1	Using the average-velocity approach.
		2	Using the constant-velocity approach.

TC Card		Iteration Parameters	
Field	Variable	Value	Description
C 1-2	IC1	TC	Card group identifier.
C 3	IC3	1	Total simulation time.
1	TMAX	+	Maximum simulation time. [T]
2	DELT	+	Time duration (period) of one tidal cycle. [T]
3	NTI	+	No. of tidal cycles.
4	NTIC	+	No. of time steps in a tidal cycle.
5	NTCK	+	No. of time step intervals to check quasi-steady flow. For instance, if NTCK = 10, we check quasi-steady flow by comparing the computational results every 10 time steps from corresponding times in successive tidal cycles.
6	NTSTO	+	No. of time step intervals to record flow results for future use after the quasi-steady condition is reached.
7	NTRANSP	+	No. of time step intervals to compute transport. For instance, if NTRANSP = 5, we perform one transport computation in five flow time steps.

OC Card		Output control parameters	
Field	Variable	Value	Description
C 1-2	IC1	OC	Card group identifier.
C 3	IC3	1	Print control parameters.
1	JOPT	0	Print at specified intervals.
		1	Print at specified set of time values.
2	KPRT	+	Specify the interval if JOPT = 0.
	NPRINT	+	Specify total number of the specified times, if JOPT=1.
Note: NPRINT new lines after OC1 card are needed if JOPT = 1.			
(the first new line)			
1	TPRT(1)	+	The 1-st specified time moment at which the associated simulation results are to be printed.
(the second new line)			
1	TPRT(2)	+	The 2-nd specified time moment at which the associated simulation results are to be printed.
			.
			.
(the NPRINT new line)			
1	TPRT(NPRINT)	+	The NPRINT-th specified time moment at which the associated simulation results are to be printed.

Field	Variable	Value	Description
C 1-2	IC1	OC	Card group identifier
C 3	IC3	2	Print options.
1	NSELT	+	Total options to be selected.
2	KPR0(i)		Print options.
		1	Print water surface elevation.
		2	Print velocity.
		3	Print water depth.

Field	Variable	Value	Description
C 1-2	IC1	OC	Card group identifier.
C 3	IC3	3	Output control for post-process.
1	IFILE	0	Save as ascii format.
		1	Save as binary format.
2	KOPT	0	Save at specified interval.
		1	Save at specified set of times.
3	KDSK	+	Save every specified interval, if KOPT=0.
	NPOST	+	Save at specified set of times, if KOPT=1.

Note: NPOST new lines after OC3 card are needed if KOPT = 1.

(the first new line)			
	TSV(1)	+	The 1-st specified time moment at which the associated simulation results are to be saved.
(the second new line)			
	TSV(2)	+	The 2-nd specified time moment at which the associated simulation results are to be saved.
			.
			.
(the NPOST new line)			
	TSV(NPOST)	+	The NPOST-th specified time moment at which the associated simulation results are to be saved.

Field	Variable	Value	Description
C 1-2	IC1	OC	Card group identifier.
C 3	IC3	4	Solution file output options.
1	KSELT	+	Total options to be selected.
2	KSAVE(i)		Save options.
		1	Save water surface elevation.
		2	Save flux.
		3	Save water depth.

MP Card — Material property parameters

Field	Variable	Value	Description
C 1-2	IC1	MP	Card group identifier.
C 3	IC3	1	Material property.
1	i	+	id of material type.
2	PROP(1,i)	+	Manning's roughness associated with the material type.
3	PROP(2,i)	+	xx-eddy viscosity associated with the material type. [L^2/T]
4	PROP(3,i)	+	yy-eddy viscosity associated with the material type. [L^2/T]
5	PROP(4,i)	+	xy-eddy viscosity associated with the material type. [L^2/T]

Field	Variable	Value	Description
C 1-2	IC1	MP	Card group identifier.
C 3	IC3	2	Density of water and acceleration of gravity.
1	ITUNIT		Index of time unit.
		1	The time unit for simulation is second.
		2	The time unit for simulation is minute.

		3	The time unit for simulation is hour.
2	ILUNIT		Index of length unit.
		1	The length unit for simulation is meter.
		2	The length unit for simulation is foot.
		3	The length unit for simulation is kilometer.
		4	The length unit for simulation is mile.
3	RHO	+	Density of water, (M/L^3).

RF Card — Rainfall parameters

Field	Variable	Value	Description
C 1-2	IC1	RF	Card group identifier.
C 3	IC3	1	Rainfall data for the simulation.
1	i	+	id of global element.
2	IRTYP(i)	+	id of xy series to describe the time-dependent rainfall rate for the element.

SS Card — Source/sink parameters

Field	Variable	Value	Description
C 1-2	IC1	SS	Card group identifier.
C 3	IC3	1	Source/sink data for the simulation.
1	i	+	id of the global node.
2	ISR(i)	+	id of xy series to describe the time-dependent source/sink rate for the node.

OB Card — Open boundary parameters

Field	Variable	Value	Description
C 1-2	IC1	OB	Card group identifier.
C 3	IC3	1	Dirichlet boundary nodes for the simulation.
1	NPDB(j)	+	id of global node corresponding to the j-th Dirichlet boundary node.
2	IDTYP(j)	+	id of xy series to describe the time-dependent water surface elevation or water depth profile associated with the Dirichlet boundary node.
3	IDBH(j)		Index of the profile type for the j-th Dirichlet boundary node.
		1	This profile is a time-dependent water surface elevation profile.
		-1	This profile is an analytical function as the form of $a\sin 2\pi(t+t_0)/T$. The associated xy series needs two points to describe a and t_0.

Field	Variable	Value	Description
C 1-2	IC1	OB	Card group identifier.
C 3	IC3	2	Flux-type boundary sides for the simulation.
1	NSCB(j,1)	+	id of global node corresponding to the 1-st node of the j-th flux-type boundary side.
2	NSCB(j,2)	+	id of global node corresponding to the 2-nd node of the j-th flux-type boundary side.
3	ICTYP(j,1)	+	id of xy series to describe the time-dependent normal flux profile associated with the open boundary side.

IC Card — Initial condition data parameters

Field	Variable	Value	Description
C 1-2	IC1	IC	Card group identifier.
C 3	IC3	H	Water surface elevation.
1	IHEAD	0	Constant water surface elevation.
		1	Variable water surface elevation. In this case, the user needs to specify an ICWD file in the super file as explained in the end of this appendix.
2	HCONST	+	Value of the constant water surface elevation for IHEAD = 0. [L]

Field	Variable	Value	Description
C 1-2	IC1	IC	Card group identifier.
C 3	IC3	U	Velocity.
1	IV	0	Constant velocity.
		1	Variable velocity. In this case, the user needs to specify an ICQL file in the super file as explained in the end of this appendix.
2	UCONST	+	Value of the constant velocity. [L/T]
3	VCONST	+	Value of the constant velocity. [L/T]

Field	Variable	Value	Description
C 1-2	IC1	IC	Card group identifier.
C 3	IC3	S	Initial condition start type.
1	ISTART	0	Cold start, water depth/water surface elevation and velocity.
		1	Hot start, water surface elevation and velocity.

Field	Variable	Value	Description
C 1-2	IC1	IC	Card group identifier.
C 3	IC3	T	Initial condition start time.
1	HSTIME	+	Time corresponding for the hot start.

XY Card — X-Y Series Parameters

Field	Variable	Value	Description
C 1-2	IC1	XY	Card group identifier.
C 3	IC3	1	Generation of any x-y series function.
1	i	+	Index number for x-y series.
2	NPOINT(i)	+	The number of x-y values in the series.
3	DELTAX	0	Dummy values.
4	DELTAY	0	Dummy values.
5	REPEAT	0	Dummy values.
6	BEGCYC	0	Dummy values.
7	TNAME	+	A character string representing the name of the XY series.
(new line)X,Y		After XY card, the x-y values of the series are listed one pair per line up to NPOINT(i).	

EN Card — End of data control

Field	Variable	Value	Description
C1-2	IC1	EN	Card group identifier.

C 3	IC3	D	End of input data.

I.3. File 3: transport file (BCTT file)

T1-T3 Cards — Job title

Only one T1, T2, and T3 card can be used.

OP Card — Run option parameters

Field	Variable	Value	Description
C 1-2	IC1	OP	Card group identifier.
C 3	IC3	1	Simulation selection.
1	IDCHEM		Index of chemical transport simulation.
		0	Chemical transport is not simulated.
		1	Chemical transport is simulated.
2	IDSED		Index of sediment transport simulation.
		0	Sediment transport is not simulated.
		1	Sediment transport is simulated.

Field	Variable	Value	Description
C 1-2	IC1	OP	Card group identifier.
C 3	IC3	2	Solver specification.
1	ILUMPT		Index of using mass lumping for transport simulations.
		0	No mass lumping.
		1	Mass lumping.
2	IPNTST		Index of using linear matrix solver for transport simulations.
		1	The pointwise iterative matrix solver.
		2	Preconditioned Conjugate Gradient Method (polynomial),
		3	Preconditioned Conjugate Gradient Method (Incomplete Cholesky).
3	IQUART		Index of using quadrature for numerical integration.
		11	Nodal quadrature for both line and element integrations.
		12	Nodal quadarature for line integration and Gaussian quadrature for element integration.
		21	Gaussian quadarature for line integration and nodal quadrature for element integration.
		22	Gaussian quadrature for both line and element integrations.
4	IADAPT		Index of using adapted implicit-explicit scheme for the predictor step.
		0	No.
		1	Yes.

Field	Variable	Value	Description
C 1-2	IC1	OP	Card group identifier.
C 3	IC3	3	Weighting factor for transport simulations.
1	WT		Time derivative weighting factor for transport simulation.
		0.5	Crank-Nicolson central.
		1.0	Backward difference.

2	OMET		Relaxation parameter for solving nonlinear matrix equations.
		0.0-1.0	Under relaxation.
		1.0	Exact relaxation.
		1.0-2.0	Over relaxation.
3	OMIT		Relaxation parameter for solving linearized matrix equation.
		0.0-1.0	Under relaxation.
		1.0	Exact relaxation.
		1.0-2.0	Over relaxation.

Field	Variable	Value	Description
C 1-2	IC1	OP	Card group identifier.
C 3	IC3	4	Preconditioned Conjugate Gradient method.
1	IEIGENT	0	GGT will not be read.
		1	GGT will be read.
2	GGT	+	Upper bound of the maximum eigenvalue of the coefficient matrix used in the Preconditioned Conjugate Gradient method.

IP Card — Iteration Parameters

Field	Variable	Value	Description
C 1-2	IC1	IP	Card group identifier.
C 3	IC3	1	Total simulation time.
1	NNITERT	+	Allowed number for the non-linear iteration.
2	NPITER	+	Allowed number for the linearized iteration.
3	TOLBC	+	Allowed relative error for getting convergent transport solutions for chemicals.
4	TOLBS	+	Allowed relative error for getting convergent transport solutions for sediments.

PT Card — Particle tracking parameters

Field	Variable	Value	Description
C 1-2	IC1	PT	Card group identifier.
C 3	IC3	1	Particle tracking controlling parameters.
1	NXWT	+	Subelement number in one direction that is used in the "in-element" particle tracking. The total subelement number included in one global element is NXWT*NXWT.
2	IDETQT		Index of particle tracking approach.
		1	Using the average-velocity approach.
		2	Using the constant-velocity approach.

MP Card — Material property parameters

Field	Variable	Value	Description
C 1-2	IC1	MP	Card group identifier.
C 3	IC3	1	Material property for transport.
1	i	+	id of material type.
2	PROPT(1,i)	+	Longitudinal dispersivity associated with the material type. [L]
3	PROPT(2,i)	+	Lateral dispersivity associated with the material type. [L]
4	PROPT(3,i)	+	Pure diffusion coefficient associated with the material type. [L^2/T]

SS card — Source/sink parameters

Field	Variable	Value	Description
C 1-2	IC1	SS	Card group identifier.
C 3	IC3	1	Source/sink profile for dissolved chemicals.
1	NP	+	id of the global node.
2	j	+	id of dissolved chemical.
3	ITSR(NP,j)	+	id of xy series to describe the time-dependent source/sink profile for the dissolved chemical at the global node.

Field	Variable	Value	Description
C 1-2	IC1	SS	Card group identifier.
C 3	IC3	2	Source/sink profile for suspended sediment.
1	NP	+	id of the global node.
2	j	+	id of suspended sediment size.
3	NCHEM	+	Number of dissolved chemicals.
4	ITSR(NP,m)	+	id of xy series to describe the time-dependent source/sink profile for the suspended sediment size at the global node, where $m = NCHEM + j$.

Field	Variable	Value	Description
C 1-2	IC1	SS	Card group identifier.
C 3	IC3	3	Source/sink profile for particulate chemicals on suspended sediments.
1	NP	+	id of the global node.
2	j	+	id of suspended sediment.
3	k	+	id of particulate chemical.
4	NCHEM	+	Number of dissolved chemicals.
5	NSSIZE	+	Number of sediment sizes.
6	ITSR(NP,m)	+	id of xy series to describe the time-dependent source/sink profile for the particulate chemical on the suspended sediment size at the global node, where $m = NCHEM + NSSIZE + (j-1)*NCHEM + k$, $j \in [1,NSSIZE]$, and $k \in [1, NCHEM]$.

DB Card — Dirichlet boundary parameters

Field	Variable	Value	Description
C 1-2	IC1	DB	Card group identifier.
C 3	IC3	1	Dirichlet boundary conditions for dissolved chemicals.
1	NP	+	id of Dirichlet boundary node.
2	NPDBT(NP)	+	id of global node corresponding to the Dirichlet boundary node.
3	i	+	id of dissolved Chemical.
4	IDTYPT(NP,i)	+	id of xy series to describe the of time-dependent concentration profile associated with the Dirichlet boundary node for the dissolved chemical.

Field	Variable	Value	Description
C 1-2	IC1	DB	Card group identifier.
C 3	IC3	2	Dirichlet boundary conditions for suspended sediments.
1	NP	+	id of Dirichlet boundary node.

2	NPDBT(NP)	+	id of global node corresponding to the Dirichlet boundary node.
3	k	+	id of suspended sediment size.
4	NCHEM	+	Number of dissolved chemicals.
5	IDTYPT(NP,i)	+	id of xy series to describe the time-dependent concentration profile associated with the Dirichlet boundary node for the suspended sediment, *where i = NCHEM+k.*

Field	Variable	Value	Description
C 1-2	IC1	DB	Card group identifier.
C 3	IC3	3	Dirichlet boundary conditions for particulate chemicals on suspended sediments.
1	NP	+	id of Dirichlet boundary node.
2	NPDBT(NP)	+	id of global node corresponding to the Dirichlet boundary node.
3	j	+	id of suspended sediment size.
4	k	+	id of particulate chemical.
5	NCHEM	+	Number of dissolved chemicals.
6	NSSIZE	+	Number of sediment sizes.
7	IDTYPT(NP,i)	+	id of xy series to describe the time-dependent concentration profile associated with the Dirichlet boundary node for the particulate chemical on the suspended sediment, *where i = NCHEM + NSSIZE + (j-1)*NCHEM + k, $j \in [1,NSSIZE]$, and $k \in [1, NCHEM]$.*

FB Card — Flux-type boundary parameters

Field	Variable	Value	Description
C 1-2	IC1	FB	Card group identifier.
C 3	IC3	1	Flux-type boundary conditions for dissolved chemicals.
1	NS	+	id of flux-type boundary side.
2	NSCBT(NS,1)	+	id of global node corresponding to the 1-st node of the flux-type boundary side.
3	NSCBT(NS,2)	+	id of global node corresponding to the 2-nd node of the flux-type boundary side.
4	NSCBT(NS,3)		Index of boundary condition type for the flux-type boundary side.
		1	This is a Variable boundary side with the time-dependent concentration specified if the flow is incoming.
		2	This is a Cauchy boundary side with the time-dependent Cauchy flux specified.
		3	This is a Neumann boundary side with the time-dependent Neumann flux specified.
5	i	+	id of dissolved Chemical.
6	ICTYPT(NS,i)	+	id of xy series to describe the of time-dependent profile associated with the flux-type boundary side for the dissolved chemical. It is (1) a concentration profile when NSCBT(j,2) = 1. (2) a Cauchy flux profile when NSCBT(j,2) = 2. (3) a Neumann flux profile when NSCBT(j,2) = 3.

Field	Variable	Value	Description
C 1-2	IC1	FB	Card group identifier.

C 3	IC3	2	Flux-type boundary conditions for suspended sediments.
1	NS	+	id of flux-type boundary side.
2	NSCBT(NS,1)	+	id of global node corresponding to the 1-st node of the flux-type boundary side.
3	NSCBT(NS,2)	+	id of global node corresponding to the 2-nd node of the flux-type boundary side.
4	NSCBT(NS,3)		Index of boundary condition type for the flux-type boundary side.
		1	This is a Variable boundary node with the time-dependent concentration specified if the flow is incoming.
		2	This is a Cauchy boundary node with the time-dependent Cauchy flux specified.
		3	This is a Neumann boundary node with the time-dependent Neumann flux specified.
5	k	+	id of suspended sediment size.
6	NCHEM	+	Number of dissolved chemicals.
7	ICTYPT(NS,i)	+	id of xy series to describe the time-dependent profile associated with the flux-type boundary side for the suspended sediment, *where i = NCHEM+k.* It is (1) a concentration profile when NSCBT(j,2) = 1. (2) a Cauchy flux profile when NSCBT(j,2) = 2. (3) a Neumann flux profile when NSCBT(j,2) = 3.

Field	Variable	Value	Description
C 1-2	IC1	FB	Card group identifier.
C 3	IC3	3	Flux-type boundary conditions for particulate chemicals on suspended sediments.
1	NS	+	id of flux-type boundary side.
2	NSCBT(NS,1)	+	id of global node corresponding to the 1-st node of the flux-type boundary side.
3	NSCBT(NS,2)	+	id of global node corresponding to the 2-nd node of the flux-type boundary side.
4	NSCBT(NS,3)		Index of boundary condition type for the flux-type boundary side.
		1	This is a Variable boundary node with the time-dependent concentration specified if the flow is incoming.
		2	This is a Cauchy boundary node with the time-dependent Cauchy flux specified.
		3	This is a Neumann boundary node with the time-dependent Neumann flux specified.
5	j	+	id of suspended sediment size.
6	k	+	id of particulate chemical.
7	NCHEM	+	Number of dissolved chemicals.
8	NSSIZE	+	Number of sediment sizes.
9	ICTYPT(NS,i)	+	id of xy series to describe the time-dependent profile associated with the flux-type boundary side for the particulate chemical on the suspended sediment, *where i = NCHEM + NSSIZE + (j-1)*NCHEM + k, j ∈ [1,NSSIZE], and k ∈ [1, NCHEM].* It is (1) a concentration profile when NSCBT(j,2) = 1. (2) a Cauchy flux profile when NSCBT(j,2) = 2.

(3) a Neumann flux profile when NSCBT(j,2) = 3.

ON Card		Ocean-type boundary parameters	
Field	Variable	Value	Description
C 1-2	IC1	ON	Card group identifier.
C 3	IC3	1	Material property for Ocean-type boundary conditions.
1	i	+	id of material type.
2	FDCAY(i)	+	Flushing decay rate. [1/T]

Field	Variable	Value	Description
C 1-2	IC1	ON	Card group identifier.
C 3	IC3	2	Ocean-type boundary conditions for dissolved chemicals.
1	NS	+	id of flux-type boundary side.
2	NSNBT(NS,1)	+	id of global node corresponding to the 1-st node of the ocean-type boundary side.
3	NSNBT(NS,2)	+	id of global node corresponding to the 2-nd node of the ocean-type boundary side.
4	i	+	id of dissolved Chemical.
5	INTYPT(NS,i)	+	material id associated with the ocean-type boundary side for specifying the flushing decay rate of the dissolved chemical.

Field	Variable	Value	Description
C 1-2	IC1	ON	Card group identifier.
C 3	IC3	3	Ocean-type boundary conditions for suspended sediments.
1	NS	+	id of ocean-type boundary side.
2	NSNBT(NS,1)	+	id of global node corresponding to the 1-st node of the ocean-type boundary side.
3	NSNBT(NS,2)	+	id of global node corresponding to the 2-nd node of the ocean-type boundary side.
4	k	+	id of suspended sediment size.
5	NCHEM	+	Number of dissolved chemicals.
6	INTYPT(NS,i)	+	material id of associated with the ocean-type boundary side for specifying the flusing decay rate of the suspended sediment, *where i = NCHEM+k.*

Field	Variable	Value	Description
C 1-2	IC1	ON	Card group identifier.
C 3	IC3	4	Ocean-type boundary conditions for particulate chemicals on suspended sediments.
1	NS	+	id of ocean-type boundary side.
2	NSNBT(NS,1)	+	id of global node corresponding to the 1-st node of the ocean-type boundary side.
3	NSNBT(NS,2)	+	id of global node corresponding to the 2-nd node of the ocean-type boundary side.
4	j	+	id of suspended sediment size.
5	k	+	id of particulate chemical.
6	NCHEM	+	Number of dissolved chemicals.
7	NSSIZE	+	Number of sediment sizes.

8	INTYPT(NS,i)	+	material id of associated with the ocean-type boundary side for specifying the flushing decay rate of the particulate chemical on the suspended sediment, *where i = NCHEM + NSSIZE + (j-1)*NCHEM + k, j ∈ [1,NSSIZE], and k ∈ [1, NCHEM].*

RS card — Rainfall source parameters

Field	Variable	Value	Description
C 1-2	IC1	RS	Card group identifier.
C 3	IC3	1	Rainfall source profile for dissolved chemicals.
1	j	+	id of dissolved chemical.
2	IRC(j)	+	id of xy series to describe the time-dependent rainfall source profile for the dissolved chemical.

IC card — Initial condition parameters

Field	Variable	Value	Description
C 1-2	IC1	IC	Card group identifier.
C 3	IC3	1	Initial condition parameters.
1	IDCONC		index of initial concentrations.
		0	constant initial concentrations.
		1	variable initial concentrations. In this case, the user needs to specify ICCN, ICCP, and ICCS files in the super file as explained in the end of this appendix.

Field	Variable	Value	Description
C 1-2	IC1	IC	Card group identifier.
C 3	IC3	2	Initially constant conditions for dissolved chemicals.
1	j	+	id of the dissolved chemical being input.
2	CCONST(j)	+	Specified initial concentration for the dissolved chemical. [M/L^3]

Field	Variable	Value	Description
C 1-2	IC1	IC	Card group identifier.
C 3	IC3	3	Initially constant conditions for particulate chemicals on suspended sediments
1	j	+	id of the particulate chemical being input.
2	i	+	id of the suspended sediment size where the particulate chemical is.
3	NCHEM	+	Number of dissolved chemicals.
4	CCONST(k)	+	Specified initial concentration for the particulate chemical on suspended sediment being input, where k = i*NCHEM + j. [M/M]

Field	Variable	Value	Description
C 1-2	IC1	IC	Card group identifier.
C 3	IC3	4	Initially constant conditions for particulate chemicals on bed sediments
1	j	+	id of the particulate chemical being input.
2	i	+	id of the bed sediment size where the particulate chemical is.
3	NCHEM	+	Number of dissolved chemicals.
4	NSSIZE	+	Number of sediment sizes.

5	CCONST(k)	+	Specified initial concentration for the particulate chemical on the bed sediment being input, where k = (I+NSSIZE)* NCHEM + j. [M/M]

Field	Variable	Value	Description
C 1-2	IC1	IC	Card group identifier.
C 3	IC3	5	Initially constant conditions for suspended sediments.
1	i	+	id of the suspended sediment size being input.
2	SCONST(i)	+	Specified initial concentration for the suspended sediment of the i-th size. [M/L^3]

Field	Variable	Value	Description
C 1-2	IC1	IC	Card group identifier.
C 3	IC3	6	Initially constant conditions for bed sediments.
1	i	+	id of the bed sediment size being input.
2	NSSIZE	+	Number of sediment sizes.
3	SCONST(k)	+	Specified initial concentration for the bed sediment of the i-th size, where k = NSSIZE + i. [M/L^3]

Field	Variable	Value	Description
C 1-2	IC1	IC	Card group identifier.
C 3	IC3	7	Initially constant conditions for dissolved chemicals in the interstitial water of bed sediments
1	i	+	id of the dissolved chemical being input.
2	NCHEM	+	Number of dissolved chemicals.
3	NSSIZE	+	Number of sediment sizes.
4	CCONST(k)	+	Specified initial concentration for the bed sediment of the i-th size, where k = NSSIZE + i. [M/L^3]

XY Card — X-Y Series Parameters

Field	Variable	Value	Description
C 1-2	IC1	XY	Card group identifier.
C 3	IC3	1	Generation of any x-y series function.
1	i	+	Index number for x-y series.
2	NPOINT(i)	+	The number of x-y values in the series.
3	DELTAX	0	Dummy values.
4	DELTAY	0	Dummy values.
5	REPEAT	0	Dummy values.
6	BEGCYC	0	Dummy values.
7	TNAME	+	A character string representing the name of the XY series.
(new line)X,Y			After XY card, the x-y values of the series are listed one pair per line up to NPOINT(i).

EN Card — End of data control

Field	Variable	Value	Description
C1-2	IC1	EN	Card group identifier.
C 3	IC3	D	End of input data.

I.4. File 4: contaminant/sediment and reaction information file (CHEM file)

T1-T3 Cards		Job title	
		Only one T1, T2, and T3 card can be used.	

RX card		Chemical reaction parameters	
Field	Variable	Value	Description
C 1-2	IC1	RX	Card group identifier.
C 3	IC3	1	Numbers of reactions and chemicals
1	NRXN	+	Number of reactions.
2	NCHEM	+	Number of dissolved chemicals.

Field	Variable	Value	Description
C 1-2	IC1	RX	Card group identifier.
C 3	IC3	2	Chemical names
1	NCHEM	+	Number of dissolved Chemical.
Note: NCHEM new lines are needed.			
(the first new line)			
CHEMN(1)		+	Name of the 1-st dissolved chemical.
(the second new line)			
CHEMN(2)		+	Name of the 2-nd dissolved chemical.
			.
			.
(the NCHEM-th new line)			
CHEMN(NCHEM)		+	Name of the NCHEM-th dissolved chemical.

Field	Variable	Value	Description
C 1-2	IC1	RX	Card group identifier.
C 3	IC3	3	Reaction rate constants and stoichiometry
1	j	+	id of chemical reaction.
2	NCHEM	+	Number of dissolved chemicals.
3	FKRX(j)	+	Forward reaction rate constant of the reaction. [reaction dependent]
4	BKRX(j)	+	Backward reaction rate constant of the reaction. [reaction dependent]
Note: Two new lines are needed.			
(the first new line)			
1	NURTS(j,1)	+	Stoichiometric coefficient of the 1-st dissolved chemical (on the reactant side) in the reaction.
2	NURTS(j,2)	+	Stoichiometric coefficient of the 2-nd dissolved chemical (on the reactant side) in the reaction.
			.
			.
up to NURTS(j,NCHEM)			
(the second new line)			
1	NUPDS(j,1)	+	Stoichiometric coefficient of the 1-st dissolved chemical (on the product side) in the reaction.
2	NUPDS(j,2)	+	Stoichiometric coefficient of the 2-nd dissolved chemical (on the product side) in the reaction.

.
.

up to NUPDS(j,NCHEM)

ST card		Sediment parameters	
Field	Variable	Value	Description
C 1-2	IC1	ST	Card group identifier.
C 3	IC3	1	Number of sediment sizes
1	NSSIZE	+	Number of sediment sizes.
2	EXCHNG	+	Exchange coefficient accounting for diffusion of chemicals between pore water and column water.

Field	Variable	Value	Description
C 1-2	IC1	ST	Card group identifier.
C 3	IC3	2	Parameter associated with each sediment size.
1	j	+	id of Sediment size.
2	SPARA(j,1)		The type of the sediment size.
		1	Cohesive sediment, e.g., clay and silt.
		2	Non-cohesive sediment, e.g., sand.
3	SPARA(j,2)	+	Settling speed of the sediment size. [L/T]
4	SPARA(j,3)	+	Critical shear stress for deposition of the sediment size. [M/L/T^2]
5	SPARA(j,4)	+	Critical shear stress for erosion of the j-th size fraction of sediment. [M/L/T^2]
6	SPARA(j,5)	+	Erodibility of the sediment size. [M/L^2]
7	SPARA(j,6)	+	Specific weight of the sediment size. [M/L^3]
8	SPARA(j,7)	+	Median diameter of particles in mixture of the sediment size. [L]
9	SPARA(j,8)	+	Critical bottom shear stress of the sediment size at which sediment movement begins. [M/L/T^2]

Field	Variable	Value	Description
C 1-2	IC1	ST	Card group identifier.
C 3	IC3	3	Sorption rate constants related to suspended sediment.
1	j	+	id of suspended sediment size.
2	i	+	id of dissolved chemical.
3	FKSPSS(j,1)	+	Forward rate constant of the sorption of i-th dissolved chemical onto the suspended sediment of the j-th size. [L^3/M/T]
4	BKSPSS(j,2)	+	Backward rate constant of the sorption of i-th dissolved chemical onto the suspended sediment of the j-th size. [1/T]

Field	Variable	Value	Description
C 1-2	IC1	ST	Card group identifier.
C 3	IC3	4	Sorption rate constants related to bed sediment.
1	j	+	id of bed sediment size.
2	i	+	id of dissolved chemical.
3	FKSPBS(j,i)	+	Forward rate constant of the sorption of i-th dissolved chemical onto the bed sediment of the j-th size. [L^3/M/T]
4	BKSPBS(j,i)	+	Backward rate constant of the sorption of i-th dissolved chemical

			onto the bed sediment of the j-th size. [1/T]
5.	FKSP2(j,i)	+	Forward rate constant of the sorption of i-th chemical in the interstitial water onto the bed sediment of the j-th size. [L^3/M/T]
6.	BKSP2(j,i)	+	Backward rate constant of the sorption of i-th chemical in the interstitial water onto the bed sediment of the j-th size. [L^3/M/T]

Field	Variable	Value	Description
C 1-2	IC1	ST	Card group identifier.
C 3	IC3	5	The intrinsic properties related to bed sediment.
1	j	+	id of bed sediment size.
2	RHOB(j)	+	Bulk density of the j-th size particle of bed sediments. [M/L^3]
3	THETA(j)	+	Porosity of the j-th size particle of bed sediments.

VO card — Volatilization parameters

Field	Variable	Value	Description
C 1-2	IC1	VO	Card group identifier.
C 3	IC3	1	Volatilization rate constants.
1	j	+	id of dissolved chemical.
2	IAP(j)	+	id of xy series to describe the time-dependent partial atmospheric pressure profile of the dissolved chemical. [atm]
3	FKVO(j)	+	Forward volatilization rate constant of the dissolved chemical. [1/T]
4	BKVO(j)	+	Backward volatilization rate constant of the dissolved chemical. [M/atm/L^3/T]

DY card — 1-st order decay parameters

Field	Variable	Value	Description
C 1-2	IC1	DY	Card group identifier.
C 3	IC3	1	Decay constants of dissolved chemicals.
1	j	+	id of dissolved chemical.
2	DECAY(j)	+	1-st order decay constant of the dissolved chemical. [1/T]

Field	Variable	Value	Description
C 1-2	IC1	DY	Card group identifier.
C 3	IC3	2	Decay constants of particulate chemicals on suspended sediments.
1	j	+	id of sediment size.
2	i	+	id of particulate chemical.
3	NCHEM	+	Number of dissolved chemicals.
4	DCY	+	Decay constant of the particulate chemical on the suspended sediment. [1/T]

Field	Variable	Value	Description
C 1-2	IC1	DY	Card group identifier.
C 3	IC3	3	Decay constants of particulate chemicals on bed sediments.
1	j	+	id of sediment size.
2	i	+	id of particulate chemical.
3	NCHEM	+	Number of dissolved chemicals.
4	NSSIZE	+	Number of sediment sizes.

5	DCY	+	Decay constant of the particulate chemical on the bed sediment. [1/T]

XY Card		X-Y Series Parameters	
Field	Variable	Value	Description
C 1-2	IC1	XY	Card group identifier.
C 3	IC3	1	Generation of any x-y series function.
1	i	+	Index number for x-y series.
2	NPOINT(i)	+	The number of x-y values in the series.
3	DELTAX	0	Dummy values.
4	DELTAY	0	Dummy values.
5	REPEAT	0	Dummy values.
6	BEGCYC	0	Dummy values.
7	TNAME	+	A character string representing the name of the XY series.
(new line)X,Y		After XY card, the x-y values of the series are listed one pair per line up to NPOINT(i).	

EN Card		End of data control	
Field	Variable	Value	Description
C1-2	IC1	EN	Card group identifier.
C 3	IC3	D	End of input data.

I.5. File 5: initial water surface elevation file (ICWD file)

This file includes the following lines:

1st line: (A7)
1. File title.

2nd line: (A7, 1X, A6)
1. Data title.
2. **BEGSCL**

3rd line: (A6)
1. **BEGSCL**

4th line: (A2,I8)
1. **ND**
2. number of nodes.

5th line: (A2,I8)
1. **EM**
2. number of elements.

6th line: (A4,1X,A40)
1. subtitle 1.
2. subtitle 2.

7th line: (A2,A4,D16.8)
1. **TI**
2. any four characters.
3. initial time.

In the next NNP (number of nodes) lines, each line contains one record stating the water surface elevation at the corresponding node.
1. initial water surface elevation.

I.6. File 6: initial velocity (ICQL file)

This file includes the following lines:

1st line: (A7)
2. File title.

2nd line: (A7, 1X, A6)
1. Data title.
2. **BEGVEC**

3rd line: (A6)
1. **BEGVEC**

4th line: (A2,I8)
1. **ND**
2. number of nodes.

5th line: (A2,I8)
1. **EM**
2. number of elements.

6th line: (A4,1X,A40)
1. subtitle 1.
2. subtitle 2.

7th line: (A2,A4,D16.8)
1. **TI**
2. any four characters.
3. initial time.

In the next NNP (number of nodes) lines, each line contains two record stating the x- and y- velocity components at the corresponding node. (Free format)

1. initial x-velocity.
2. initial y-velocity.

I.7. File 7: initial dissolved chemical concentration file (ICCN file)

This file includes the following lines

1st line: (A7)
3. File title.

2nd line: (A7, 1X, A6)
1. Data title.
2. **BEGSCL**

3rd line: (A6)
1. **BEGSCL**

4th line: (A2,I8)
1. **ND**
2. number of nodes.

5th line: (A2,I8)
1. **EM**
2. number of elements.

6th line: (A4,1X,A40)
1. subtitle 1.
2. subtitle 2.

7th line: (A2,A4,D16.8)
1. **TI**
2. any four characters.
3. initial time.

In the next NCHEM*NNP (number of nodes) lines, the user input the dissolved concentrations according to the following logic. (Free format)

```
DO I = 1,NCHEM
  DO NP=1,NNP
    C(NP,I)  CB(NP,I)
  ENDDO
ENDDO
```

where C(NP, I) and CB(NP,I) are the initial dissolved concentration in the water column and in the interstitial water, respectively, associated with the I^{th} chemical at the NP^{th} node.

I.8. File 8: initial particulate chemical concentration file (ICPN file)

This file includes the following lines

1st line: (A7)
1. File title.

2nd line: (A7, 1X, A6)
1. Data title.
2. **BEGSCL**

3rd line: (A6)
1. **BEGSCL**

4th line: (A2,I8)
1. **ND**
2. number of nodes.

5th line: (A2,I8)
1. **EM**
2. number of elements.

6th line: (A4,1X,A40)
1. subtitle 1.
2. subtitle 2.

7th line: (A2,A4,D16.8)
1. **TI**
2. any four characters.
3. initial time.

In the next NCHEM*NSSIZE*NNP (number of nodes) lines, the user input the particulate chemical concentrations according to the following logic. (Free format)

```
DO I = 1,NCHEM
  DO J=1,NSSIZE
    DO NP=1,NNP
      PS(NP,J,I)  PB(NP,J,I)
    ENDDO
  ENDDO
ENDDO
```

where PS(NP,J,I) and PB(NP,J,I) are the initial particulate chemical concentration associated with the I^{th} chemical on the J^{th} suspended and bed sediments, respectively, at the NP^{th} node.

I.9. File 9: initial sediment concentration file (ICSN file)

This file includes the following lines

1st line: (A7)
1. File title.

2nd line: (A7, 1X, A6)
1. Data title.
2. **BEGSCL**

3rd line: (A6)
1. **BEGSCL**

4th line: (A2,I8)
1. **ND**
2. number of nodes.

5th line: (A2,I8)
1. **EM**
2. number of elements.

6th line: (A4,1X,A40)
1. subtitle 1.
2. subtitle 2.

7th line: (A2,A4,D16.8)
1. **TI**
2. any four characters.
3. initial time.

In the next NSSIZE*NNP (number of nodes) lines, the user input the sediment concentrations according to the following logic. (Free format)

```
DO J=1,NSSIZE
  DO NP=1,NNP
    SS(NP,J)   BS(NP,J)
  ENDDO
ENDDO
```

where SS(NP,J) and BS(NP,J) are the initial suspended and bed sediment concentrations, respectively, at the NPth node.

In the table below, we give brief description on the files that should be included in the super files for achieving desired simulations. In the super file, the BCFT file is a MUST in order to read in the simulation control index, KMOD, as defined above. Both the BCTT and CHEM files need to be included in the super file when transport simulations are desired. When variable initial conditions are to be read, more files need to be taken into account in the super files, as stated in the table below.

Index in the super file	Data File Description
GEOM	geometry file
BCFT	flow file
BCTT	transport file
CHEM	Chemistry file
ICWD	initial water surface elevation
ICQL	initial velocity
ICCN	initial concentrations of dissolved chemicals: data are read chemical by chemical; for each chemical, the concentration in the water column is listed first, followed by that in the interstitial water
ICPN	initial concentrations of particulate chemicals: data are read chemical by chemical; for each particulate chemical on a sediment size, the particulate chemical concentration on the suspended sediment is first listed, then the corresponding one on the bed sediment
ICSN	initial concentrations of sediments: data are read size by size; for each sediment size, the suspended sediment concentration is first listed, followed the bed sediment concentration
HSOL	computational results of flow, including both water surface elevation, velocity, and depth
CSOL	computational results of dissolved chemical concentrations: for each chemical, the concentration in the water column is listed first, followed by that in the interstitial water
PSOL	computational results of particulate chemical concentrations: for each particulate chemical on a sediment size, the particulate chemical concentration on the suspended sediment is first listed, then the corresponding one on the bed sediment
SSOL	computational results of sediment concentrations: for each sediment size, the suspended sediment concentration is first listed, followed the bed sediment concentration

Note: All files above are ASCII files. We also store computational results in a binary file, best.sto, for plotting purposes.

Here we provide an example to show the contents of a super file. Suppose we are to simulate both flow and transport, the initial conditions are variable, and we want to print the computational results of flow as well as transport, then we'll have a super file as follows.

WMS2DSUP
GEOM test.2dm
BCFT test.2bc
BCTT test.2tp
CHEM test.2ch

ICWD test.ich
ICQL test.icv
ICCN test.icc
ICPN test.icp
ICSN test.ics
HSOL test_f.dat
CSOL test_c.dat
PSOL test_p.dat
SSOL test_s.dat

Thus, we have test.2dm describing the geometry, test.2bc specify the flow simulation, test.2tp specify the transport simulation, test.2ch provide contaminant/sediment as well as reaction information, test.ich, test.icv, test.icc, test.icp, and test.ics provide the initial conditions, and test_f.dat, test_c.dat, test_p.dat, and test_s.dat record the computational results at desire times. The following give the idea of how computational results are recorded in HSOL, CSOL, PSOL, and SSOL files.

HSOL file: hydrodynamic variables

```
DO NP = 1,NNP
  NP  X(NP)  Y(NP)  ETA(NP)  U(NP)  V(NP)  D(NP)
ENDDO
```

CSOL file: Dissolved chemicals in the water column and the interstitial water

```
DO I = 1,NCHEM
 DO NP=1,NNP
   I  NP  X(NP)  Y(NP)  C(NP,I)  CB(NP,I)
 ENDDO
ENDDO
```

PSOL file: Particulate chemicals on suspended and bed sediments

```
DO I = 1,NCHEM
 DO J=1,NSSIZE
  DO NP=1,NNP
   I  J  NP  X(NP)  Y(NP)  PS(NP,J,I)  PB(NP,J,I)
  ENDDO
 ENDDO
ENDDO
```

SSOL file: Suspended and bed sediments

```
DO J=1,NSSIZE
 DO NP=1,NNP
  J  NP  X(NP)  Y(NP)  SS(NP,J)  BS(NP,J)
 ENDDO
ENDDO
```

Appendix II. PROGRAM STRUCTURE AND SUBROUTINE DESCRIPTION

In this appendix, we are to give plots showing the structure of the computer program and provide description for each subroutine.

II.1. Program structure

1. Main program and subroutines it calls to.

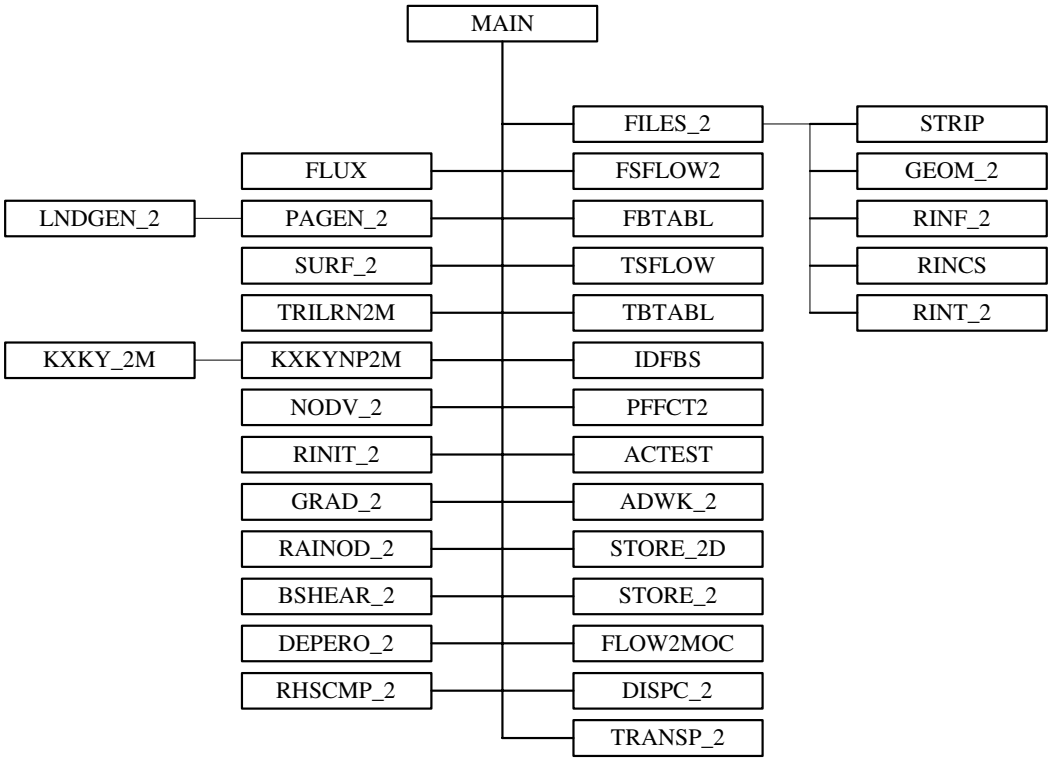

2. Subroutines concerning the computation of water flow.

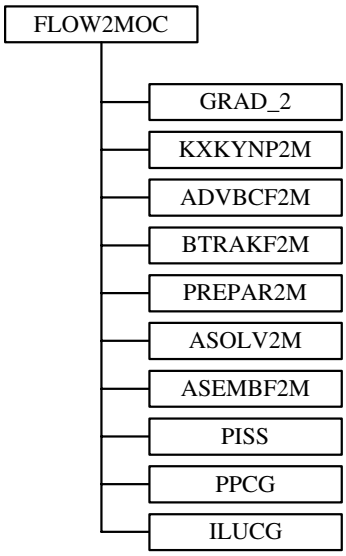

3. Subroutines concerning the computation of chemical/sediment transport.

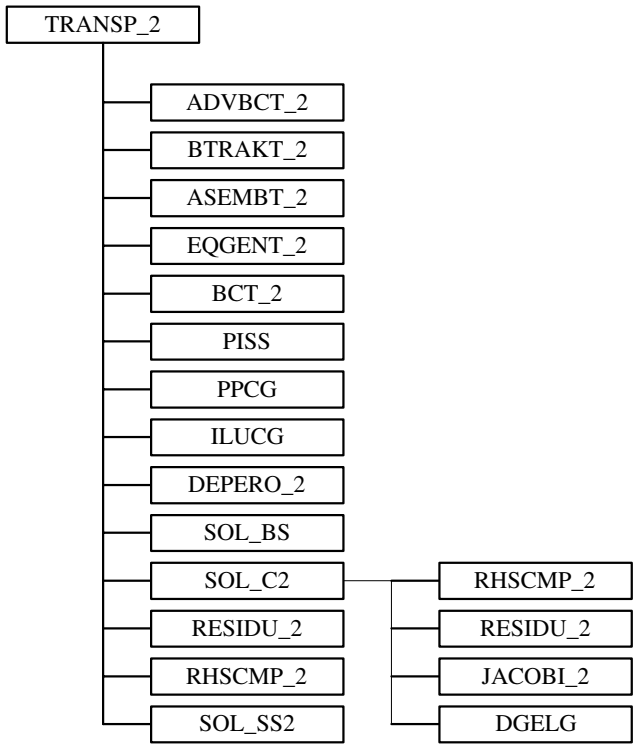

4. Subroutines concerning backward particle tracking.

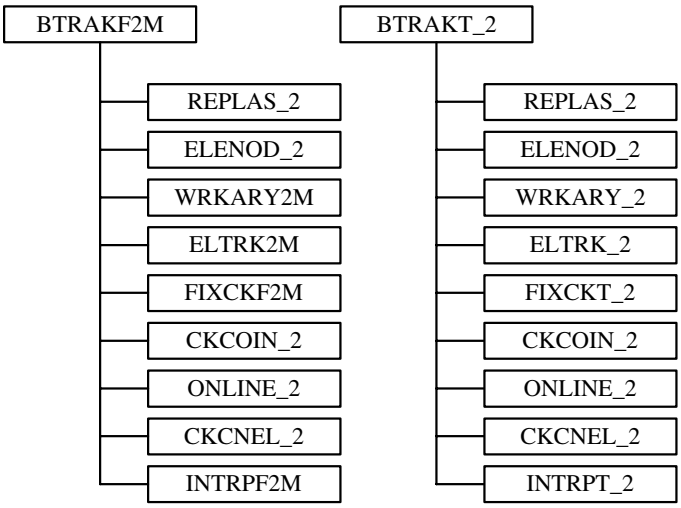

5. Subroutines concerning particle tracking in a subelement.

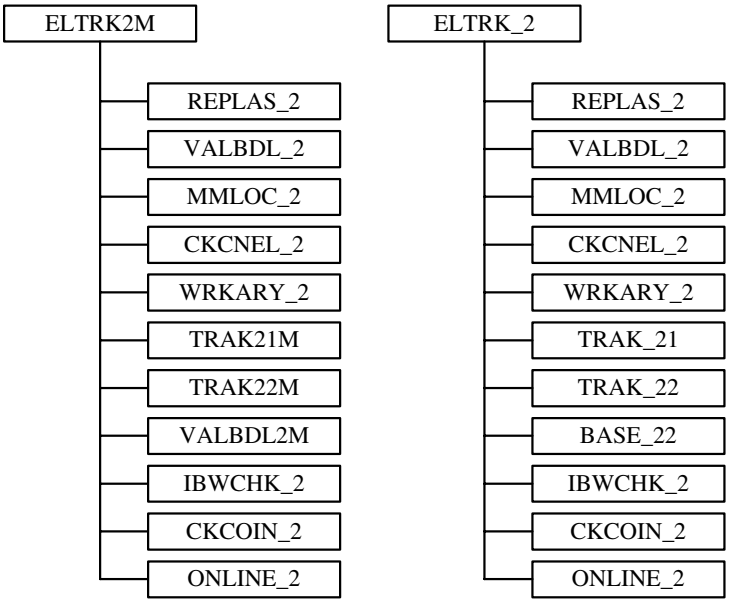

II.2. Subroutine description

MAIN

This main program serves the purpose of controlling the flow path of desired simulations. It calls to Subroutine FILES_2 to read in necessary data to undergo numerical simulations. It calls to Subroutine FLOW2MOC to compute 2-D flow and Subroutine TRANSP_2 to calculate 2-D sediment and chemical transprot. In addition, it calls to needed subroutines to print or store numerical results at desired times.

Subroutine ACTEST

This subroutine is used to determine a quasi-steady flow by checking the maximum absolute error of water stages between two successive tidal cycles.

Subroutine ADVBCF2M

This subroutine is to implement boundary conditions for the computation in the Lagrangian step of solving the 2-D flow equations when the method of characteristics is applied. In this subroutine, boundary conditions with either water stage or inflow flux specified are implemented to obtain water stage or normal flux, respectively, at associated boundary nodes.

Subroutine ADVBCT_2

This subroutine is to implement boundary conditions for the computation in the Lagrangian step of solving the 2-D transport equations of (1) suspended sediment, (2) dissolved chemicals, and (3) particulate chemicals on suspended sediments. Since the diffusive flux is neglected in the Lagrangian Step, only are Dirichlet, Cauchy, and variable boundary conditions are applied.

Subroutine ADWK_2

This subroutine is to determine the working arrays of coordinates (XW), velocities (VXW), subelement indices (IEW), subelement boundary index (IBW), and subelement connectivity (NLRLW and LRLW) in the element being considered in order to perform the 2-D “in-element” particle tracking.

Subroutine ALGBY_2

This subroutine is to achieve particle tracking along the 2-D unspecified boundary. Water flow is considered parallel to the boundary on the unspecified boundary. This subroutine also considers the first-order growth/decay term along characteristics.

Subroutine ALGBYF2M

This subroutine is to achieve particle tracking along the 2-D unspecified boundary. Water flow is considered parallel to the boundary on the unspecified boundary. It is used only when the method of characteristics is employed to solve the 2-D flow equation.

Subroutine AREA

This subroutine is to compute the area of a 2-D element, either quadrilateral or triangular.

Subroutine ASEMBF2M

This subroutine is to compose the global matrix equation to adjust 2-D velocity in the last part of the method of characteristic approach when eddy viscosity is taken into account.

Subroutine ASEMBT_2

This subroutine is to compute global coefficient matrices CMATRX1 and CMATRX2 for 2-D transport equations. CMATRX1 is a mass matrices that takes into account the total time derivative term, while CMATRX2 is stiffness matrices that considers the dispersion term.

Subroutine ASOLV2M

This subroutine is to construct and solve a set of three algebraic equations (Eqs. (3.129) through (3.131)) that is formed by using the method of characteristics to solve the dynamic wave model.

Subroutine BASE_21

This subroutine is to compute the shape functions and their derivatives at a point located in a quadrilateral element, given the local coordinates at the point.

Subroutine BASE_22

This subroutine is to compute the shape functions at a point located in a 2-D element (either triangular or quadrilateral), given the Cartesian coordinates both at the point and element nodes.

Subroutine BCT_2

This subroutine is to implement boundary conditions, including Dirichlet, Cauchy, Neumann, and variable types, for 2-D transport. Dirichlet boundary conditions are specified at boundary nodes, while the other types of boundary conditions are categorized as flux-type boundary conditions and are specified on boundary sides. Dirichlet, Cauchy, Neumann, and conventional variable boundary conditions are prescribed with time-dependent profiles.

Subroutine BSHEAR_2

This subroutine is to achieve the calculation of bottom shear stress at all nodes.

Subroutine BTRAKF2M

This subroutine is to implement backward particle tracking to obtain the water depth at all 2-D global nodes. Since a first-order approach is used for both kinematic and diffusion models and all source/sink rate terms can be expressed a linear function of water depth, we thus take into account the first-order decay/growth rate along the characteristics when we implement backward particle tracking. As for the zeroth-order source/sink rate, we simply multiply this rate by the time-step size being considered and add the product to the outcome of backward particle tracking.

Subroutine BTRAKT_2

This subroutine is to implement backward particle tracking to obtain the Lagrangian values of concentrations of (1) dissolved chemicals, (2) suspended sediments, and (3) particulate chemicals on suspended sediments at all 2-D global nodes.

Subroutine CHNGSN

This subroutine is to change sign of the velocities at point P (the starting location), point Q (the ending location), and working subelement nodes in the process of 2-D or 3-D “in-element” particle tracking.

Subroutine CKCNEL_2

This subroutine is to determine the element that connects to a specified element through the element side with the N1-th and N2-th global nodes serving as the two end nodes of the 2-D side.

Subroutine CKCOIN_2

This subroutine is to determine whether or not a specific node coincides with the N1-th global node or the N2-th global node.

Subroutine CRACKD

This subroutine is to read real numbers in order from a line data record.

Subroutine CRACKI

This subroutine is to read integer numbers in order from a line data record.

Subroutine DEPERO_2

This subroutine is to compute the deposition and erosion rates either at a global node. Both cohesive and non-cohesive cases are taken into account. Eqs. (3.129) and (3.130) are employed for cohesive sediments, while Eqs. (3.131) through (3.134) are used for non-cohesive sediments.

Subroutine DGELG

This subroutine is to solve matrix equations by a direction solver incorporated with full-pivoting.

Subroutine DISPC_2

This subroutine is to compute dispersion coefficients for 2-D transport simulations. The coefficient is evaluated at every quadrature node of elements.

Function DOTPRD

This function is to compute the inner product of two given vectors.

Subroutine ELENOD_2

This subroutine is to determine the number of element nodes for a specified 2-D element.

Subroutine ELTRK_2

This subroutine is to implement the 2-D "in-element" particle tracking in a specified element. The first-order growth/decay term is also taken into account in the tracking.

Subroutine ELTRK2M

This subroutine is to implement the 2-D "in-element" particle tracking in a specified element. It is used only when the method of characteristics is used to solve the 2-D flow equation.

Subroutine EQGENT_2

This subroutine is to generate matrix equations for 2-D transport simulations. When IDC = 0, it is for the transport of the IDS-th suspended sediment. When IDS = 0, it is for the transport of the IDC-th dissolved chemical. When neither IDC nor IDs equals zero, it is for the IDC-th particulate chemical on the IDS-th suspended sediment.

Subroutine FBTABL

This subroutine is to write out mass balance table of flow at desired times.

Function FCOS_2

This is to determine the direction of the outer product of two 2-D vectors.

Subroutine FFLUX

This subroutine is to compute the normal flow flux through each boundary node.

Subroutine FILES_2

This subroutine is to read in information in order to perform 2-D simulations. The information includes (1) geometry data, (2) flow simulation data, (3) transport simulation data, and (4) 1-D/2-D and 2-D/3-D interface data.

Subroutine FIXCKF2M

This subroutine is to handle the case in the particle tracking of 2-D water flow when a particle encounters the boundary. If this boundary is a specified (flow-through) boundary, the current particle tracking stops here and interpolation is employed to compute the Lagrangian value. If this boundary is unspecified (closed), on the other hand, the flow direction is parallel to the boundary and particle tracking along the boundary proceeds until either the available tracking time is completely consumed or a specified boundary is reached. It is used only when the method of characteristics is employed to solve the 2-D flow equation.

Subroutine FIXCKT_2

This subroutine is to handle the case in the particle tracking of 2-D chemical transport when a particle encounters the boundary. If this boundary is a specified (flow-through) boundary, the current particle tracking stops here and interpolation is employed to compute the Lagrangian value. If this boundary is unspecified (closed), on the other hand, the flow direction is parallel to the boundary and particle tracking along the boundary proceeds until either the available tracking time is completely consumed or a specified boundary is reached.

Function FKAPA_2

This function is to compute the bottom friction coefficient, κ, as defined as follows.

$$\kappa = \frac{gn\left|\nabla(h+Z_o)\right|^{1/2}\left[1+(\nabla Z_o)^2\right]^{2/3}}{h^{2/3}} \qquad \text{(II.1)}$$

Subroutine FLOW2MOC

This subroutine serves as the control panel of computing 2-D flow by using the method of characteristics to solve the dynamic model. The Picard method is used to deal with nonlinearity. During each nonlinear iteration, The characteristic equation (Eq. (3.15)) is solved first by the backward particle tracking along three characteristics. After $H^{\#}$, $u^{\#}$, and $v^{\#}$ are determined, we compute H, u, and v by solving Eqs. (3.64) through (3.66). Convergence is determined by checking the maximum relative error of H, u, and v. Relaxation technique is applied to update the working water stage and velocity for the next iteration if convergence has not been reached.

Subroutine FLUX

This subroutine is to compute mass flux of the given mobile material at boundary nodes.

Subroutine FSFLOW2

This subroutine is to compute the data needed in the mass balance table of flow.

Subroutine FTAUB_2

This subroutine is to calculate bottom shear stress at an node. The bottom shear stress is computed according to the following equations.

$$\tau_x^b = u\rho g n\left|\nabla(h+Z_o)\right|^{1/2}\left[1+(\nabla Z_o)^2\right]^{2/3} h^{1/3} \quad \text{(II.2)}$$

$$\tau_y^b = v\rho g n\left|\nabla(h+Z_o)\right|^{1/2}\left[1+(\nabla Z_o)^2\right]^{2/3} h^{1/3} \quad \text{(II.3)}$$

where τ_x^b and τ_y^b are bottom shear stress in x- and y-directions, respectively; u and v are velocity components in x- and y-directions, respectively; ρ is water density; g is gravity; n is Manning's n; h is water depth; Z_o is bottom elevation.

Subroutine GAUPNT_2

This subroutine is to compute shape functions and their derivatives at quadrature nodes.

Subroutine GEOM_2

This subroutine is to read in 2-D geometry, including coordinates and element indices.

Subroutine GRAD_2

This subroutine is to compute the spatial derivatives of water depth, stage, flow velocity, and Manning's n as desired in 2-D simulations. In addition, the second spatial derivatives of water depth and stage are calculated as needed.

Subroutine IBWCHK_2

This subroutine is to determine the two global nodes that serve as the two end node of an element side. This element side is the side that the particle has encountered when it passes through the element being considered.

Subroutine IDFBS

This subroutine is to relate flux-type boundary sides with global boundary sides. The relationship is stored in two arrays: one for flow simulations and the other for transport simulations.

Subroutine ILUCG

This subroutine is to solve the linearized matrix equation that is sparse asymmetric with the preconditioned conjugate gradient method using the incomplete Cholesky decomposition as a preconditioner.

Subroutine INTRPF2M

This subroutine is to determine the Lagrangian characteristic quantities by interpolation after backward particle tracking in solving flow governing equations when the method of characteristics is used to deal with the dynamic wave model.

Subroutine INTRPT_2

This subroutine is to determine the Lagrangian chemical and suspended sediment concentrations by interpolation after backward particle tracking in the Lagrangian step of solving 2-D transport governing equations.

Subroutine JACOBI_2

This subroutine is to compute the Jacobian for the chemical system at the NP-th node. The Jacobian

elements are defined as in Eqs. (3.113) through (3.128).

Subroutine KXKY_2M

This subroutine is to determine characteristic directions at a 2-D global node for flow simulations, based on the velocity, the spatial velocity derivatives, and the spatial stage derivatives at the node. This subroutine is needed only when the method of characteristics is employed to solve the 2-D flow equation.

Subroutine KXKYNP2M

This subroutine is to determine characteristic directions at all 2-D global nodes for flow simulations. This subroutine is needed only when the method of characteristics is employed to solve the 2-D flow equation.

Subroutine LLTINV

This subroutine is to solve for a modified residual that is to be used in the preconditioned conjugate gradient algorithm.

Subroutine LNDGEN_2

This subroutine is to determine node-node and node-element connectivity in 2-D simulations, based on the given element indices.

Subroutine LOCQ_2

This subroutine is to locate the target point and its velocity for a tracking path in a 2-D subelement of particle tracking. The available tracking time left after this tracking path is also computed.

Subroutine LOCQ2M

This subroutine is to locate the target point and its velocity for a tracking path in a 2-D subelement of particle tracking. The available tracking time left after this tracking path is also computed. It is used since the method of characteristics is employed to solve the 2-D flow equation.

Subroutine MMLOC_2

This subroutine is to specify the starting location to start the 2-D “in-element” particle tracking in an element.

Subroutine NELIM2

This subroutine is to prepare an array consisting of nodal numbers from a set of element face data.

Subroutine NODV_2

This subroutine is to calculate Manning’s n at every 2-D global node.

Subroutine OBCOEF2M

This subroutine is to determine the coefficient of a characteristic at an open boundary node. The characteristic has been determined coming from the outside of the domain. This subroutine is needed only when the method of characteristics approach is taken to solve 2-D flow equations.

Subroutine ONLINE_2

This subroutine is to adjust the coordinates of a specified point if needed, such that this point will be located on the line segment with two given 2-D nodes serving as its end nodes.

Subroutine PAGEN_2

This subroutine is to generate 2-D pointer arrays needed for numerical simulations.

Subroutine PFFCT2

This subroutine is to determine the functional values of an array by interpolation from a series of given profiles.

Subroutine PISS

This subroutine is to solver the linearized matrix equation with a pointwise iteration solution strategy.

Subroutine POLYP

This subroutine is to solve a modified residual that is to be used in the preconditioned conjugate gradient algorithm.

Subroutine PPCG

This subroutine is to solve the linearized matrix equation with the preconditioned conjugate gradient method by using a polynomial as a preconditioner.

Subroutine PREPAR2M

This subroutine is to prepare for data needed to construct and solve the set of algebraic equations in Subroutine ASOLV2M.

Subroutine Q2FLUX

This subroutine is to perform boundary integration over a 2-D boundary side.

Subroutine Q3D

This subroutine is to compute element flux matrices due to dispersion for mobile materials, where the element is triangular.

Subroutine Q3T

This subroutine is to determine the triangular element coefficient matrices and load vectors to sole 2-D transport equation in the Eulerian step.

Subroutine Q4D

This subroutine is to compute element flux matrices due to dispersion for mobile materials, where the element is quadrilateral.

Subroutine Q4T

This subroutine is to determine the quadrilateral element coefficient matrices and load vectors to sole 2-D transport equation in the Eulerian step.

Subroutine Q34FM

This subroutine is to determine the element coefficient matrices, including mass matrices and the stiffness matrices taking into account eddy viscosity in soling 2-D dynamic wave model.

Subroutine Q34F1

This subroutine is to determine element coefficient matrices and load vectors to compute the gradients of bottom elevation, water stage, velocities, and Manning's n in 2-D flow simulations.

Subroutine Q34F2

This subroutine is to determine element coefficient matrices and load vectors to compute the gradients of the derivatives of bottom elevation in 2-D flow simulations.

Subroutine RAINOD_2

This subroutine is to determine rainfall rate at 2-D global nodes.

Subroutine REPLAS_2

This subroutine is to write the values of the first four arguments into the last four arguments.

Subroutine RESIDU_2

This subroutine is to compute the residual of the 2-D transport equations of (1) dissolved chemicals (when ID = 1), (2) particulate chemicals on suspended sediments (when ID = 1), (3) particulate chemicals on bed sediments (when ID = 1), and (4) suspended sediments (when ID = 2) at the NP-th node. The residuals are defined as in Eqs. (3.109) through (3.112) for contaminant transport equations and in the following equation for the sediment transport equations.

$$\mathbf{RESS_n} = \mathbf{h}(S_n)^{N+1/2} + \Delta\tau\,(RHSS_n)^{N+1} - \Delta\tau\,(RHSS_n)^{N} \qquad n \in [1,N_s] \tag{II.4}$$

where $(RHSS_n)^{N+1}$ is evaluated with ID = 22 in Subroutine RHSCOMP1, whereas $(RHSS_n)^{N}$ is calculated with ID = 21.

Subroutine RHSCMP_2

This subroutine is to compute the right-hand side of the 2-D transport governing equations of (1) dissolved chemicals (when ID = 1), (2) particulate chemicals on suspended sediments (when ID = 1), (3) particulate chemicals on bed sediments (when ID = 1), and (4) suspended sediments (when ID = 21 or 22) at the NP-th node. The right-hand sides are defined as in Eqs. (3.102), (3.104), (3.106), and (3.108) for contaminant transport equations and in the following equation for the transport equations of suspended sediments.

(a) when ID = 21,

$$\mathbf{RHSS_n} = \left[M_n^s + R_n - D_n\right] - \left[R - I\right]S_n \qquad n \in [1,N_s] \tag{II.5}$$

(a) when ID = 22,

$$\mathbf{RHSS_n} = \left[M_n^s + R_n - D_n\right] \qquad n \in [1,N_s] \tag{II.6}$$

Subroutine RINCS

This subroutine is to read in chemistry and sediment information.

Subroutine RINF_2

This subroutine is to read in information for 2-D flow simulations.

Subroutine RINIT_2

This subroutine is to read in the initial condition for 2-D flow and/or transport simulations.

Subroutine RINT_2

This subroutine is to read in information for 2-D transport.

Subroutine SOL_BS

This subroutine is to solve the transport governing equation of bed sediments at the NP-th river/stream or node.

Subroutine SOL_C2

This subroutine is to solve for the concentrations of dissolved chemicals, particulate chemicals on suspended sediments, and particulate sediments on bed sediments at 2-D global nodes. This subroutine serves as the corrector step in our predictor-corrector approach to solve transport equations of chemicals. The Newton-Raphson method is employed to solve the nonlinear system of chemical reactions. The full-pivoting technique is incorporated into a direct solver to handle linearized matrix equations.

Subroutine SOL_SS2

This subroutine is to solve the concentrations of suspended sediments at the NP-th node in the corrector step, where the time-implicit scheme is employed.

Subroutine SOLVE

This subroutine is to solve band matrix equations by using a direct solver. The band matrix equation is triangulized when the indicator KKK is set to 1, while back substitution is implemented when KKK = 2.

Subroutine STAR2M

This subroutine is to determine the Lagrangian values (i.e., H_1^*, u_1^*, v_1^*, H_2^*, u_2^*, v_2^*, H_3^*, u_3^*, v_3^* appeared in Section 3.2.1) associated with each characteristic.

Subroutine STORE_2

This subroutine is to write out the computer results at desired times in ascii files by taking the TECPLOT format for achieving the purpose of post-processing (e.g., plotting). Four files are to be generated in this subroutine. They are (1) a file to store data of water surface elevation, water depth, and velocity, (2) a file to store concentrations in water body and interstitial phase, (2) a file to store concentrations of both suspended and bed sediments, and (4) a file to store information of particulate chemicals adsorbed on suspended and bed sediments.

Subroutine STORE_2D

This subroutine is to store the computer results at desired times in a binary file for further plotting purposes.

Subroutine STRIP

This subroutine is to read in a character variable.

Subroutine SURE_2

This subroutine is to analytically determine the target location of a 2-D tracking path when the single-velocity approach is applied.

Subroutine SURE2M

This subroutine is to analytically determine the target location of a 2-D tracking path when the single-velocity approach is applied. It is used only when the method of characteristics is employed to solve the 2-D flow equation.

Subroutine SURF_2

This subroutine is to generate boundary arrays for implementing boundary conditions in 2-D simulations.

Subroutine TBTABL

This subroutine is to write the mass balance table of mobile materials at desired times.

Subroutine TRAK_21

This subroutine is to determine (1) whether or not a particle will pass through the working subelement being considered and (2) the location of the target location if the particle will pass through the working subelement. This subroutine is employed when the starting location is where an subelement node is located.

Subroutine TRAK_22

This subroutine is to determine (1) whether or not a particle will pass through the working subelement being considered and (2) the location of the target location if the particle will pass through the working subelement. This subroutine is employed when the starting location is not where an subelement node is located.

Subroutine TRAK21M

This subroutine is to determine (1) whether or not a particle will pass through the working subelement being considered and (2) the location of the target location if the particle will pass through the working subelement. This subroutine is employed when the starting location is where an subelement node is located. It is used only when the method of characteristics is employed to solve the 2-D flow equation.

Subroutine TRAK22M

This subroutine is to determine (1) whether or not a particle will pass through the working subelement being considered and (2) the location of the target location if the particle will pass through the working subelement. This subroutine is employed when the starting location is not where an subelement node is located. It is used only when the method of characteristics is employed to solve the 2-D flow equation.

Subroutine TRANSP_2

This subroutine serves as the control panel to compute both chemical and sediment transport. The predictor-corrector numerical approach is employed to solve the transport equations of mobile materials, such as dissolved chemicals, suspended sediments, and particulate chemicals on suspended sediments. During each time step, The predictor step is first implemented to obtain the intermediate values for mobile materials.

Sediment equations are then solved by using the Picard to handle their nonlinearity. The concentrations of chemicals are the last to solve for. The set of nonlinear ordinary differential equations is solved with the Newton-Raphson method node by node in the corrector step.

Subroutine TRILRN2M

This subroutine is to generate pointer arrays for the use in constructing the matrix equation for adjusting 2-D flow velocity in the last part of the method of characteristic approach.

Subroutine TSCONV

This subroutine is to retrieve desired profiles from given x-y series curves.

Subroutine TSCONVV

This subroutine is to retrieve desired profiles from given x-y series curves.

Subroutine TSCONV2

This subroutine is to retrieve desired profiles from given x-y series curves.

Subroutine TSFLOW

This subroutine is to compute the data needed in the mass balance table of mobile material.

Subroutine VALBDL_2

This subroutine is to compute the velocity at a specified 2-D node by interpolation.

Subroutine VALBDL2M

This subroutine is to compute the velocity at a specified 2-D node by interpolation. It is used only when the method of characteristics is employed to solve the 2-D flow equation.

Subroutine WRKARY_2

This subroutine is to prepare working arrays for particle tracking in either a 2-D element or a 2-D subelement.

Subroutine WRKARY2M

This subroutine is to prepare working arrays for particle tracking in either a 2-D element or a 2-D subelement. It is employed only when the method of characteristics is employed to solve the 2-D flow equation.

Subroutine XSI_2

This subroutine is to determine the local coordinates of a specified node that is located in a 2-D quadrilateral element, given the original Cartesian coordinates of both the node and element nodes.

REFERENCES

Abbott, M. B., 1966, *An introduction to the method of characteristics*, American Elsevier, 243p.

Anastasiou, K and C. T. Chan, 1997, *Solution of the 2D shallow water equations using the finite volume method on unstructured triangular meshes*, International Journal for Numerical Methods in Fluids, 24(11), 1225-1245.

Blumberg, A. F., Z.-G. Ji, and C. K. Ziegler, 1996, *Modeling outfall plume behavior using far field circulation model*, Journal of hydraulic Engineer, 122(11), 610-615.

Casulli, V. and R. T. Cheng, 1990, *Stability analysis of Eulerian-Lagrangian methods for the one-dimensional shallow-water equations*, Applied Mathematical Modelling, 14(3), 122-131.

Cecchi, M. M., A. Pica, and E. Secco, 1998, *Projection method for shallow water equations*, International Journal for Numerical Methods in Fluids, 27(special issue), 81-95.

Cheng, H. P. and G. T. Yeh, 1998, *Development of a three-dimensional model of subsurface flow, heat transfer, and reactive chemical transport: 3DHYDROGEOCHEM*, Journal of Contaminant Hydrology (in press).

Cheng, J. R., H. P. Cheng, and G. T. Yeh, 1996a. *A Lagrangian-Eulerian method with adaptively local zooming and peak/valley capturing approach to solve two-dimensional advection-diffusion transport equations.* International Journal for Numerical Methods in Engineering, 39(6), 987-1016.

Cheng, H. P., J. R. Cheng, and G. T. Yeh, 1996b, *A particle tracking technique for the Lagrangian-Eulerian finite element method in multi-dimensions.* International Journal for Numerical Methods in Engineering, 39(7), 1115-1136.

Chilakapathi, A., 1995, *A simulator for reactive flow and transport of groundwater contaminants*, Report PNL-10636, Pacific Northwest Laboratory, USA.

Chow, V. T, 1973, *Open channel hydraulics*, McGraw-Hill, 680p.

Falconer, R. A. and B. Lin, 1997, *Three-dimensional modelling of water quality in the Humber estuary*, Water Research, 31(5), 1092-1102.

Falconer, R. A., 1990, *Engineering problems and the application of mathematical models relating to combating water pollution*, Municipal Engineer, 7(6), 281-291.

Fennema, J. F. and M. H. Chaudhry, 1989, *Implicit methods for two-dimensional unsteady free-*

surface flows, Journal of Hydraulic Research, 27(3), 321-332.

Graf, W. H., 1984, *Hydraulics of Sediment Transport,* Water Resources Publication.

Hansen, E. A. and L. Arneborg, 1997, *Use of a discrete vortex model for shallow water flow around islands and coastal structures*, Coastal Engineering, 32(2), 223-246.

Hirsch, Ch., C. Lacor, and H. Deconinck, 1987, *Convection algorithms based on a diagonalization procedure for the multidimensional Euler equations*, AIAA Journal, Vol. 25, 667-676.

Lai, C., 1987, *Comprehensive method of characteristics models for flow simulation*, J. of Hydraulic Engineering, Vol. 114, No. 9, 1074-1097.

Lai, C., 1977, *Computer simulation of two-dimensional unsteady flows in estuaries and embayments by the method of characteristics — basic theory and the formulation of the numerical method*, Report USGS Water-Resources Investigations 77-85, Reston, MA, USA.

Laible, J. P. and T. P. Lillys, 1997, *A filtered solution of the primitive shallow-water equations*, Advances in Water Resources, 20(1), 23-35.

Muccino, J. C., W. G. Gray, and M. G. G. Foreman, 1997, *Calculation of vertical velocity in three-dimensional, shallow water equation, finite element models*, International Journal for Numerical Methods in Fluids, 25(7), 779-802.

Ors, H., 1997, *Contaminant transport model for the Bosphorus Strait*, Journal of Environmental Science and Health, Part A: Environmental Science and Engineering & Toxic and Hazardous Substance Control, 32(3), 699-714.

Ozkan-Haller, H. T. and J. T. Kirby, 1997, *Fourier-Chebyshev collocation method for the shallow water equations including shoreline runup*, Applied Ocean Research, 19(1), 21-34.

Park, K. and A. Y. Kuo, 1996, *Multi-step computation scheme: decoupling kinetic processes from physical transport in water quality models*, Water Research, 30(10), 2255-2264.

Park, S. S., K. F. Najjar, and C. G. Uchrin, 1995, *Water quality management model for the lakes bay estuarine embayment 2: hydrodynamic tidal model*, Journal of Environmental Science and Health, Part A: Environmental Science and Engineering & Toxic and Hazardous Substance Control, 30(5), 1077-1204.

Paulsen, S. C. and R. M. Owen, 1996, *Quantitative model of sediment dispersal and heavy mineral distribution in North Cardigan Bay, Irish Sea*, Mirine Georesources and Geotechnology, 14(2), 143-159.

Petera, J. and V. Nassehi, 1996, *New two-dimensional finite element model for the shallow water equations using a lagrangian framework constructed along fluid particle trajectories*, International Journal for Numerical Methods in Engineering, 39(24), 4159-4182.

Press, W. H., S. A. Teukolsky, W. T. Vetterling, and B. P. Flannery, 1992, *Numerical Recipes*, 2nd edition, Cambridge, 963p.

Salvage, K. M., 1998, *Reactive contaminant transport in variably saturated porous media: biogeochemical model development, verification, and application*, Ph. D. thesis in Civil and Environmental Engineering, The Pennsylvania State University, USA.

Shi, J. and E. F. Toro, 1996, *Fully discrete high-order shock-capturing numerical schemes*, International Journal for Numerical Methods in Fluids, 23(3), 241-269.

Sommeijer, B. P. and J. Kok, 1996, *Splitting methods for three-dimensional bio-chemical transport*, Applied Numerical Mathematics, 21(3), 303-320.

Spitaleri, R. M. and L. Corinaldesi, 1997, *Multigrid semi-implicit finite difference method for the two-dimensional shallow water equations*, International Journal for Numerical Methods in Fluids, 25(11), 1229-1240.

Stumm, W. and J. J. Morgan, 1981, *Aquatic chemistry — an introduction emphasizing chemical equilibria in natural waters*, John Wiley & Sons, 780 p.

Tseng, M. H. and S.-J. Liang, 1997, *Comparison of second-order accurate TVD scheme and p-version space-time least-squares finite-element method for nonlinear hyperbolic problems*, HPC Asia'97 Proceedings for the 2nd High Performance Computing on the Information Superhighway, 289-294.International Journal for Numerical Methods in Fluids, 24(1), 61-79.

Wang, J. D. and J. J. Connor, 1975, *Mathematical modeling of near coastal circulation*, Report MITSG 75-13, Massachusetts Institute of Technology, MA, USA.

Wood, T. M. and Baptista, A. M., 1992, *Modeling the pathways of nonconservative substances in estuaries*, Proceedings of the 2nd International Conference on Estuarine and Coastal Modeling, 280-291.

Yeh, G. T., G. Iskra, J. M. Zachara, and J. E. Szecsödy, 1998, *Development and verification of a mixed chemical kinetic and equilibrium model*, Advances in Environmental Research, 2(1), 24-56.

Yeh, G. T., J. R. Chang, and T. E. Short, 1992, *An exact peak capturing and oscillation-free scheme to solve advection-dispersion transport equations*, Water Resources Research, 28(11), 2937-2951.

Yeh, G. T., 1990, *A Lagrangian-Eulerian method with zoomable hidden fine-mesh approach to solving advection-dispersion equations*, Water Resources Research, 26(6), 1133-1144.

Yeh, G. T. and V. S. Tripathi, 1990, *HYDROGEOCHEM: A Coupled Model of HYDROlogical Transport and GEOCHEMical Equilibria in Reactive Multicomponent Systems*, Report ORNL-6371, Oak Ridge National Laboratory, Oak Ridge, TN, USA.

Yeh, G. T., 1983, *CHNTRN: A ChaNnel TRaNsport Model for Simulating Sediment and Chemical Distribution in a Stream/River Network*, ORNL-5882, Oak Ridge National Laboratory, Oak Ridge, Tennessee 37830.

Yeh, G. T. and C. Kalasinsky, 1977, A two-dimensional finite element circulation model (CAFE), Report EN-139, Stone & Webster, Boston.

For more information about the
National Shipbuilding Research Program
please visit:

http://www.nsrp.org/

or

http://www.USAShipbuilding.com/